



OPTIMIZATION OF DONEPEZIL HYDROCHLORIDE-LOADED
MICROPARTICLES PRODUCED BY DOUBLE EMULSION TECHNIQUE



By
MISS Lalinthip SUTTHAPITAKSAKUL

A Thesis Submitted in Partial Fulfillment of the Requirements
for Master of Pharmacy (PHARMACEUTICAL SCIENCES)

Graduate School, Silpakorn University

Academic Year 2020

Copyright of Graduate School, Silpakorn University

การหาสภาวะที่เหมาะสมในการผลิตไมโครพาร์ทีเคิลบรรจุยาโคนิฟิซิลไฮโดรคอลลอยด์
ด้วยเทคนิคอิมัลชันสองชั้น



โดย
นางสาวลลิตทิพย์ สุทธาพิทักษ์สกุล

วิทยานิพนธ์นี้เป็นส่วนหนึ่งของการศึกษาตามหลักสูตรเภสัชศาสตรมหาบัณฑิต
สาขาวิชาวิทยาการทางเภสัชศาสตร์ แผน ก แบบ ก 1 เภสัช ระดับปริญญาามหาบัณฑิต
บัณฑิตวิทยาลัย มหาวิทยาลัยศิลปากร
ปีการศึกษา 2563
ลิขสิทธิ์ของบัณฑิตวิทยาลัย มหาวิทยาลัยศิลปากร

OPTIMIZATION OF DONEPEZIL HYDROCHLORIDE-LOADED
MICROPARTICLES PRODUCED BY DOUBLE EMULSION
TECHNIQUE



A Thesis Submitted in Partial Fulfillment of the Requirements
for Master of Pharmacy (PHARMACEUTICAL SCIENCES)
Graduate School, Silpakorn University
Academic Year 2020
Copyright of Graduate School, Silpakorn University

Title Optimization of donepezil hydrochloride-loaded microparticles
produced by double emulsion technique
By Lalinthip SUTTHAPITAKSAKUL
Field of Study (PHARMACEUTICAL SCIENCES)
Advisor Professor Pornsak Sriamornsak , Ph.D.

Graduate School Silpakorn University in Partial Fulfillment of the
Requirements for the Master of Pharmacy

.....Dean of graduate school
(Associate Professor Jurairat Nunthanid, Ph.D.)

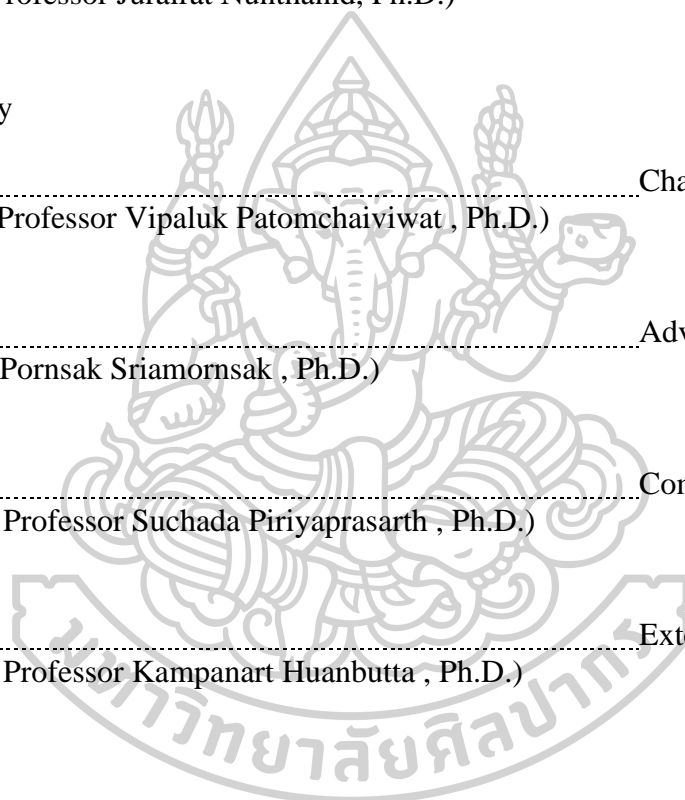
Approved by

.....Chair person
(Assistant Professor Vipaluk Patomchaiwiwat , Ph.D.)

.....Advisor
(Professor Pornsak Sriamornsak , Ph.D.)

.....Committee
(Associate Professor Suchada Piriyaprasarth , Ph.D.)

.....External Examiner
(Associate Professor Kampanart Huanbutta , Ph.D.)



59364202 : Major (PHARMACEUTICAL SCIENCES)

Keyword : donepezil hydrochloride, double emulsion, taste-masking, Box-Behnken design, orally disintegrating tablets

MISS LALINTHIP SUTTHAPITAKSAKUL : OPTIMIZATION OF DONEPEZIL HYDROCHLORIDE-LOADED MICROPARTICLES PRODUCED BY DOUBLE EMULSION TECHNIQUE THESIS ADVISOR : PROFESSOR PORNSAK SRIAMORNSAK, Ph.D.

Donepezil hydrochloride (DPH) is a bitter indanone and piperidine derivative that acts as a reversible cholinesterase inhibitor and has been approved for use in all stages of Alzheimer's disease. Patients with Alzheimer's disease may experience swallowing difficulties as the disease progresses. Orally disintegrating tablets (ODTs) with DPH have been created to make drug administration easier. As ODTs are designed to disintegrate quickly in the mouth, they may come into contact with taste receptors, resulting in a bitter taste. As a result, the objectives of this study were to mask the bitter taste of DPH and create ODTs with taste-masked microparticles. Microencapsulation by double emulsion solvent evaporation technique using aminoalkyl methacrylate copolymer (AMC) as an encapsulation polymer was used to prepare taste-masked DPH-loaded microparticles. A Box-Behnken design was employed to investigate the effect of AMC amount, stirring time, and volume of outer water phase on particle size, *in vitro* drug dissolution at 5 min (Q_5) in simulated saliva fluid, and mean dissolution time (MDT) in simulated gastric fluid. The results demonstrated that AMC amount and stirring time had a significant influence on particle size. While Q_5 and MDT was influenced by AMC amount and volume of external water phase. After validation of the developed model, the optimization was carried out. AMC amount of 5.7 g, stirring time of 148 s, and volume of external phase of 350 mL were the optimum condition to prepare microparticles with desired properties. The optimized product was further characterized and incorporated in ODTs, which prepared by the direct compression method. The effect of super-disintegrants, i.e., sodium starch glycolate, croscarmellose sodium, and crospovidone, on wetting time and *in vitro* disintegration time were studied. The ODT containing 4% crospovidone was chosen for *in vivo* evaluation as it provided short wetting time and rapid *in vitro* disintegration. The *in vivo* results showed that the taste-masked microparticles-loaded ODTs with acceptable palatability were successfully prepared. From the results, it can be concluded that the taste-masked microparticles were successfully prepared by double emulsion solvent evaporation technique. The effect of independent factors and optimization can be determined by implementing Box-Behnken design. Lastly, the ODTs containing taste-masked microparticles with acceptable properties were successfully prepared.

ACKNOWLEDGEMENTS

Firstly, I would like to express my sincere gratitude to my thesis advisor, Professor Dr. Pornsak Sriamornsak, for invaluable guidance, patience, and encouragement throughout my study period. Without his guidance and persistent help, my thesis would not have been accomplished.

Additionally, I wish to express my gratitude to Associate Professor Dr. Sontaya Limmatvapirat and Associate Professor Dr. Thawatchai Phaechamud for their insightful comment and discussion about my research in our laboratory meeting.

I wish to express my appreciation to Assistant Professor Dr. Vipalak Patomchaiwiwat and Associate Professor Dr. Suchada Piriyaprasarth for their valuable guidance and being on my proposal and thesis examination committee. I also wish to thank Associate Professor Dr. Kampanart Huanbutta for their helpful suggestion and for being on my thesis examination committee.

I wish to thank all laboratory members at Pharmaceutical Technology Building for their help and friendships along my study.

I cannot forget to acknowledge the Graduate School and Faculty of Pharmacy, Silpakorn University for financial support. I also would like to acknowledge Graduate Development Scholarship 2020, National Research Council of Thailand for financial support.

Eventually, I wish to give my special thanks to my beloved dad, mom, family, and friends for their meaningful emotional support and understanding. I cannot go through any trouble without their caring.

Lalinthip SUTTHAPITAKSAKUL

TABLE OF CONTENTS

| | Page |
|--|-------------|
| ABSTRACT..... | D |
| ACKNOWLEDGEMENTS..... | E |
| TABLE OF CONTENTS..... | F |
| LIST OF TABLES..... | K |
| LIST OF FIGURES..... | L |
| CHAPTER 1 Introduction..... | 15 |
| CHAPTER 2 Literature review..... | 18 |
| 2.1 Background of donepezil hydrochloride (DPH)..... | 20 |
| 2.1.1 Drug development history..... | 20 |
| 2.1.2 Physicochemical properties..... | 20 |
| 2.1.3 Dosing strategies..... | 21 |
| 2.1.4 Adverse event..... | 21 |
| 2.2 The major challenges of DPH for dosage form development..... | 21 |
| 2.2.1 Bitter taste of DPH..... | 21 |
| 2.2.1.1 Taste-masking by organoleptic method..... | 22 |
| 2.2.1.2 Taste-masking by application of physical barrier..... | 22 |
| 2.2.2 Adverse event of DPH..... | 24 |
| 2.3 Novel dosage forms and development technologies..... | 24 |
| 2.3.1 Oral drug administration..... | 24 |
| 2.3.2 Topical and transdermal drug administration..... | 25 |
| 2.3.3 Parenteral drug administration..... | 26 |
| 2.3.4 Nasal drug administration..... | 26 |
| 2.4 Microencapsulation by double emulsion solvent evaporation technique for taste-masking of DPH..... | 27 |
| 2.4.1 Double emulsion..... | 27 |
| 2.4.1.1 Techniques to produce double emulsion..... | 29 |

| | |
|--|----|
| 2.4.1.1.1 Two-step emulsification | 29 |
| 2.4.1.1.2 Membrane emulsification | 30 |
| 2.4.1.1.3 Microfluidic method | 31 |
| 2.4.2 Double emulsion solvent evaporation technique (DESE) | 31 |
| 2.4.3 Commonly used polymers in DESE..... | 34 |
| 2.4.3.1 Biodegradable polymer | 34 |
| 2.4.3.2 Non-biodegradable polymer | 34 |
| 2.4.4 Factors affecting on microparticle preparation by DESE | 36 |
| 2.5 ODTs..... | 38 |
| 2.5.1 Techniques to produce ODTs..... | 38 |
| 2.5.1.1 Compression technique | 38 |
| 2.5.1.2 Lyophilization | 38 |
| 2.5.1.3 Molding | 39 |
| 2.5.1.4 Sublimation | 39 |
| 2.5.1.5 Cotton candy process..... | 39 |
| 2.5.2 Characterization of ODTs | 40 |
| 2.6 Design of experiment (DoE) approach for optimization | 41 |
| 2.6.1 DoE..... | 41 |
| 2.6.2 Types of DoE..... | 42 |
| 2.6.2.1 Full factorial design..... | 42 |
| 2.6.2.2 Fractional factorial design | 42 |
| 2.6.2.3 Central composite design (CCD) | 42 |
| 2.6.2.4 Box-Behnken design (BBD) | 43 |
| 2.6.3 BBD for optimization of drug-loaded microparticles by DESE | 44 |
| CHAPTER 3 Materials and methods..... | 46 |
| 3.1 Materials | 48 |
| 3.2 Preliminary study on double emulsion preparation | 48 |
| 3.3 Characterization of DPH-loaded double emulsion | 49 |
| 3.3.1 Viscosity of oil phase measurement | 49 |

| | |
|---|----|
| 3.3.2 Double emulsion droplet morphology characterization | 49 |
| 3.3.3 Double emulsion droplet size measurement..... | 49 |
| 3.4 Identification of relevant factors on microparticles preparation using quality risk management approach | 50 |
| 3.5 Study on factors affecting microparticle preparation | 50 |
| 3.5.1 Effect of pH of external water phase..... | 50 |
| 3.5.2 Effect of ultrasonication time | 51 |
| 3.5.3 Effect of polymer amount..... | 51 |
| 3.5.4 Effect of stirring time | 51 |
| 3.5.5 Effect of volume of external water phase..... | 51 |
| 3.5.6 Statistical analysis | 51 |
| 3.6 Optimization of DPH-loaded microparticles by BBD..... | 52 |
| 3.7 Characterization of DPH-loaded microparticles..... | 52 |
| 3.7.1 Morphology of microparticles..... | 52 |
| 3.7.2 Image analysis of microparticles..... | 53 |
| 3.7.3 Residual solvent determination | 53 |
| 3.7.4 Fourier transform infrared (FTIR) spectroscopy..... | 53 |
| 3.7.5 Powder X-ray diffractometry (PXRD)..... | 53 |
| 3.7.6 Differential scanning calorimetry (DSC) | 54 |
| 3.7.7 Drug content determination..... | 54 |
| 3.7.8 <i>In vitro</i> dissolution test | 55 |
| 3.8 Preparation and evaluation of ODTs | 56 |
| 3.8.1 Preparation of ODTs | 56 |
| 3.8.2 Evaluation of physical properties | 57 |
| 3.8.2.1 Thickness, diameter, and hardness measurement..... | 57 |
| 3.8.2.2 Friability test..... | 57 |
| 3.8.3 Wetting test..... | 57 |
| 3.8.4 <i>In vitro</i> disintegration test..... | 58 |
| 3.8.5 <i>In vitro</i> dissolution test | 59 |

| | |
|---|-----|
| 3.8.6 <i>In vivo</i> evaluation | 59 |
| 3.8.6.1 Perception and bitterness threshold determination..... | 59 |
| 3.8.6.2 Palatability test | 60 |
| CHAPTER 4 Results and discussion | 61 |
| 4.1 Study on factors affecting microparticle preparation | 62 |
| 4.1.1 Effect of pH of external water phase..... | 63 |
| 4.1.2 Effect of ultrasonication time | 64 |
| 4.1.3 Effect of polymer amount..... | 66 |
| 4.1.4 Effect of stirring time | 72 |
| 4.1.5 Effect of volume of external phase..... | 75 |
| 4.2 Determination of factors and factor levels for optimization based on risk assessment approach..... | 78 |
| 4.3 DoE in microparticle preparation | 79 |
| 4.3.1 Particle size of DPH-loaded microparticles | 80 |
| 4.3.2 Q5 in SSF | 82 |
| 4.3.3 MDT in SGF..... | 85 |
| 4.3.4 Validation of mathematical model | 87 |
| 4.3.5 Optimization of DPH-loaded microparticles preparation | 88 |
| 4.4 Characterization of optimized DPH-loaded microparticles..... | 90 |
| 4.4.1 Residual solvent determination | 90 |
| 4.4.2 FTIR spectroscopy | 90 |
| 4.4.3 PXRD | 91 |
| 4.4.4 DSC | 92 |
| 4.5 Preparation and evaluation of ODTs | 93 |
| 4.5.1 Physical properties of ODTs | 93 |
| 4.5.2 Wetting test and <i>in vitro</i> disintegration test..... | 94 |
| 4.5.3 <i>In vitro</i> dissolution test | 96 |
| 4.5.4 <i>In vivo</i> evaluation | 98 |
| CHAPTER 5 Conclusion and future prospect | 100 |

REFERENCES 102
VITA..... 114



LIST OF TABLES

| | Page |
|--|-------------|
| Table 1 List of highly water-soluble and small molecules encapsulated by DESE.... | 33 |
| Table 2 Impact of formulation and operating factors on microparticles properties ... | 37 |
| Table 3 Alternative disintegration testing of ODTs..... | 41 |
| Table 4 List of factors and levels for BBD | 45 |
| Table 5 Formulation of blank ODT with total weight of 200 mg..... | 56 |
| Table 6 Formulation of ODT containing DPH or DPH-loaded microparticles | 57 |
| Table 7 Risk value of formulation factors and operating condition of microparticle preparation | 63 |
| Table 8 EE of microparticles prepared by different stirring times and AMC amounts | 74 |
| Table 9 EE of microparticles prepared by different volumes of external phase and AMC amounts | 78 |
| Table 10 Independent factors, level of each factor and responses in BBD of DPH-loaded microparticles preparation | 79 |
| Table 11 Summary of independent factors, level of factor, and responses in Box-Behnken design of DPH-loaded microparticles preparation | 80 |
| Table 12 ANOVA results of the fitted model for predicting Y_1 | 81 |
| Table 13 ANOVA results of the fitted model for predicting Y_2 | 83 |
| Table 14 ANOVA results of the fitted model for predicting Y_3 | 86 |
| Table 15 Comparison of the difference between actual and predicted value of responses | 87 |
| Table 16 Physical properties of blank ODTs | 93 |
| Table 17 Physical properties of ODTs containing taste-masked microparticles | 96 |

LIST OF FIGURES

| | Page |
|---|-------------|
| Figure 1 Chemical structure of DPH | 20 |
| Figure 2 Schematic of $W_1/O/W_2$, and $O_1/W/O_2$ emulsions | 28 |
| Figure 3 (a) schematic and (b)optical microscopic image of double emulsion droplets | 28 |
| Figure 4 Schematic illustration of $W_1/O/W_2$ emulsion preparation by two-step emulsification..... | 29 |
| Figure 5 Schematic of different membrane emulsification methods (adapted from Vladislavljević and coworkers (60)) | 30 |
| Figure 6 Schematic of double emulsion prepared by (a) microfluidic device consisted of an upstream cross junction connected to a downstream T-junction, and (b) a glass capillary device with double bore injection capillary (adapted Vladislavljević and coworkers (64)) | 31 |
| Figure 7 Diagram of CCD for three factors | 43 |
| Figure 8 Diagram of BBD for three factors | 44 |
| Figure 9 Schematic diagram showing the setup for wetting test | 58 |
| Figure 10 Schematic diagram showing the setup for in vitro disintegration test..... | 58 |
| Figure 11 Fishbone diagram of factors affecting the properties of DPH-loaded microparticles..... | 62 |
| Figure 12 Effect of pH of external water phase on EE of microparticles..... | 64 |
| Figure 13 Effect of ultrasonication time on double emulsion droplets size | 65 |
| Figure 14 Effect of ultrasonication time on size of microparticles..... | 65 |
| Figure 15 Optical microscopic images of emulsion droplets containing AMC amount of (a) 1, (b) 2, (c) 3, (d) 4, (e) 5, (f) 6, and (g) 7 g | 66 |
| Figure 16 SEM images (left) and microscopic images (right) of microparticles containing AMC amount of (a, b) 1, and (c, d) 7 g..... | 67 |
| Figure 17 SEM images showing surface morphology of microparticles containing AMC amount of (a) 1, (b) 2, (c) 3, (d) 4, (e) 5, (f) 6, and (g) 7 g | 68 |
| Figure 18 Size of microparticles prepared with different amounts of AMC | 68 |

| | |
|--|----|
| Figure 19 In vitro drug release profiles in SSF of DPH-loaded microparticles containing different amounts of AMC | 69 |
| Figure 20 Q ₅ in SSF of microparticles containing different amounts of AMC | 69 |
| Figure 21 Cumulative in vitro drug dissolution in SGF of microparticles containing different amounts of AMC | 70 |
| Figure 22 MDT in SGF of microparticles containing different amounts of AMC | 70 |
| Figure 23 Viscosity profiles of oil phase containing different amounts of AMC | 71 |
| Figure 24 Size of microparticles prepared by different stirring times | 72 |
| Figure 25 Q ₅ in SSF of microparticles prepared by different stirring times | 73 |
| Figure 26 MDT in SGF of microparticles prepared with different stirring times | 74 |
| Figure 27 Size of microparticles prepared with different volumes of external water phase | 75 |
| Figure 28 Q ₅ in SSF of microparticles prepared by different volumes of external water phase | 76 |
| Figure 29 MDT in SGF of microparticle prepared by different volumes of external water phase | 77 |
| Figure 30 Three-dimensional plot showing the effect of independent factors on size of microparticles | 82 |
| Figure 31 Three-dimensional plot showing the effect of independent factors on Q ₅ in SSF | 84 |
| Figure 32 In vitro drug dissolution profiles of standard run 5, 7, and 8 in (a) SSF, and (b) SGF | 84 |
| Figure 33 Three-dimensional plot showing the effect of independent factors on MDT of drug release in SGF | 86 |
| Figure 34 SEM images of (a) optimized microparticles and (a) its surface morphology | 89 |
| Figure 35 FTIR spectra of DPH, AMC, PVA, physical mixture, and optimized microparticles | 91 |
| Figure 36 Powder X-ray diffraction patterns of DPH, AMC, PVA, physical mixture, and optimized microparticles | 92 |
| Figure 37 DSC thermograms of (a) DPH, (b) AMC, (c) PVA, (d) physical mixture, and (e) optimized microparticles | 92 |
| Figure 38 Microscopic images of (a) DPH-ODT and (b) F12-ODT | 95 |

| | |
|--|----|
| Figure 39 Stages of wetting test of F10-ODT (with 4% sodium starch glycolate), F11-ODT (with 2% croscarmellose sodium), and F12-ODT (with 4% crospovidone) | 96 |
| Figure 40 In vitro drug dissolution profiles of native DPH, DPH-ODT, optimized microparticles, and F12-ODT in (a) SSF, and (b) SGF | 97 |
| Figure 41 VAS scores of (a) bitterness, (b) tablet handling, (c) grittiness, and (d) overall palatability | 99 |



CHAPTER 1

Introduction

Alzheimer's disease is an incurable progressive neurodegenerative disease combining with cognitive impairment. Patients may experience a slow decline in memory, problem-solving and other cognitive skills (1). Generally, Alzheimer's is a disease of elderly population. The number of people influenced by this disease is expected to rise to 152 million worldwide by 2050 (2). The prevalence continues to increase with age and influence 10% of people over the age of 65 years and about 50% of people over 85 years (3). The reduction of skeletal muscle mass and tissue elasticity with advanced aging results in diminished muscle strength and range of motion. In addition, the depletion of oral moisture, taste and smell acuity can also negatively influence the efficient swallowing of food through the upper gastrointestinal tract (4, 5). Therefore, swallowing disorders or dysphagia can be observed in this population. In addition, the neuropathological changes in Alzheimer's disease could also worsen the problem. The accumulation of beta-amyloid and tau protein, which are the hallmark lesions of the disease, causes the loss of neurons and synapses in brain cortex which involved in voluntary control of swallowing (6). Therefore, most patients exhibit a slow swallowing. Subsequently, they may encounter weight loss and increased feeding-tube dependency, leading to an increased risk of aspiration pneumonia, a major cause of death among this group (7). Swallowing difficulty is an important issue that should be considered at early stage of the oral dosage form development for Alzheimer's disease for patient. Nowadays, there is no effective medicine available to terminate or reverse the destruction of neurons. The available medicines only palliate the cognitive function. Promising medicines are in the class of cholinesterase inhibitors, including donepezil hydrochloride (DPH) that prevent the breakdown of acetyl choline.

To address the swallowing problem, orally disintegrating tablets (ODTs) have been developed. These tablets differ from conventional immediate release tablets in that they can be administered without taking of water. When the ODTs contact with the tongue, they rapidly disintegrate or dissolve and form suspension with the saliva, which easily swallow (8, 9). For DPH, the preparation of ODTs may be a useful resolution for

swallowing difficulties. However, a lasting bitter taste with numbness feeling of DPH may become an important issue. After ODTs completely disintegrate in oral cavity, the active drug and other components would likely produce unpleasant taste or grittiness feelings, which leads to poor patient compliance. Therefore, taste-masking may be a crucial prerequisite for DPH formulation.

In recent decades, several taste-masking techniques have been used to mask unpleasant taste of DPH. The simplest approach is organoleptic method. However, only this technique is inadequate for masking the taste of DPH (10, 11). The efficient approach may be the application of physical barrier by different techniques including polymer coating (12), solid dispersion (13), ion exchange resin complexation (14), inclusion complex formation (15), and microencapsulation (16). Among these taste-masking approaches, microencapsulation technique has gained much attention. It can be used to entrap active agent within a carrier to protect active agent against unfavorable environment, control release and also mask unpleasant taste. The selection of microencapsulation technique would provide sufficient drug encapsulation and effective taste masking. Since DPH is a hydrophilic drug, oil-in-water emulsion solvent evaporation technique which is generally used for drug encapsulation may not suitable because DPH may diffuse to the external water phase during preparation or may not dissolve in the internal oil phase. The water-in-oil-in-water (W/O/W) double emulsion solvent evaporation may be a useful choice to encapsulate DPH.

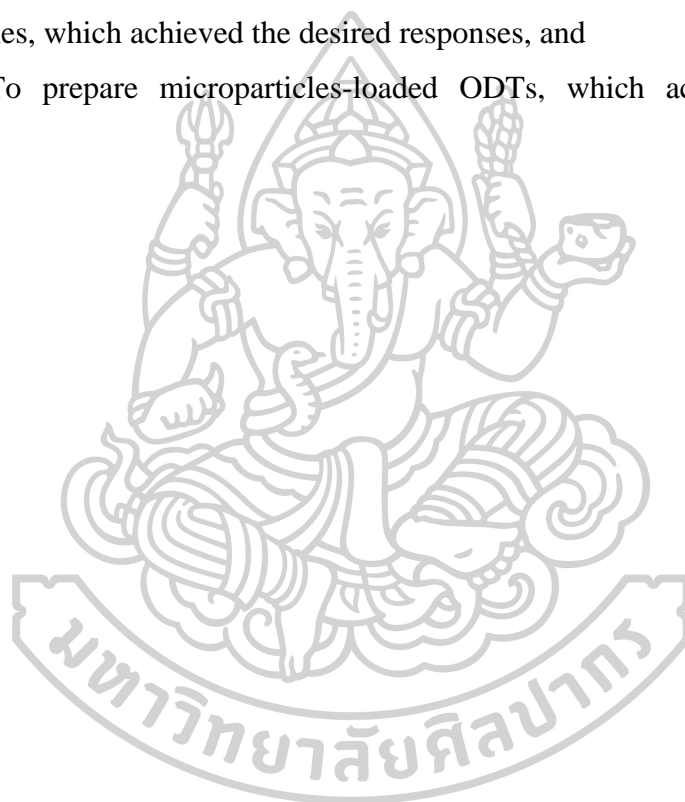
In this study, aminoalkyl methacrylate copolymer was used as an encapsulation polymer. It is soluble in gastric solution up to pH 5 but insoluble in neutral and alkaline solution above pH 5. It has potential to use as a taste-masked polymer by preventing drug release in the oral cavity at pH of around 7, thus releasing active drug rapidly in the stomach. Moreover, to maintain the stability of double emulsion during preparation, partially hydrolyzed polyvinyl alcohol was employed as a stabilizer of emulsion droplets.

Since double emulsion is a complex and thermodynamically unstable system, several factors could affect the properties of taste-masked microparticles including formulation factors, processing factors, and environmental factors (16-19). The experimental design may be a beneficial approach to investigate the effect and interaction between factors. It also reduce cost, time, and number required for

experimental investigation (19). Moreover, the optimized microparticles, which provide taste-masked microparticles with desired properties, can be obtained. The optimized microparticles can then be incorporated in ODTs. The effect of super-disintegrant on the disintegration time of ODTs can be investigated to obtain fast disintegrating tablets with suitable mechanical properties. Subsequently, ODTs properties can be evaluated by both *in vitro*, and *in vivo* testing.

The objectives of this study were:

1. To find the optimum process conditions for the preparation of taste-masked microparticles, which achieved the desired responses, and
2. To prepare microparticles-loaded ODTs, which achieved the desired properties.



CHAPTER 2

Literature review

- 2.1 Background of donepezil hydrochloride (DPH)
 - 2.1.1 Drug development history
 - 2.1.2 Physicochemical properties
 - 2.1.3 Dosing strategies
 - 2.1.4 Adverse event
- 2.2 The major challenges of DPH for dosage form development
 - 2.2.1 Bitter taste of DPH
 - 2.2.1.1 Taste-masking by organoleptic method
 - 2.2.1.2 Taste-masking by application of physical barrier
 - 2.2.2 Adverse event of DPH
- 2.3 Novel dosage forms and development technologies
 - 2.3.1 Oral drug administration
 - 2.3.2 Topical and transdermal drug administration
 - 2.3.3 Parenteral drug administration
 - 2.3.4 Nasal drug administration
- 2.4 Microencapsulation by double emulsion solvent evaporation technique for taste-masking of DPH
 - 2.4.1 Double emulsion
 - 2.4.1.1 Techniques to produce double emulsion
 - 2.4.1.1.1 Two-step emulsification
 - 2.4.1.1.2 Membrane emulsification
 - 2.4.1.1.3 Microfluidic method
 - 2.4.2 Double emulsion solvent evaporation technique (DESE)
 - 2.4.3 Commonly used polymers in DESE
 - 2.4.3.1 Biodegradable polymer
 - 2.4.3.2 Non-biodegradable polymer
 - 2.4.4 Factors affecting on microparticle preparation by DESE
- 2.5 ODTs

2.5.1 Techniques to produce ODTs

2.5.1.1 Compression technique

2.5.1.2 Lyophilization

2.5.1.3 Molding

2.5.1.4 Sublimation

2.5.1.5 Cotton candy process

2.5.2 Characterization of ODTs

2.6 Design of experiment (DoE) approach for optimization

2.6.1 DoE

2.6.2 Types of DoE

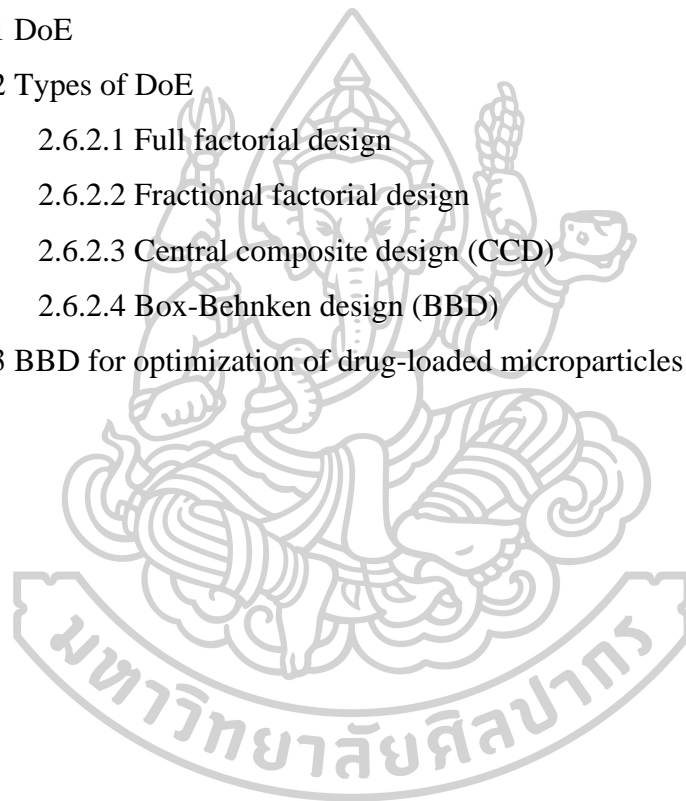
2.6.2.1 Full factorial design

2.6.2.2 Fractional factorial design

2.6.2.3 Central composite design (CCD)

2.6.2.4 Box-Behnken design (BBD)

2.6.3 BBD for optimization of drug-loaded microparticles



2.1 Background of donepezil hydrochloride (DPH)

2.1.1 Drug development history

DPH was first synthesized in 1983 by Eisai Co., Ltd. in order to solve the adverse event of physostigmine and tacrine, which is first generation cholinesterase inhibitors. It was developed based on the cholinergic hypothesis which hypothesize that the memory and cognitive dysfunction in Alzheimer's patient related to the deficiency of cholinergic innervation of forebrain (20, 21). In 1997, E2020 (or DPH) was successfully discovered, and launched in Atlanta. It prevents acetylcholine breakdown by selective inhibition of acetylcholinesterase over butyrylcholinesterase. DPH has been approved by USFDA to use in the treatment of mild, moderate, and severe stages Alzheimer's disease patients (1). Moreover, it improves the cognitive function without hepatotoxicity (22).

2.1.2 Physicochemical properties

DPH is a member of second generation cholinesterase inhibitors having N-benzylpiperidine and indanone group as illustrated in Fig. 1. The tertiary amine group has a high pK_a of 8.9. The molecular weight of DPH is 425.96 g/mol with log P of 4.27. It has high solubility in water of 55 g/L at 25°C and high permeability. In addition, it is freely soluble in chloroform, and acetic acid. The thermal analysis shows a melting point at approximate 224°C (23, 24).

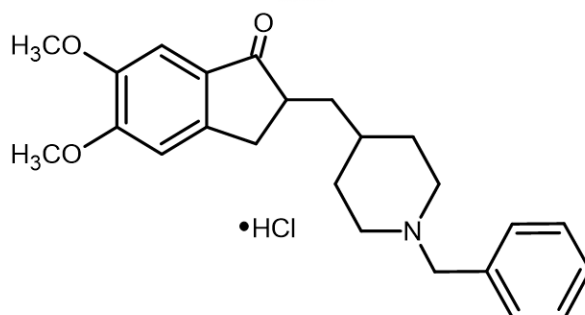


Figure 1 Chemical structure of DPH

Although DPH in the form of hydrochloride salt has been approved, donepezil free base form has also been used as an active drug among some research groups. In contrast to DPH, it is less water-soluble of 33 g/L at 25°C with the melting point of 85.6°C (25). It has bitter taste with numbness feeling on the tongue. Previous studies reported different bitterness thresholds of 15 to 20 µg/mL (12) and 150 µg/mL (26).

2.1.3 Dosing strategies

In mild to moderate Alzheimer's disease patients, DPH of 5 mg per day is a recommended starting dose. After maintaining for four to six weeks, it can be increased to 10 mg per day. For patients who have been on a stable dose of 10 mg for at least three months, a 23-mg sustained release tablet can be given after long-term safety and tolerability evaluation (27-29).

2.1.4 Adverse event

The adverse events of DPH are dose-dependent including nausea, diarrhea, insomnia, muscle cramps, fatigue, vomiting, and anorexia. Due to an increasing of cholinergic system activity, it also stimulates the movement of abdominal organs, and gastric fluid secretion. Subsequently, many patients who have been prescribed may have a risk of developing long-term adverse event such as peptic ulcer, or gastrointestinal bleeding (30, 31).

2.2 The major challenges of DPH for dosage form development

2.2.1 Bitter taste of DPH

A bitter taste of DPH may be a critical obstacle for dosage form development. In case of Aricept[®], an innovator product of DPH, carrageenan is used as a taste-masking agent. Since DPH is intermediate within helical form of hydrated carrageenan, its bitter taste is suppressed (28, 32). Moreover, there have been several attempts to mask bitter taste of such drug such as taste masking by organoleptic method, and application of physical barrier.

2.2.1.1 Taste-masking by organoleptic method

The unpleasant taste of drug substance can be easily masked by organoleptic method, which involved addition of sweeteners and flavors. This approach is the simplest and convenience for taste-masking since exclusive equipment and complex technique are less required. Regarding to study of Liew and coworkers (10), the bitter taste of DPH-loaded orodispersible film (ODF) was masked by addition of artificial sweeteners such as aspartame, sucralose, or saccharin sodium. Although the formulation consisted of sucralose, which was the sweetest substance of approximately 300- to 1,000-times sweeter than sucrose, received maximum score from the volunteers, a large amount of sucralose was added. Typically, less than 1% of these sweeteners are recommended as it may leave a distinct bitter aftertaste. In addition, a natural sweetener, ammonium glycyrrhizinate (30- to 50-times sweeter sucrose) was also investigated among this research group for taste-masking of ODT (11). Despite the bitter taste of DPH was successfully masked, the use of large quantities of sweetener may lead to an increasing of cost and manufacturing difficulties.

2.2.1.2 Taste-masking by application of physical barrier

The application of physical barrier may be an efficient approach to mask the unpleasant taste, as it prevents the contact of active substance and taste receptor, thus blocking taste signal transduction (33, 34). Several technique used including polymer coating, solid dispersion, ion exchange resin complexation, inclusion complex formation, and microencapsulation.

According to the research work of Yan and coworkers, AMC (Eudragit E), a pH-responsive polymer, was used as a spray-dried polymer to prepare DPH-loaded microspheres. Depending on the solubility of AMC, which insoluble but swellable above pH 5, it was a great choice to prevent DPH release in saliva at the pH of around 7. By comparing with the bitterness threshold, the result demonstrated that bitter taste was successfully masked. However, it should be remarked that the taste suppression was resulted from the synergistic effecting between polymer and aspartame (180- to 200-times sweeter than sucrose) of 1% (12). Regarding to the study of Han and coworkers, the bitter taste of DPH was masked by incorporating it in ODF containing hydroxypropyl methylcellulose and hydroxypropyl cellulose at the ratio of 5: 1. The

result showed that the optimized film received good score from the volunteers (13). Since a large amount of sucralose of 12% was added, it should be noted that the taste-masking effect may associate with combination result of polymer and sweeteners.

Ion exchange resin complexation can also use for taste masking. It is a high molecular weight polymer, which capable of exchanging anion or cation. The formation of opposite charged drug-resin complex or so called resinates, which does not breakup in oral cavity but completely release drug in gastrointestinal tract, offers potential benefits for unpleasant taste-masking (33, 35). Based on the study of Kim and coworkers, a spray-drying technique was used to prepare DPH-Amberlite IRP-64 complex with the purpose to mask bitter taste of active drug. The *in vitro* taste evaluation using electronic taste sensor system showed a large Euclidean distance to DPH, indicating a great reduction of bitter taste. However, *in vivo* taste evaluation showed that the bitterness index was higher than bitterness threshold of DPH, indicating that the unpleasant taste was not completely masked (14).

Next technique is inclusion complex formation. Among several complexing agent, beta-cyclodextrin has earned much attention from researchers. The formation of drug-cyclodextrin complex can be employed for taste-masking purpose as it decreases the exposure of drug molecule to taste bud, thus preventing unpleasant taste sensation. The native cyclodextrin, on the other hands, has some limitations including a facile separation of complex upon dilution and appropriate size requirement of active molecule (34). So, various modified cyclodextrins has been continuously developed. Such technique was used by Liu and coworkers to mask the bitter taste of DPH. The complex of DPH and hydroxypropyl-beta-cyclodextrin prepared with liquid-liquid solvent extraction method. Then, the complex was incorporated in ODF. The *in vitro* taste evaluation result showed that Euclidean distance of optimized product was greater than other sample, demonstrating successful taste-masking (15).

Among several techniques for providing physical barrier, microencapsulation technique has received much attention. It is a method in which an active substance is coated by specialized polymers to make small particles in micrometer size range. The coating act as a physical barrier to the active substances, so minimizing interaction between active substance and taste cells. The active molecules can be encapsulated by three different groups including chemical, physical, and physico-chemical process. In

pharmaceutical industry, microencapsulation by emulsification solvent evaporation is widely used (16).

2.2.2 Adverse event of DPH

As DPH is a cholinesterase inhibitor, the enhancement of cholinergic nervous system resulted in an increasing of stomach and intestinal mobility, gastric fluid secretion. It may cause peptic ulcer and/or gastrointestinal bleeding, which should be carefully monitored (30, 31). While using the highest strength, the occurrence of this adverse effect increased by around 2-fold. It is correlated with the fluctuation of DPH plasma concentration levels, the gradual dose titration within four to six weeks is therefore recommended to allow patients to adapt to the pharmacodynamic effect of DPH. Additionally, it is believed that the gastrointestinal adverse event is associated with a rapid activation of the cholinergic system as a result of the drug's rapid absorption. Co-administration of food can help by delaying the onset of drug concentration (36, 37).

Recently, various novel dosage forms have been developed to overcome the gastrointestinal adverse events of DPH. It can be classified by the route of administration including oral, topical, parenteral, and nasal route.

2.3 Novel dosage forms and development technologies

2.3.1 Oral drug administration

To reduce the gastrointestinal adverse event following oral administration, the smectite clays with acid absorption capacity were used to intercalated DPH. The hybrid was then coated by spray drying with aminoalkyl methacrylate copolymer (Eudragit E) in order to modify drug release. The fast drug release was obtained from all hybrids. Therefore, they hypothesized that such hybrid can be used to overcome the adverse event of DPH. However, the gastric acid reduction capacity of new hybrid was not characterized in this study (38). In another study, donepezil free base form (DPB)-loaded lyotropic liquid crystalline mesophases were developed by mixing glyceryl monooleate, DPB-oleic acid solution, and water. The mesophases overcome gastrointestinal problem by maintaining consistent drug concentration level over 24 h,

as observed in drug release testing. Therefore, the authors concluded that such formulation may be used to improve gastrointestinal adverse event of DPH (25).

2.3.2 Topical and transdermal drug administration

The topical and transdermal drug administration provide various benefits over other routes including circumvent of first fast metabolism, non-invasive, and convenience for self-administration. Especially, it also offers more uniform drug level, thus minimizing gastrointestinal adverse event of DPH. However, the main obstacle for such route is poor permeation because the stratum corneum, the outermost layer of the skin, acts as a barrier. Moreover, the hydrophilic property of DPH may be another limitation. This route has gained a significant interest from Teikolu Pharma Inc., (USA) and Eisai Co. Ltd., the originator of Aricept. The licensing application of Aricept transdermal patches for once-weekly administration was submitted to the US FDA in 2010. However, it was withdrawn in 2012 (39).

Recently, donepezil transdermal patches were developed by Icure Pharmaceutical Inc. (South Korea). It has been tested in phase III clinical trial, comparing the efficacy and safety of the patches and Aricept tablets in mild to moderate AD patients (40).

In addition, several studies have also been conducted to overcome these limitations. The most popular technique to enhance skin permeation is addition of penetration enhancer to the transdermal patches or film i.e., stearic acid, palmitic acid, oleic acid, palmitoleic acid (41), *dl*-limonene (42), and lecithin (43).

In another study, DPH was transformed to ionic liquid in order to disrupt cell membrane integrity after application on skin, thus facilitating drug permeation (44). DPH delivery by iontophoretic technique was also investigated using wearable electronic drug delivery patches. The *in vivo* test across abdominal region of rats showed that an increasing of current density increased plasma drug level (45).

To circumvent the limitation of stratum corneum, DPH was loaded in the tips of microneedle prepared by different concentrations of hydroxypropyl methyl cellulose using micro-molding technique. The authors suggested that their microneedles provided high C_{max} of over four folds comparing to that of oral administration (46). The DPH-loaded hydrogel-forming microneedle films were prepared by blending of

Gantrez S-97, polyethylene glycol, and sodium carbonate (47). After microneedle puncture, which can bypass stratum corneum, DPH was directly delivered to the underlying microcirculation. Therefore, high plasma drug level was obtained from pharmacokinetic test in these studies. Although various drug delivery systems have been developed to deliver DPH or DPB across the skin, the ability of these product to overcome the gastrointestinal adverse event were not clearly elucidated.

2.3.3 Parenteral drug administration

DPH was directly delivered to the systemic by some research group. The injectable DPH-loaded poly (d,l-lactic-co-glycolic acid) microspheres were prepared in order to sustain drug release by emulsion solvent evaporation. Drug release testing results showed a sustained drug release of over 80% over 10 days. In this study, DPH was then modified to DPB in order to control drug release. The DPB microspheres demonstrated sustained drug release of 90% over 42 days (48). Although gastrointestinal adverse event was raised as the main objective of the study, this point was not directly evaluated. In addition, the compliance of the product may be questionable because of the subcutaneous injection of microspheres, which is an invasive route.

2.3.4 Nasal drug administration

Regarding previous routes, DPH was delivered through oral, transdermal, or parenteral administration. The drug molecule is supposed to deliver to the brain through systemic circulation. In case of nose-to-brain drug delivery, the drug molecule is directly delivered through neuronal route. This route has multiple advantages compared with others including patient convenience, blood brain barrier (BBB) circumvention, avoiding first-pass metabolism, increasing patient compliance, and rapid achievement of therapeutic drug level. The therapeutic efficacy of DPH is influenced not only by a decreasing of drug concentration in the brain due to the presence of the BBB, but also by its low brain permeability. After passing to posterior region of nasal cavity, drug molecule will contact to respiratory and olfactory region and deliver to the brain by the following pathway: olfactory nerve, trigeminal nerve, lymphatic, vestibular, and cerebrospinal fluid. Among these pathways, olfactory nerve and trigeminal nerve are

major pathways. Moreover, drug molecules can be absorbed through nasal blood vessels to enter the systemic circulation. These drugs, especially small, and lipophilic molecule, access the brain region by crossing BBB. Regarding the nasal route, the mucociliary clearance in vestibular region while drug molecule enters to nasal cavity and enzymatic degradation may be the main limitations for this route of administration (49-51). Therefore, various drug delivery systems, especially nanotechnology-based, have been developed.

Comparing to DPH, DPB has received more attention to use as an active molecule among several research group because of its lipophilicity and compatibility with lipid excipient. For example, DPB-loaded chitosan nano-suspension (52), DPB-loaded liposome (53), and DPB-loaded solid lipid nanoparticles (54). The *in vitro* drug release test and/or *in vivo* test results of these formulations showed an improvement of drug release and/or pharmacokinetic parameters.

In addition, the nanotechnology-based drug delivery system was used in combination with the permeation enhancer i.e., butter oil and omega-3 fatty acid to prepare DPH microemulsions for intranasal administration. The *in vivo* pharmacokinetic study showed higher drug extent comparing to the control group, suggesting a promising approach for nose-to-brain drug delivery (55). In another study, ligand-based approach was also used along with solid lipid nanoparticles for intranasal DPB administration. Apolipoprotein E, a ligand of lipoprotein receptor on BBB, was targeted on solid lipid nanoparticles. The results showed that DPB cellular uptake was increased in a cell line and co-culture BBB model (56). These findings suggested a promising approach to overcome the limitations of BBB.

2.4 Microencapsulation by double emulsion solvent evaporation technique for taste-masking of DPH

2.4.1 Double emulsion

Double emulsion is the simplest type of multiple emulsion, also known as emulsion of emulsion which the droplets of dispersed phase consist of small droplets of different phases inside them (18). Typically, double emulsion droplets prepared by conventional method have a broad size distribution. There are two main types of double

emulsions which demonstrated in Fig. 2 i.e., water-in-oil-in-water ($W_1/O/W_2$), and oil-in-water-in-oil ($O_1/W/O_2$).

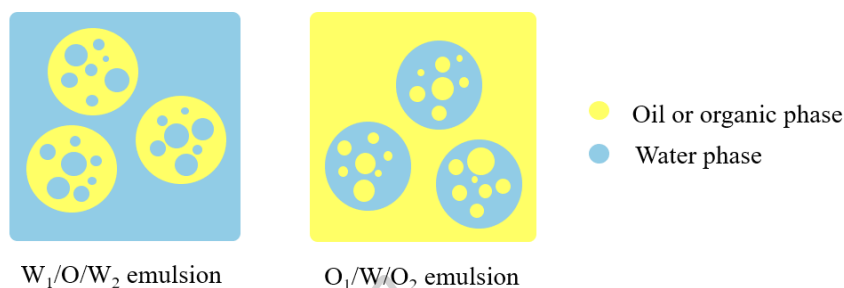


Figure 2 Schematic of $W_1/O/W_2$, and $O_1/W/O_2$ emulsions

Each double emulsion droplet may contain few small emulsion droplets, or over 100 emulsion droplets. They can be classified to three different types according to internal droplets arrangement as illustrated in Fig. 3. The small double emulsion droplet consisting of few or only one single internal droplet is observed in type A arrangement. While type B demonstrated larger double emulsion droplet consisting of several small internal droplets. The complicated arrangement is observed in type C droplet which consist of several large internal emulsion droplets. Due to high internal content of type C droplet, it has the potential to serve as an entrapment device which control the release of active component in the internal phase or polymer matrix (16).

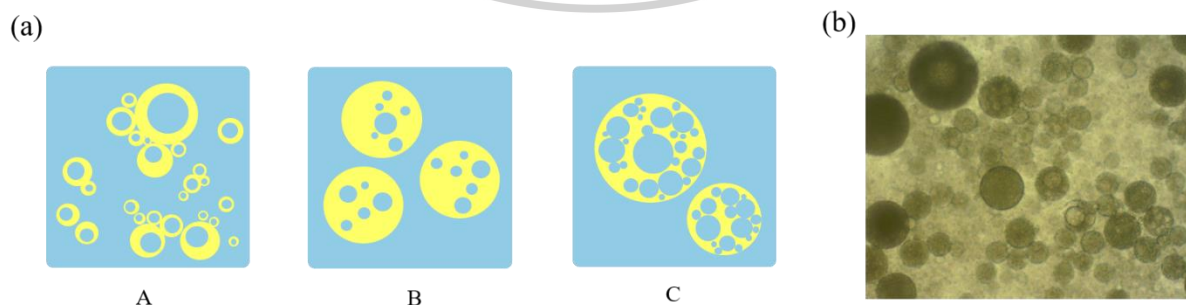


Figure 3 (a) schematic and (b) optical microscopic image of double emulsion droplets

2.4.1.1 Techniques to produce double emulsion

Double emulsion can be prepared by three different techniques such as two-step emulsification, membrane emulsification, or microfluidic method. This study would mainly focus on W/O/W double emulsion preparation.

2.4.1.1.1 Two-step emulsification

Two-step emulsification is the conventional method to produce double emulsion, comprising of two steps: preparation of primary emulsion, and preparation of double emulsion. To prepare $W_1/O/W_2$ emulsion, the internal water phase containing hydrophilic drug, and organic phase containing polymer or hydrophobic drug are first prepared separately as illustrated in Fig. 4. After that, both phases are vigorously mixed using homogenizing device. Due to the small volume of internal water phase comparing with that of oil phase, the primary W/O emulsion is prepared. In some case, a hydrophobic stabilizer or gelling agent can be added to stabilize or adjust the viscosity of internal phase (57, 58). Secondly, the primary emulsion is dispersed in external water phase containing hydrophilic stabilizer for breaking it into small droplets, $W_1/O/W_2$ double emulsion is obtained (17, 59). While droplet size uniformity can be neglected, this method offers benefit in food and cosmetic industries as it is very convenience for large-scale production (60).

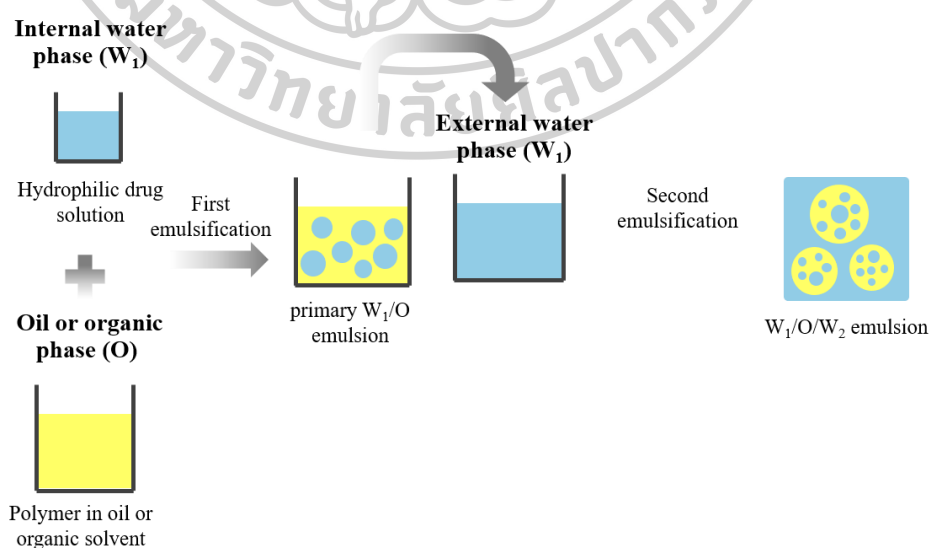


Figure 4 Schematic illustration of $W_1/O/W_2$ emulsion preparation by two-step emulsification

2.4.1.1.2 Membrane emulsification

To address the broad size distribution problem of double emulsion prepared by two-step emulsification technique, uniform-sized emulsion can be prepared using membrane emulsification. The first membrane is developed by Nakashima and coworkers (61) in the 1980s, namely Shirasu porous glass membrane, which is a microporous membrane with uniform size distribution. In addition to Shirasu porous glass membrane, several types of membrane materials, i.e., ceramic, metallic, and polymer with different pores size, and surface affinity are available in the market (59, 61).

This method can be classified to three different methods: conventional direct membrane emulsification, and premix membrane emulsification as shown in Fig. 5. Using direct membrane emulsification method, a pure liquid is used as dispersed phase, after pressuring through porous membrane, the fine simple emulsion droplets are formed at the interface of membrane and continuous phase. The shear stress generated by flowing, recirculating, or vibration of continuous phase ensures the detachment of droplet from the membrane. In case the coarse emulsion is used, it can be considered as premix membrane emulsification (60, 62).

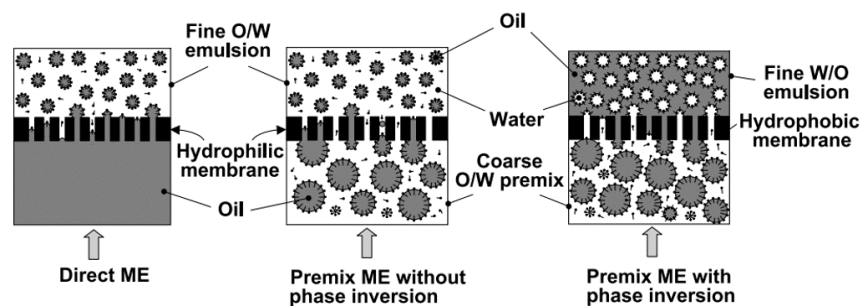


Figure 5 Schematic of different membrane emulsification methods (adapted from Vladisljević and coworkers (60))

Comparing to two-step emulsification, membrane emulsification can generate a uniform-sized emulsion with controllable size by selecting membrane pore size. In addition, since the emulsion is prepared under mild condition, low shear force is required to prepare emulsion (62).

2.4.1.1.3 Microfluidic method

Microfluidic devices allow efficient preparation of complex emulsion with low size distribution and almost 100% encapsulation efficiency (EE). Typically, microfluidic devices are classified into two main types: two-dimensional, and coaxial assemblies of glass capillaries microfluidic device. The channel surface of these devices is first treated with some treatments to modify its wettability (hydrophobicity or hydrophilicity). To prepare double emulsion by this method, as shown in Fig. 6, the droplet formation occurs in the device by different modes such as dripping, jetting, or squeezing. After the droplet formed at upstream junction, it is then carried and enclosed to double emulsion droplet at the downstream junction. Size, and number of enclosed droplets can be precisely controlled by adjusting viscosity, phase flow rate, junction distance, rate of droplet generation, etc. (59, 63, 64).

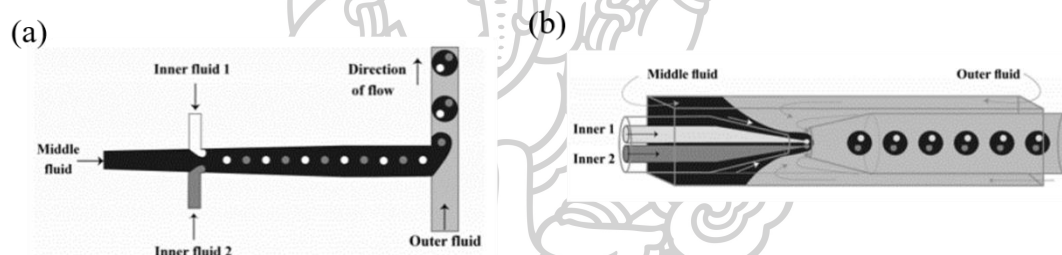


Figure 6 Schematic of double emulsion prepared by (a) microfluidic device consisted of an upstream cross junction connected to a downstream T-junction, and (b) a glass capillary device with double bore injection capillary (adapted Vladislavjević and coworkers (64))

2.4.2 Double emulsion solvent evaporation technique (DESE)

Non-aqueous double emulsion droplets are always an intermediate material, which can be transformed to solid particles after polymerization or solvent removal. The combination of double emulsion and solvent evaporation technique was initially adopted for encapsulation active substance (65-67). After double emulsion is prepared by traditional two-step emulsification, the solvent evaporation is carried out, leading to a hardening of solid particles. The solvent can be evaporated by mechanical stirring at

room temperature, or it can be accelerated under low pressure condition using vacuum oven, freeze dryer, or rotary evaporator.

Several studies demonstrated that both hydrophobic and hydrophilic drugs can be encapsulated by this technique. However, hydrophobic drug is frequently encapsulated by single W/O or O/O emulsion solvent evaporation techniques, which is easy and less complex. Since hydrophilic drug fails to encapsulate by single emulsion as it may be expelled from hydrophobic polymer during preparation step, DESE is often used to encapsulate hydrophilic drug (16, 17). Table 1 demonstrates the list of highly water-soluble and small molecules encapsulating by this technique.



Table 1 List of highly water-soluble and small molecules encapsulated by DESE

| Active molecule | Emulsion type | Production technique | Polymer used | Organic solvent | Stabilizer | Objective | Reference |
|--|----------------------------------|-------------------------|-------------------------------------|--------------------|----------------------------|--|-----------|
| Pseudoephedrine hydrochloride | W ₁ /O/W ₂ | Two-step emulsification | Poly (methyl methacrylate) | Methylene chloride | PVA | To investigate the effect of process and formulation factors on drug-loaded microspheres prepared by DESE | (65) |
| Brilliant blue | W ₁ /O/W ₂ | Two-step emulsification | Poly(lactic acid) | Methylene chloride | PVA | To investigate DESE and improve entrapment efficiency of soluble dyes | (67) |
| Propranolol hydrochloride and nifedipine | W ₁ /O/W ₂ | Two-step emulsification | Eudragit RS: RL | Methylene chloride | PVA | To co-encapsulate propranolol hydrochloride and nifedipine within mom-biodegradable polymer and study drug release kinetics | (68) |
| Levobunolol hydrochloride | W ₁ /O/W ₂ | Two-step emulsification | Polycaprolactone | Methylene chloride | PVA or Poloxamer188 | To investigate the effect of process and formulation factors on drug-loaded microparticles prepared by DESE | (69) |
| Alendronate sodium | W ₁ /O/W ₂ | Two-step emulsification | PLGA and Pluronic F68 | Ethyl acetate | CaCl ₂ solution | To investigate the effect of process and formulation factors on drug-loaded microparticles prepared by DESE | (70) |
| Trimebutine maleate | W ₁ /O/W ₂ | Two-step emulsification | Polyvinylacetal diethylaminoacetate | Methylene chloride | PVA | To mask bitter taste of trimebutine maleate by encapsulation in microspheres | (71) |
| Doxorubicin hydrochloride | W ₁ /O/W ₂ | Two-step emulsification | PLGA | Methylene chloride | PVA | To develop doxorubicin-PEGylated TNF-related apoptosis inducing-ligand-loaded microspheres for sustained release drug delivery | (72) |
| Clonidine hydrochloride | W ₁ /O/W ₂ | Two-step emulsification | PLGA | Methylene chloride | PVA | To prepare drug-loaded microparticles with controlled release property of over 4-6 weeks | (73) |
| Sildenafil citrate | W ₁ /O/W ₂ | Two-step emulsification | PLGA | Methylene chloride | PVA | To investigate and optimize process and formulation factors on drug-loaded microparticles prepared by DESE | (74) |
| Metformin hydrochloride | W ₁ /O/W ₂ | Two-step emulsification | PLA | Methylene chloride | PVA | To investigate and optimize process and formulation factors on drug-loaded microparticles prepared by DESE | (75) |

Key: W/O/W: water-in-oil-in-water emulsion, PVA: polyvinyl alcohol, PLGA: Poly (lactic-co-glycolic-acid), DESE: double emulsion solvent evaporation technique

2.4.3 Commonly used polymers in DESE

There are two groups of polymers, which have been used for drug encapsulation including biodegradable polymer, and polymethacrylate copolymer.

2.4.3.1 Biodegradable polymer

Biodegradable polymer can be degraded into non-toxic components and release active molecules. It is a synthetic homo- or copolymer consisting of different proportions of lactic acid, glycolic acid, lactide, glycolide and ϵ -hydroxycaproic acid. Several polymers have been investigated for drug encapsulation by DESE in recent years such as poly (L-lactic acid) (PLA), poly (lactic-co-glycolic acid) (PLGA), and polycaprolactone (PCL).

PLA is approved by the USFDA for human use as it is biodegradable, compatible, and less toxicity. Its properties such as crystallinity, or hydrophilicity can be modified by preparing copolymer, interacting other monomer, or modification of functional group. These modifications significantly affect to drug release, permeability, and degradation rate of encapsulated drug.

PLGA is another type of biodegradable polymer which commonly used for drug encapsulation by double emulsion technique. It has also been approved for human use by USFDA. This polymer is gradually degraded through hydrolysis reaction, producing lactic acid, and glycolic acid which are non-toxic metabolites. The degradation interval depends on the proportion of components.

PCL is also biodegradable and biocompatible polymer with low melting point and glass transition temperature. Due to a slow degradation rate, it is suitable for developing sustained release dosage form. After degradation, its metabolites can be eliminated by congenital metabolic system (16, 76).

2.4.3.2 Non-biodegradable polymer

Non-biodegradable polymers with biocompatible property are also used as a carrier for drug encapsulation, such as ethyl cellulose, and polymethacrylate copolymer (77).

Ethyl cellulose is non-biodegradable and biocompatible polymer. It is gastric fluid-resistance polymer, which is suitable for duodenal or colonic delivery, and prolonged release drug delivery.

The polymethacrylate copolymer groups (Eudragit[®]) can be prepared by reacting methacrylic acid with acrylic ester in different proportions. It consists of anion or cation. Typically, it has high molecular weight of over 10,000 g/mol. It frequently used as a film-former or matrix carrier. The dissolution and permeability of aminoalkyl methacrylate copolymer (Eudragit[®] E), methacrylic acid copolymer type A (Eudragit[®] L), and type B (Eudragit[®] S) are pH-dependent. While ammonio methacrylate copolymer type A (Eudragit[®] RL), type B (Eudragit[®] RS), ethyl acrylate and methyl methacrylate copolymer (Eudragit[®] NE) are pH-independent.

Aminoalkyl methacrylate copolymer is a cationic polymer. It is soluble in gastric fluid or weak acid buffer solution up to pH 5. However, it is swellable and permeable above pH 5. It is light yellow color powder with amine odor. It is usually used as a film coating polymer for taste and odor-masking and moisture protection of immediate release formulations (76, 78).

Methacrylic acid copolymer is synthesized from methacrylic acid and methyl methacrylate. The ratio of free carboxylic to ester group is 1: 1, and 1: 2 for Eudragit[®] L, and S, respectively. These polymers are soluble in neutral pH (pH 6 to 7). It forms salt with alkali, creating gastric acid resistance film. However, it soluble in intestinal fluid. It is applied as an enteric coating polymer.

Ammonio methacrylate copolymer is a product of the polymerization between acrylic acid and methacrylic acid esters. These polymers are water-insoluble. The ammonium groups are responsible for the permeability of polymer. The percentage of these groups in Eudragit[®] RL, and RS is 10%, and 5%, respectively. Eudragit[®] RL is highly water permeability while Eudragit[®] RS is less water permeability. The film prepared from these polymers are usually used for sustained release formulations.

Methyl methacrylate copolymer is synthesized from polymethacrylic acid esters. It is available as aqueous dispersion of 30%, and 40% for Eudragit[®] NE 30 D, 40 D, respectively. The film is insoluble but swellable and permeable in water. These polymers are used as a film coating for sustained release formulations (76).

2.4.4 Factors affecting on microparticle preparation by DESE

In order to prepare microparticles for encapsulation of highly water-soluble and small molecules by DESE, there are several factors affecting on particle size, EE, and drug release. The impact of formulation and operating factors on these properties is demonstrated in Table 2.



Table 2 Impact of formulation and operating factors on microparticles properties

| Factors | Microparticles properties (reference) | |
|--|--|--|
| | Particle size | EE |
| Formulation factors: | | |
| Increase of drug amount | Bigger diameter (75) | Increased (65, 69) |
| Decrease of drug to polymer ratio | Bigger diameter (74) | N/A |
| Increase of organic solvent amount | N/A | Increased (65) |
| Increase of polymer amount | Bigger diameter (70, 73, 79) | Increased (65, 73) |
| Increase of polymer molecular weight | Increase (73) | Increased (73) |
| Increase of stabilizer concentration in external phase (W ₂) | Smaller (65, 75) or bigger diameter (69, 75) | Increased (65, 69) or no impact (70, 74, 75) |
| Increase of pH of external water phase (W ₂) | Bigger (71) or smaller diameter (75) | Decreased (65, 69) or increased (68, 71, 73, 75) |
| Increase of volume of internal phase (W ₁) | Smaller diameter (73) | Decreased (65, 73) or no impact (71) |
| Increase of volume of oil phase (O) | Bigger diameter (73) | Increased (73) |
| Increase of volume of external water phase (W ₂) | Smaller diameter (69) | Decreased (65, 68, 69) or increased (71) |
| Increase of water to solvent ratio in primary emulsion | Bigger diameter (74) | Increased or decreased (74) |
| Addition of electrolytes to external water phase (W ₂) | N/A | Increased (65) or decreased (70) |
| Operating factors: | | |
| Increase of stirring time in the first emulsification | Smaller diameter (73) | N/A |
| Increase of ultrasonication time in the first emulsification | Smaller diameter (79) | N/A |
| Increase of stirring time in the second emulsification | Smaller diameter (73, 79) | Decreased (65) |
| Increase of stirring rate in the second emulsification | Bigger or smaller diameter (75) | Decreased (75) |
| Increase of ultrasonication time in the second emulsification | Smaller diameter (70) | N/A |
| Drug dissolution | | |
| No impact (73) | | |
| Decreased (74) | | |
| N/A | | |
| Decreased (73) | | |
| Decreased (73) | | |
| Decreased (69, 74) | | |
| N/A | | |
| Increased (65) | | |
| N/A | | |
| Increased (71) | | |
| Increased or decreased (74) | | |
| N/A | | |

Key: W₁/O: water-in-oil emulsion, N/A: not available

2.5 ODTs

ODT is a subtype of orally dispersible formulation, which rapidly disintegrate or dissolve after placing on the tongue. Initially, this dosage form was designed to facilitate the administration in pediatric and geriatric patient, or patients with swallowing difficulties. In addition, the convenience use of such dosage form would improve patient compliance of the treatment. As demonstrated in recent study (80), ODTs received a well acceptability among the children and older adult groups.

2.5.1 Techniques to produce ODTs

Various methods are employed to prepare ODTs including compression, lyophilization, molding, sublimation, mass extrusion, cotton candy process, and others.

2.5.1.1 Compression technique

Compression method is a conventional technique to prepare tablets. This involves only two simple steps: ingredient blending and tableting. Since it provides adequate tablet strength for handling and almost no special equipment is required for the production, there is a growing interest in the utilization of such technique. To achieve rapid disintegration, type and amount of super-disintegrant may be carefully determined. In addition, the effervescent agent can be added to accelerate the tablet disintegration. Examples of patented technologies based on this technique include OraSolv[®] (with effervescent agent), Durasolv[®] (with or without effervescent agent), and Flashtab[®] (combination of dry and wet granulation before tableting) (9, 81).

2.5.1.2 Lyophilization

Lyophilization technique offers an efficient way to increase the porosity of final ODTs enabling rapid disintegration. The mixture of active compound and excipients in form of aqueous solution, suspension, or emulsion of actives are poured into blister packs, and then passed through a freezing process. Such technique can provide an ultra-fast disintegration time with great mouthfeel. It is useful for heat sensitive actives. However, it is an expensive and time consume technique, and requires a special handling and package owing to the fragility of final product. Presently, there are three

patented technologies based on lyophilization technique comprising of Zydis[®], Lyoc[®], and Quicksolv[®] (9, 81).

2.5.1.3 Molding

There are two approaches to produce ODTs by molding technique, including compression molding and heat molding. The compression molding is a simple method, which the blend of actives and excipients moisten by hydro-alcoholic solvent before air drying. The mass is then compressed in the mold with low force, resulting in porous and less compact final product enhancing rapid disintegration. The patented production technology based on compression molding is WOWtab[®].

In comparison to heat molding, the molten mass of actives with water soluble sugars and agar is first prepared before pouring into a mold. The mixture is allowed to solidify under room temperature and dry at low temperature under vacuum condition. Despite, this technique is convenience for large scale production, the molded ODTs have poor mechanical properties. Hence, some additives are frequently added to improve this property such as acacia, polyvinylpyrrolidone, and polyethylene glycol (81, 82).

2.5.1.4 Sublimation

The disintegration time of ODTs prepared by sublimation method is enhanced by the formation of numerous pores within tablets. The volatile substances, such as urea, camphor, ammonium carbonate, benzoic acid, hexamethonium tetramine, etc., are incorporated in the formulation and tableted. After that, these substances are removed by sublimation, which creates a porous structure shortening tablet disintegration time (9, 82).

2.5.1.5 Cotton candy process

Cotton candy process is also known as floss formation technique involving polysaccharides matrix formation by flash melting and spinning. The resultant product is cotton candy-like fiber, which is blended with actives and excipient and compressed to ODTs. Although the mechanical strength of ODTs may be improved by the recrystallization of cotton candy matrix, this technique is inappropriate for heat-labile

actives. Flashdose[®] is an example of patented technology according to cotton candy process (82).

2.5.2 Characterization of ODTs

The standard test, i.e., tablet hardness, and friability, can be performed as specified in pharmacopoeias. However, there is some special concerns relevant to the disintegration test of ODTs. Regarding to the European Pharmacopoeia, drug product can be labeled as ODTs when it disintegrates in water within 3 min based on *in vitro* disintegration test. USFDA Guidance for Industry recommends disintegration time limit of less than 30 s for ODTs, which closely relevant to the real condition. The disintegration testing is recommended to carry out based on the pharmacopoeia or alternative test that provide an equivalent result to that of compendial method (8, 9). However, the test conducted in 900-mL purified water under vigorous agitation, which aids disintegration, may be unable to simulate *in vivo* condition properly. Since it has been reported that the volume of saliva in oral cavity is in the range of 0.09 – 1.86 mL. The average secretion rate of saliva at rest is 0.5 mL/min; it can be increased to 2 mL/min during stimulation (83-85). Therefore, several alternative disintegration test methods have been proposed to simulate the oral cavity conditions.

Wetting test can be used as a screening tool for ODTs development. It can be performed by placing the ODT on the wetted filter paper or folded tissue paper. Time required for the ODT to disintegrate into small particles is noted as wetting time; a lower wetting time implies a quicker disintegration of the ODTs (86). Park and coworkers (87) proposed a modified version of this test using a circular filter paper and testing in 12-well polystyrene plate. The volume of dye solution added depends on ODT weight. Time required for the dye solution to diffuse and cover the surface of ODT is defined as a simulated wetting time. Moreover, alternative disintegration methods in Table 3 have been developed in recent years to determine the disintegration time of ODTs.

Table 3 Alternative disintegration testing of ODTs

| Apparatus | Test condition | Disintegration time | Reference |
|---------------------------------------|--|---|-----------|
| Modified USP dissolution apparatus II | The test is operated in 900-mL dissolution medium with paddle speed of 100 rpm. | Time required for the ODT to pass through a sinker screen | (88) |
| Charge coupled device (CCD) camera | The ODT is placed on a stainless-steel grid over disintegration medium tank. | Disintegration time monitored by a CCD camera. | (89) |
| Shaking bath | The ODT is placed in glass cylinder with a mesh screen. Then, it is placed in a shaking bath. | Time required for the ODT to pass through a mesh screen | (90) |
| Rotary shaft | The ODT is placed on a wire gauze and immersed in the medium. It is then compressed by a rotary shaft. | Time required for the ODT to completely disintegrate | (91) |
| Texture analyzer | The ODT is attached to the probe. Then, the probe is lowered and immersed in medium. | Time required for the ODT to completely disintegrate | (92) |

2.6 Design of experiment (DoE) approach for optimization

2.6.1 DoE

DoE is a statistical approach to determine the relationship between factors affecting processes and responses. Traditionally, one factor at a time (OFAT) approach is used to study the effect of each factor by varying one factor while others are kept constant. However, there are a number of factors as specified above; so, it is impossible to investigate all factors in one experiment. Additionally, with OFAT approach, the interactions between related factors are not considered and optimum condition cannot be determined. Therefore, to address these obstacles, DoE approach may be adopted. It provides multiple advantages over OFAT approach as it can be used to determine the effect of each factor on the responses, improve a yield and minimize variability of the experiment. Initially, the screening experiment should be performed to investigate whether the factor has an effect to the response or not. Moreover, the direction of relationship between factor and response can also be obtained. After that, the obtained data is used for optimization in the second step in order to determine optimum condition (19).

2.6.2 Types of DoE

2.6.2.1 Full factorial design

In full factorial design, the experimental condition can be formed by systematically varying the level of at least two factors and all possible combinations of the level of factor. So, it is called crossed factor DoE. Not only the main factors are investigated, the interactions between each factor are also considered. The replication of an experiment at the central point allows the estimation of the experimental variability. Two-level full factorial design is a common design, where two level, low and high level, are studied. The required number of experiments can be calculated as following Equation:

$$\text{Number of experiments} = 2^n \quad (1)$$

where n is the number of factors.

While the number of factors increases, a number of experiments that must be conducted is rapidly increased, which may be a main limitation of this design (19, 93).

2.6.2.2 Fractional factorial design

The fractional factorial design or reduced design can be employed to reduce the number of experiments to be carried out in full factorial design. In this study, the main effects and low order interactions are investigated, while the high order interactions are negligible. The reduced number of required experiments can be calculated as follow (19, 93):

$$\text{Number of experiments} = 2^{n-k} \quad (2)$$

where n is the number of factors, k is the step of reduction.

2.6.2.3 Central composite design (CCD)

Central composite design is a combination of full factorial or fractional factorial design with additional star point. The number of star point is two-fold of factor number. As illustrated in Fig. 7, it allows the curvature estimation according to quadratic model.

The number of experiments using full factorial and fractional factorial design can be calculated by Equation 3 and 4, respectively:

$$\text{Number of experiments} = 2^n + 2n + C_0 \quad (3)$$

$$\text{Number of experiments} = 2^{n-k} + 2n + C_0 \quad (4)$$

where n is the number of factors, k is the step of reduction, C_0 is the number of central points.

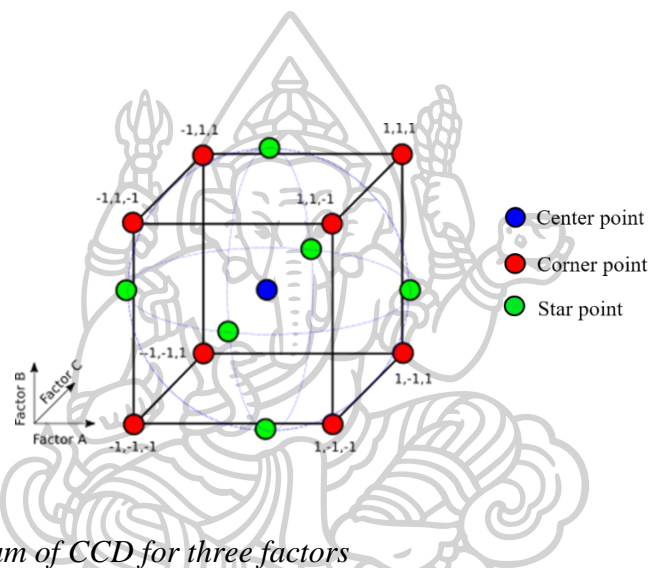


Figure 7 Diagram of CCD for three factors

2.6.2.4 Box-Behnken design (BBD)

BBD is an incomplete block design (Fig. 8). It requires three levels of each factor to run an experiment. As it does not include the combination of factor on the highest and lowest level, offering a benefit when the conducting of the experiment at the corner point is impossible or too expensive. The main advantage of such experiment is the reduction of experiment number. The number of experiments can be calculated by the following Equation:

$$\text{Number of experiments} = 2n(n-1) + C_0 \quad (5)$$

where n is the number of factors, C_0 is the number of central points.

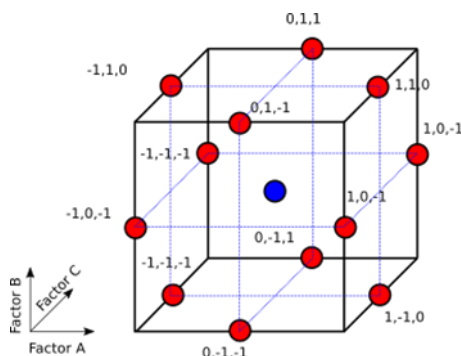


Figure 8 Diagram of BBD for three factors

2.6.3 BBD for optimization of drug-loaded microparticles by DESE

During the preparation of drug-loaded microparticles by DESE, the final product properties can be affected by several factors including formulation factors (drug amount, polymer amount, stabilizer concentration, viscosity of polymer solution, volume of internal and external phase and pH of external phase), process factors (stirring rate, stirring time and evaporation temperature), environmental factors (temperature and humidity) (16, 17).

Regarding to the study of Bouriche and coworkers (75), BBD was successfully used to determine the effect of factors and optimum condition for drug-loaded microparticles using DESE. The optimization of metformin hydrochloride-loaded microparticles by W/O/W DESE was carried out. PLA was used as an encapsulation polymer. BBD was used to optimize the effect of the amount of metformin in the inner aqueous phase (X_1), pH of external aqueous phase (X_2), amount of PVA in the external phase (X_3) and stirring rate (X_4) on the EE (%), particle size (μm), and zeta potential. The factors and level are listed in Table 4. According to the ANOVA results, the Equations for each response were developed. They demonstrated that the model was suitable with p value of the model of less than 0.05 and p value of the lack-of-fit of more than 0.05. These models were reliable with R^2 of 0.79, 0.83 and 0.89, respectively.

Table 4 List of factors and levels for BBD

| Factors | Levels | | |
|------------------------------|----------|-------------|-----------|
| | Low (-1) | Central (0) | High (+1) |
| Amount of metformin | 25 | 50 | 75 |
| pH of external aqueous phase | 4 | 5.5 | 7 |
| Amount of PVA (% w/v) | 0.5 | 1 | 1.5 |
| Stirring rate (rpm) | 400 | 800 | 1200 |

The following models presenting a relationship between the parameters and EE, mean particle size, and zeta potential of this study.

$$EE = 12.35 - 9.56X_1 + 4.87X_3 - 8.89X_4 - 10.69X_1X_3 + 18.54X_1^2$$

$$\text{Mean particle size} = 343.61 - 396.36X_3 - 8.89X_4 - 596.39X_1X_2 + 351.84X_1X_3 + 256.18X_2^2 - 250.34X_4^2$$

$$\text{Zeta potential} = -8.38 - 7.23X_1 + 1.87X_3 + 10.69X_3X_4 - 3.02X_1^2 - 6.28X_2^2 - 10.53X_3^2 - 4.5X_4^2$$

After that, to maximize the EE, the optimization process was carried out, resulting in the following optimum condition with the desirability of 0.998: $X_1 = 25$ mg, $X_2 = 4$, $X_3 = 1.5\%$, and $X_4 = 400$ rpm. The predicted EE of 82.15% was predicted under the optimum condition while the actual EE of optimized formulation was 78.05% (75).

CHAPTER 3

Materials and methods

- 3.1 Materials
- 3.2 Preliminary study on double emulsion preparation
- 3.3 Characterization of DPH-loaded double emulsion
 - 3.3.1 Viscosity of oil phase measurement
 - 3.3.2 Double emulsion droplet morphology characterization
 - 3.3.3 Double emulsion droplet size measurement
- 3.4 Identification of relevant factors on microparticles preparation using quality risk management approach
- 3.5 Study on factors affecting microparticle preparation
 - 3.5.1 Effect of pH of external water phase
 - 3.5.2 Effect of ultrasonication time
 - 3.5.3 Effect of polymer amount
 - 3.5.4 Effect of stirring time
 - 3.5.5 Effect of volume of external phase
 - 3.5.6 Statistical analysis
- 3.6 Optimization of DPH-loaded microparticles by BBD
- 3.7 Characterization of DPH-loaded microparticles
 - 3.7.1 Morphology of microparticles
 - 3.7.2 Image analysis of microparticles
 - 3.7.3 Residual solvent determination
 - 3.7.4 Fourier transform infrared (FTIR) spectroscopy
 - 3.7.5 Powder X-ray diffractometry (PXRD)
 - 3.7.6 Differential scanning calorimetry (DSC)
 - 3.7.7 Drug content determination
 - 3.7.8 *In vitro* dissolution test
- 3.8 Preparation and evaluation of ODTs
 - 3.8.1 Preparation of ODTs
 - 3.8.2 Evaluation of physical properties

3.8.2.1 Thickness, diameter, and hardness measurement

3.8.2.2 Friability test

3.8.3 Wetting test

3.8.4 *In vitro* disintegration test

3.8.5 *In vitro* dissolution test

3.8.6 *In vivo* evaluation

3.8.6.1 Perception and bitterness threshold determination

3.8.6.2 Palatability test



3.1 Materials

1. Donepezil hydrochloride (Lot number 000000085, Siam Pharmaceutical Co., Ltd, Thailand)
2. Aminoalkyl methacrylate copolymer (AMC; Eudragit[®] E PO, Lot number G170331544, Evonik Röhm GmbH, Germany)
3. Polyvinyl alcohol, molecular weight of 85,000 Da to 124,000 Da, and degree of hydrolysis of 87% to 89% (Lot number 16796TJV, Sigma-Aldrich, USA)
4. Mannitol (Lot number 302004308, Shandong Tianli Pharmaceutical Co., LTD, China)
5. Spray-dried lactose monohydrate (Supertab[®]11SD, Lot number 23034009, DMV-Fonterra Excipients GmbH & Co., Germany)
6. Sodium starch glycolate (Primojel[®], Lot number 10519TW, DMV-Fonterra Excipients GmbH & Co., Germany)
7. Microcrystalline cellulose (Comprecel[®]M101D+, Lot number C2006037, Mingtai Chemical Co., LTD, China)
8. Croscarmellose sodium (Disolcel[®], Lot number D02003103, Mingtai Chemical Co., LTD, China)
9. Crospovidone (Polyplasdone XL[®], Lot number 0002434812, Ashland Chemical Inc., USA)
10. Polyvinylpyrrolidone (PVP) K-30 (Lot number 002377911, Ashland Chemical Inc., USA)
11. Magnesium stearate (Kemilub EM-F-V[®], Lot number 67991, Italmatch Chemicals, Spain)
12. Dichloromethane, AR grade (Lot number AR1040A, RCI Labscan, Thailand)
13. Methyl alcohol, HPLC grade (Lot number LC1005, RCI Labscan, Thailand)
14. Acetonitrile, HPLC grade (Lot number LC1115, RCI Labscan, Thailand)

3.2 Preliminary study on double emulsion preparation

In the present study, two-step emulsification technique was used to prepare double emulsion. Initially, the internal water phase (W_1) was prepared by dissolving DPH in 10 mL of distilled water to produce a transparent solution at a concentration of

50 mg/mL. The primary water-in-oil emulsion was prepared by emulsifying W_1 with 25 mL of oil phase (O) containing AMC in dichloromethane by H14 ultrasonic probe (model UP400S, Hielscher, Germany) with an ultrasound capacity of 100% (400 W, 24 kHz). It was then mixed with 1% PVA, an external water phase (W_2), by a turbine stirrer (model SS20, Stuart, UK) at 500 rpm to produce $W_1/O/W_2$ emulsion.

To study the effect of polymer amount, double emulsion was prepared by varying AMC amount of 1, 2, 3, 4, 5, 6, and 7 g, while other parameters were kept constant (ultrasonication time of 120 s, volume of the external water phase of 450 mL, and stirring time in the second emulsification of 180 s).

Moreover, to study the effect of ultrasonication time, double emulsion was prepared with the ultrasonication capacity of 100% (400 W, 24 kHz) while varying ultrasonication time from 30 s to 180 s. Meanwhile, the AMC amount of 7 g, volume of the external water phase of 450 mL and stirring time in the second emulsification of 180 s were kept constant.

3.3 Characterization of DPH-loaded double emulsion

3.3.1 Viscosity of oil phase measurement

The cone and plate (CP1/50, SR1233) rheometer (model Kinexus, Malvern, UK) was used to measure the viscosity of oil phase containing of different amounts of AMC in DPH. The shear rate of 0.1 to 100.0 s^{-1} at the temperature of $25 \pm 0.1^\circ C$ was used.

3.3.2 Double emulsion droplet morphology characterization

Double emulsion was sampling (5 mL) at the midpoint between the surface of emulsion and the top of stirrer, dropped onto a clean glass slide and covered with cover slip. The emulsion images were recorded by a light microscope (model CX41RF, Olympus, Japan).

3.3.3 Double emulsion droplet size measurement

After sampling, the size of double emulsion droplets was measured by light scattering particle size analyzer (model LA-950, Horiba, Japan) with fraction cell mode. The size was reported as median while the size distribution was reported as span.

3.4 Identification of relevant factors on microparticles preparation using quality risk management approach

To facilitate a suitable decision making on microparticle preparation, the quality risk assessment approach was employed in this study. Initially, regarding to the literature information, the relevant factors affecting properties of drug-loaded microparticles prepared by DESE were identified using fishbone diagram. According to Annex 2: WHO guidelines on quality risk management (94), the risk matrix was constructed to prioritize a factor risk by multiplying the probability and its impact. The probability can be classified based on the number of events reported into 5 levels including (1) rare, (2) unlikely, (3) possible, (4) likely, (5) almost certain. The impact can also be classified based on magnitude of consequence into 5 levels including (1) negligible, (2) marginal, (3) moderate, (4) critical, (5) catastrophic. After that, the risk value of the factor was categorized into high (12 to 25), medium (5 to 10), and low (1 to 4). The preliminary study was then conducted. The information from risk assessment step and preliminary study were used for determining factor and factor level for further study.

3.5 Study on factors affecting microparticle preparation

Double emulsion was prepared using the methods described above and then stirred at ambient temperature for 3 to 5 h to allow complete solvent evaporation until constant weight was achieved. The microparticles were recovered through ultracentrifugation at 7,000 rpm for 10 min and washed in triplicate with distilled water to remove DPH and PVA residues. The obtained microparticles were dried at 30°C for 12 h under a vacuum oven and then stored in a desiccator for future characterization.

3.5.1 Effect of pH of external water phase

To study the effect of pH of external water phase, double emulsion was prepared using different buffer solutions, including acetate buffer (pH 5), phosphate buffer (pH 7), and carbonate-bicarbonate buffer (pH 10) to prepare 1% PVA solution. The AMC amount of 7 g, volume of external phase of 450 mL, and stirring time in the second emulsification of 180 s were used.

3.5.2 Effect of ultrasonication time

To study the effect of ultrasonication time, double emulsion was prepared with the ultrasonication capacity of 100% (400 W, 24 kHz), while varying ultrasonication time from 30 s to 180 s. The AMC amount of 7 g, volume of external phase (pH 10) of 450 mL, stirring time in the second emulsification of 180 s were used.

3.5.3 Effect of polymer amount

To study the effect of polymer amount, double emulsion was prepared with the volume of external phase (pH 10) of 450 mL, while varying AMC amount of 1, 2, 3, 4, 5, 6, and 7 g. Other factors were kept constant (ultrasonication time of 120 s, volume of the external water phase of 450 mL, and stirring time of 180 s).

3.5.4 Effect of stirring time

To study the effect of stirring time, double emulsion was prepared using different stirring periods (30, 60, 90, 120, 150, and 180 s). The AMC amount studied was 3 and 7 g. Other factors were kept constant (ultrasonication time of 120 s and volume of the external water phase of 450 mL).

3.5.5 Effect of volume of external water phase

To study the effect of volume of external water phase, double emulsion was prepared with different volumes (150, 250, 350, and 450 mL). The AMC amount studied was 3 and 7 g. Other factors were kept constant (ultrasonication time of 120 s and stirring time of 180 s).

3.5.6 Statistical analysis

The statistical analysis was performed by one-way analysis of variance (ANOVA) with homogeneity of variance test. The multiple comparison *post-hoc* test was also carried out with Sceffé or Games-Howell test on the basis of homogeneity test result. The *p*-value of less than 0.05 was considered significant different.

3.6 Optimization of DPH-loaded microparticles by BBD

To optimize formulation and processing factors, BBD was employed to investigate their effect on the responses. The levels of each factor were determined based on the preliminary study results. The experimental design and analysis were performed with Design-Expert® software version 8.0.7.1. The 17 total experimental runs with center points were constructed and randomly performed as per the run order. The statistical significance of the model was determined by *p*-value of less than 0.05. The adequacy of the model was determined by an insignificant lack-of-fit. The goodness of fit of model was determined by high coefficient of determination (R^2).

The proposed model was validated by performing additional experiments. The root mean square error (RSME) was calculated to measure the difference between predicted value and actual value by the following Equation:

$$\text{RMSE} = \sqrt{\frac{\sum_{i=1}^n (p_i - a_i)^2}{n}} \quad (6)$$

where p_i and a_i are predicted value and actual value of experiment, respectively, n is number of experiments.

Regarding to the criteria for each response, the optimum conditions for preparing DPH-loaded microparticles with desired properties were determined. The percentage of prediction error were calculated as follows:

$$\text{Prediction error} = \left| \frac{p_i - a_i}{a_i} \right| \times 100 \quad (7)$$

3.7 Characterization of DPH-loaded microparticles

3.7.1 Morphology of microparticles

Scanning electron microscope (SEM; model MIR3, TESCAN, Czech Republic) was used to examine the shape and surface morphology of microparticles. Adhesive tape was used to adhere the microparticles to the stub. A thin gold layer was then applied to the surface of the microparticles in a vacuum chamber. The images were obtained with the accelerating voltage of 5.0 kV.

3.7.2 Image analysis of microparticles

The microparticles were mounted on a clean glass slide and covered by cover slip. The light microscope (model CX41RF, Olympus, Japan) was used to capture images of total 50 microparticles (10 microparticles/frame, 5 frames). JMicroVision software, an image analysis software, was used to measure Feret diameter of each particles. The particle size and size distribution were reported as median and standard deviation. Each formulation was measured in triplicate.

3.7.3 Residual solvent determination

The residual dichloromethane in DPH-loaded microparticles was determined by headspace technique with TRACE1310 gas chromatograph (GC; Thermo Fisher Scientific, USA) connected with TriPlus RSH autosampler (Thermo Fisher Scientific, USA) and TSQ9000 mass spectrometer (Thermo Fisher Scientific, USA). The sample was separated in Rtx-624 (30 m x 0.32 mm, 1.80 μm ; Restek Corporation, USA). The initial temperature of GC oven was programmed at 35°C for 10 min, increased to 200°C, and held for 2 min with a ramp rate of 10°C/min. Residual amount of dichloromethane was calculated from a calibration curve.

3.7.4 Fourier transform infrared (FTIR) spectroscopy

To investigate interaction and compatibility of DPH, AMC, and PVA, the samples were pulverized with dried potassium bromide pellets and compressed into a disc by hydraulic press machine. The sample disc was analyzed by FTIR spectrophotometer (model Nicolet 4700, Thermo Electron Corporation, USA) over a scan range of 4,000 to 400 cm^{-1} .

3.7.5 Powder X-ray diffractometry (PXRD)

The powder X-ray diffractometer (model Miniflex II, Rigaku, Japan) was used to obtain the crystalline and amorphous characteristics of the DPH, AMC, PVA, physical mixture and optimized microparticles. The sample was tightly packed on a glass slide and its upper surface was pressed to get a smooth and flat surface. Afterward, it was positioned on a sample holder. The PXRD pattern was recorded at 30 kV and 15

mA over 2-theta range of 5 to 50 degree with graphite monochromatized Cu K α radiation. The scan speed was set at 4 degree/min.

3.7.6 Differential scanning calorimetry (DSC)

The differential scanning calorimeter (model DSC8000, Perkin Elmer, USA) was used to investigate the thermal characteristic of DPH, AMC, PVA, physical mixture, and optimized microparticles. Approximately 2 to 5 mg of sample were placed on a sample pan, covered with its lid, and sealed by standard sample pan crimper press. The sample was heated and the DSC thermogram was recorded at a temperature of 30 to 300°C with heating rate of 10°C/min.

3.7.7 Drug content determination

The amount of DPH encapsulated in microparticles was analyzed by high performance liquid chromatography (HPLC; model Jasco PU2089, Jasco, Japan) equipped with quaternary gradient pump and multi-wavelength UV-Vis detector (model Jasco UV2070, Jasco, Japan). Mobile phase was prepared by combining 0.01 M phosphate buffer, methyl alcohol and acetonitrile (50: 30: 20 v/v) and adjusted with phosphoric acid to a pH 2.7 \pm 0.1. The test solution was prepared by placing microparticles in 25-mL volumetric flask and dissolving with 10 mL of mobile phase with the aid of ultrasonic bath until a transparent solution was obtained. The solution was then adjusted to its final volume by addition of mobile phase, mixed, and filtered through a nylon syringe filter with the pore size of 0.45 μ m. The sample of 20 μ L was injected to a 4.6 \times 250 mm column packed with 5- μ m Luna C18(2) octadecylsilane (Phenomenex, USA). The analysis was carried out under isocratic condition with mobile phase flow rate of 1 mL/min. DPH concentration was measured by UV absorption at 270 nm and calculated based on linear standard curve. Moreover, drug loading and EE of the microparticle were calculated with the following Equation:

$$\% \text{ Drug loading} = \frac{\text{Amount of DPH in microparticles}}{\text{Amount of microparticles}} \times 100 \quad (8)$$

$$\% \text{ EE} = \frac{\text{Amount of drug in microparticles}}{\text{Amount of theoretical drug loading}} \times 100 \quad (9)$$

3.7.8 *In vitro* dissolution test

In vitro dissolution test in simulated saliva fluid (SSF) pH 6.75 was used as a tool to determine the taste-masking efficiency of DPH-loaded microparticles. To simulate the biological condition in oral cavity, the flow-through cell (USP apparatus 4) in a close loop configuration equipped with CE7 smart dissolution testing unit, CP7 piston pump, and C613 fraction collector (Sotax, Switzerland) was used to determine drug dissolution. The cell for powders and granulates (diameter of 12 mm) was assembled by placing a 5-mm ruby glass bead on the tip of cell cone and filling with 1-mm glass beads using measuring spoon. Then, the elements were placed in the following order from bottom to top; a wire mesh (0.2-mm pore size), glass fiber filter (2.7- μ m pore size), and a wire mesh. The microparticles equivalent to 5 mg DPH was weighed and placed in a cell chamber, followed by placing an application for powder. Then, a wire mesh, a glass fiber filter with pore size of 2.7 μ m, and 0.7 μ m, respectively, were placed before assembling the filter head on outlet opening. All test cells were inserted on a cell block. The dissolution test was conducted under sink condition in 50-mL SSF at the temperature of $37 \pm 0.5^\circ\text{C}$ with 4 mL/min flow rate. Aliquots of 3 mL of dissolution medium were withdrawn at 2, 5, 10, 15, 20, 30 and 60 min and replaced with equal volumes of fresh medium. After that, Q_5 in SSF was calculated.

In case of simulated gastric fluid (SGF) pH 1.2, drug dissolution test was also conducted with similar method. However, SGF was used as a dissolution medium instead of SSF. MDT in SGF was calculated based on the following Equation:

$$\text{MDT} = \frac{\sum_{j=1}^n \hat{t}_j \Delta M_j}{\sum_{j=1}^n \Delta M_j} \quad (10)$$

where j is number of samples, n is the number of dissolution sample times, \hat{t}_j is the time at midpoint between t_j and t_{j-1} , which can be calculated with the Equation: $\hat{t}_j = (t_j + t_{j-1})/2$, and ΔM_j is the additional amount of drug dissolved between t_j and t_{j-1} (95).

3.8 Preparation and evaluation of ODTs

3.8.1 Preparation of ODTs

Table 5 demonstrates the formulation of 200-mg ODT. To study the effect of super-disintegrant on wetting time and *in vitro* disintegration time, F1-ODT to F9-ODT were first prepared without addition of DPH or DPH-loaded microparticles. Before mixing, super-disintegrants (sodium starch glycolate, croscarmellose sodium, or crospovidone), and mannitol were sieved through a 425- μ m sieve. Then, mannitol, spray-dried lactose monohydrate, microcrystalline cellulose, and super-disintegrant were blended in a plastic bag with geometric blending technique to produce a homogeneous mixture. The rest of the ingredients (PVP K-30 and magnesium stearate) were blended one by one for 1 min. The hydraulic press machine (model SPECAC15011, Specac Ltd., UK) was used to compress the mixture with a force of 1 ton, and dwelling time of 10 s. The flat surface punch set with diameter of 9.65 mm was used. The resultant ODTs were kept in sealed plastic bag and stored over silica gel bed in desiccator for further evaluation.

Table 5 Formulation of blank ODT with total weight of 200 mg

| Ingredient | Quantity (mg/tablet) | | | | | | | | |
|---------------------------------|----------------------|--------|--------|--------|--------|--------|--------|--------|--------|
| | F1-ODT | F2-ODT | F3-ODT | F4-ODT | F5-ODT | F6-ODT | F7-ODT | F8-ODT | F9-ODT |
| Mannitol | 90 | 90 | 90 | 90 | 90 | 90 | 90 | 90 | 90 |
| Spray-dried lactose monohydrate | 81 | 77 | 73 | 81 | 77 | 73 | 81 | 77 | 73 |
| Microcrystalline cellulose | 21 | 21 | 21 | 21 | 21 | 21 | 21 | 21 | 21 |
| Sodium starch glycolate | 4 | 8 | 12 | - | - | - | - | - | - |
| Croscarmellose sodium | - | - | - | 4 | 8 | 12 | - | - | - |
| Crospovidone | - | - | - | - | - | - | 4 | 8 | 12 |
| PVP K-30 | 2 | 2 | 2 | 2 | 2 | 2 | 2 | 2 | 2 |
| Magnesium stearate | 2 | 2 | 2 | 2 | 2 | 2 | 2 | 2 | 2 |

After conducting wetting time and *in vitro* disintegration time test, F10-ODT, F11-ODT, and F12-ODT containing optimized microparticles of 28.5 mg (equivalent to DPH of 5 mg) and DPH-ODT were prepared (Table 6).

Table 6 Formulation of ODT containing DPH or DPH-loaded microparticles

| Ingredient | Quantity (mg/tablet) | | | |
|---------------------------------|----------------------|---------|---------|---------|
| | F10-ODT | F11-ODT | F12-ODT | DPH-ODT |
| Optimized microparticles | 28.5 | 28.5 | 28.5 | - |
| DPH | - | - | - | 5 |
| Mannitol | 90 | 90 | 90 | 90 |
| Spray-dried lactose monohydrate | 48.5 | 52.5 | 48.5 | 72 |
| Microcrystalline cellulose | 21 | 21 | 21 | 21 |
| Sodium starch glycolate | 8 | - | 12 | - |
| Croscarmellose sodium | - | 4 | - | - |
| Crospovidone | - | - | 8 | 8 |
| PVP K-30 | 2 | 2 | 2 | 2 |
| Magnesium stearate | 2 | 2 | 2 | 2 |

3.8.2 Evaluation of physical properties

3.8.2.1 Thickness, diameter, and hardness measurement

The hardness tester (model TBH225TD, Erweka GmbH, Germany) was used to determine the thickness, diameter, and hardness of each formulation (in triplicate).

3.8.2.2 Friability test

The friability tester (model TA120, Erweka GmbH, Germany) was used to determine %friability. The ODTs of approximately 6.5 g tablet weight were sampled, dedusted, and accurately weighed before placing in the drum. The friability tester was rotated 25 rpm for 4 min. After taking all tablets out, the loose dust was removed, and weighed. The friability of each formulation was calculated as in Equation 11:

$$\text{Friability} = \frac{\text{Initial weight (g)} - \text{Final weight (g)}}{\text{Initial weight (g)}} \times 100 \quad (11)$$

3.8.3 Wetting test

The wetting test was modified from the method proposed by Park and coworker (87). The test was conducted by placing Whatman filter paper with a diameter of 21 mm on the bottom of well (Corning® polystyrene, 12-well plate with a well diameter of 22 mm). A 1.25 mL of 0.1% w/w brilliant blue dye solution was dropped into each well.

The forceps were used to place an ODT on a filter paper (as presented in Fig. 9). Each formulation was tested in triplicate. The video record was used to determine the wetting time, which was the time needed for the dye solution to be diffused and completely covered the surface of ODT.

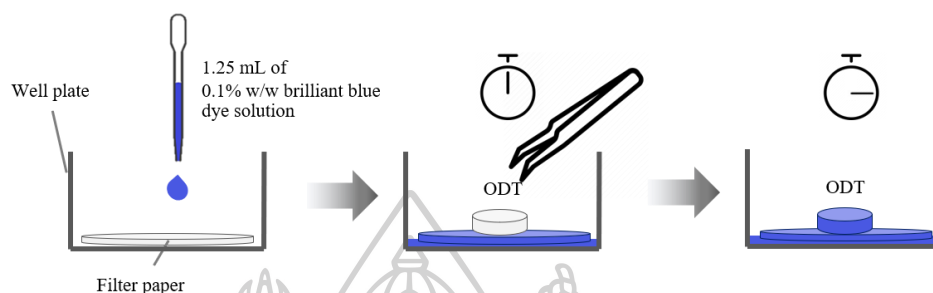


Figure 9 Schematic diagram showing the setup for wetting test

3.8.4 *In vitro* disintegration test

In vitro disintegration time was determined following *in vitro* disintegration test established by Hoashi and coworkers (96). The setup of experiment apparatus comprised of upper and lower wire mesh, a ring weight (20 g), and SSF-filled pipette, which is schematically shown in Fig. 10.

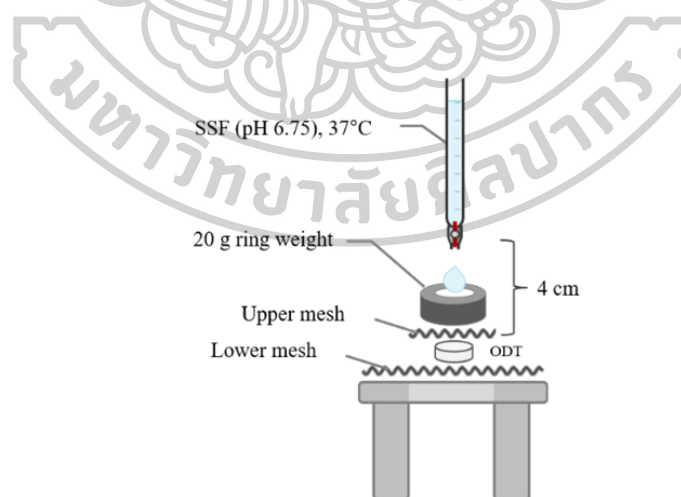


Figure 10 Schematic diagram showing the setup for *in vitro* disintegration test

Initially, a pair of forceps was used to place an ODT on the lower mesh and covered with the upper mesh. Then, a ring weight of 20 g was applied on top of the

assembly. The SSF-filled pipette was lowered at the distance of 4 cm and then dropped on the ODT with 4 mL/min flow rate. The experiment was performed in triplicate. The time needed for the upper mesh to completely reach the lower mesh was determined as an *in vitro* disintegration time based on the video record.

3.8.5 *In vitro* dissolution test

The *in vitro* dissolution testing of ODTs in SSF and SGF were conducted with the method specified in section 3.7.8 *In vitro* dissolution test. However, a tablet cell with inner diameter of 12 mm was used instead of cell for powders and granulates.

3.8.6 *In vivo* evaluation

The *in vivo* evaluation was performed in 6 healthy volunteers, as recommended in British Pharmacopoeia (97). Two males and four females were recruited with age range of 23 to 30 years according to the ethical approval research protocol approved by the Ethics Committee for Human Research of Silpakorn University (COE63.0922-079). The volunteers were asked to sign a consent form after reading entire protocol and being advised about the risk/benefit of the experiment.

3.8.6.1 Perception and bitterness threshold determination

The determination of perception and bitterness threshold was first carried out. The serial dilution of DPH was carried out with deionized water to prepare the following solution: (A) 0 µg/mL, (B) 12.5 µg/mL, (C) 25 µg/mL, (D) 37.5 µg/mL, (E) 50 µg/mL, (F) 62.5 µg/mL, (G) 75 µg/mL, (H) 87.5 µg/mL, (I) 100 µg/mL. Before testing began, the volunteers were asked to thoroughly rinse their mouth with deionized water. They were asked to hold 10 mL of solution (A) in their mouth and slowly move it along the surface of the tongue for 30 s. Then, they were asked to test the moderate level concentration, solution (E). After spitting out test solution and rinsing their mouth with deionized water, the volunteers were asked to evaluate test solution by giving one of these following answers:

- (1) I did not feel any different between solution A and E
- (2) I felt something, but I could not distinguish its taste
- (3) I felt a bitter taste

The volunteers who replied answer 1 or 2 were then asked to try solution F, which had a higher concentration. In contrast, the volunteers who replied answer 3 were asked to try solution D, which had a lower concentration. There was a 10 min wash-out period between trials. The lowest concentration at which the volunteers could still felt some tastes was determined as perception threshold while the lowest concentration at which the volunteers could felt a bitter taste was determined as bitterness threshold of DPH.

3.8.6.2 Palatability test

Prior evaluation of ODTs, the volunteer training was conducted to ensure that the results were comparable. The volunteers were first asked to rinse their mouth with deionized water and hold three DPH solution (solution (A), (E), and (I)), which had different concentrations. Then, they were told the bitterness score of each solution (0, 50, and 100).

The palatability test was performed. The volunteers were first asked to rinse their mouth with deionized water. Then, the DPH-ODT or F12-ODT (with 8 mg of crosopvidone) was randomly gave to the volunteers who were asked to place the sample on the center of the tongue and hold in their mouth. The stopwatch was used to record the disintegration time of tablet. The volunteers were asked to hold the tablet for another 30 s after it completely disintegrated. However, they were allowed splitting the sample out if the bitter taste was too strong. After test finished, the volunteers were asked to give a score to the sample on its bitterness, tablet handling, grittiness, and overall palatability by making a mark on a 100-mm visual analog scale (VAS). The scores were measured in millimeters and the VAS score median of DPH-ODT and F12-ODT were compared using a paired-samples T-test. The *p*-value of less than 0.05 was considered significant difference and represented by the asterisk.

CHAPTER 4

Results and discussion

4.1 Study on factors affecting microparticle preparation

4.1.1 Effect of pH of external phase

4.1.2 Effect of ultrasonication time

4.1.3 Effect of polymer amount

4.1.4 Effect of stirring time

4.1.5 Effect of volume of external phase

4.2 Determination of factors and factor levels for optimization based on risk assessment approach

4.3 DoE in microparticle preparation

4.3.1 Particle size of DPH-loaded microparticles

4.3.2 Q₅ in SSF

4.3.3 MDT in SGF

4.3.4 Validation of mathematical model

4.3.5 Optimization of DPH-loaded microparticle preparation

4.4 Characterization of optimized DPH-loaded microparticles

4.4.1 Residual solvent determination

4.4.2 FTIR spectroscopy

4.4.3 PXRD

4.4.4 DSC

4.5 Preparation and evaluation of ODTs

4.5.1 Physical properties of ODTs

4.5.2 Wetting test and *in vitro* disintegration test

4.5.3 *In vitro* dissolution test

4.5.4 *In vivo* evaluation

4.1 Study on factors affecting microparticle preparation

The factors affecting the properties of microparticles were identified on the basis of literature review of a highly water-soluble and small molecules encapsulating using DESE, including materials, environment, double emulsion preparation condition, and solvent evaporation condition (15, 16, 66, 68-75), as illustrated in fishbone diagram in Fig. 11.

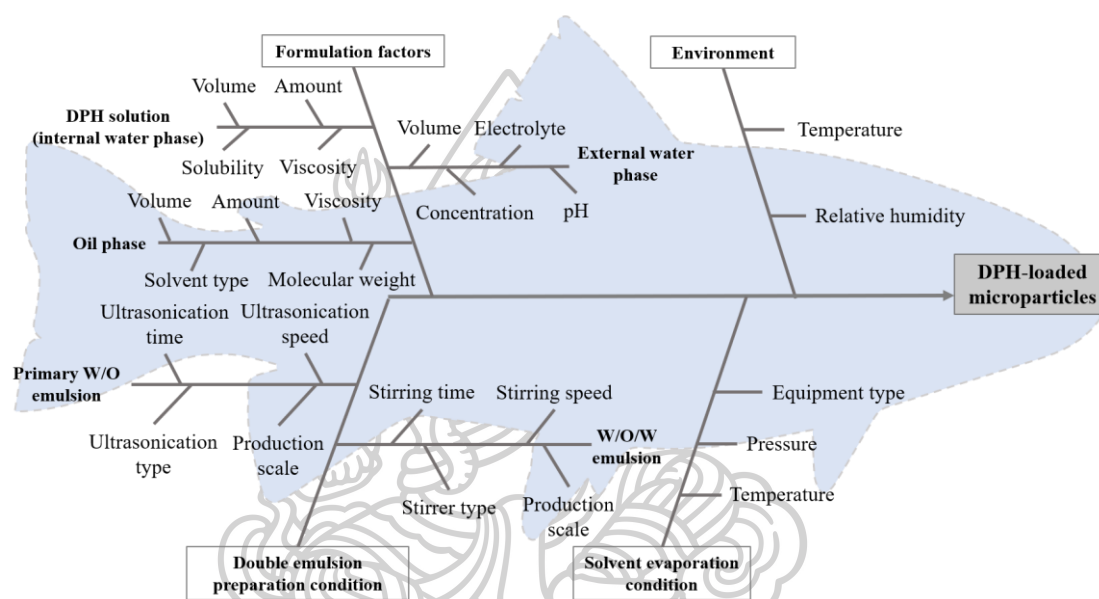


Figure 11 Fishbone diagram of factors affecting the properties of DPH-loaded microparticles

In this study, material type, ultrasonicator type used in the first emulsification, stirrer type used in the second emulsification, solvent evaporation condition, and production scale were kept constant while temperature and relative humidity were monitored during the experiment. Therefore, these factors were excluded from the risk assessment. Then, the risk matrix was developed (Table 7) based on published information to prioritize the effect of these relevant factors on critical quality attributes (CQAs) of DPH-loaded microparticles. For bitter taste-masking and ODTs production, the CQAs of DPH-loaded microparticles were particle size, and drug dissolution.

Table 7 Risk value of formulation factors and operating condition of microparticle preparation

| Factors | CQAs | |
|--|---------------|------------------|
| | Particle size | Drug dissolution |
| Formulation factors: | | |
| Drug amount | Medium | Low |
| Organic solvent amount | Low | Low |
| Polymer amount | High | High |
| Stabilizer concentration | High | High |
| pH of external water phase | Low | Low |
| Volume of internal phase | Medium | Medium |
| Volume of oil phase | Medium | Low |
| Volume of external water phase | High | High |
| Operating condition: | | |
| Ultrasonication time in the first emulsification | Medium | Low |
| Stirring time in the second emulsification | High | High |
| Stirring rate in the second emulsification | Medium | Low |

The studies were further performed to investigate the effect of high-risk factors, having high risk value on both particle size and drug dissolution, including polymer amount, stabilizer concentration, volume of external water phase, and stirring time in the second emulsification.

4.1.1 Effect of pH of external water phase

According to the preliminary study, PVA concentration (1%), which can maintain the size of double emulsion throughout preparation process, was used as a stabilizer in external water phase. The effect of pH of external water phase on EE was studied. DPH-loaded double emulsion was prepared using 1% PVA solubilized in different buffers, including acetate buffer (pH 5), phosphate buffer (pH 7), and carbonate-bicarbonate buffer (pH 10). The results demonstrated that an increase of pH of external water phase from pH 5 to pH 10 resulted in a sharply increase in EE from 8.14 to 49.27% (Fig. 12). This phenomenon was also observed in other studies (71, 73, 75) and can be explained by the pH-solubility relationship. Typically, the basic drug solubility could be calculated with following Equation:

$$\log S = \log S_0 + \log (10^{\text{pK}'_a - \text{pH}} + 1) \quad (12)$$

where S is the solubility, S_0 is the solubility of unionized drug, and pK'_a is drug dissociation constant (98).

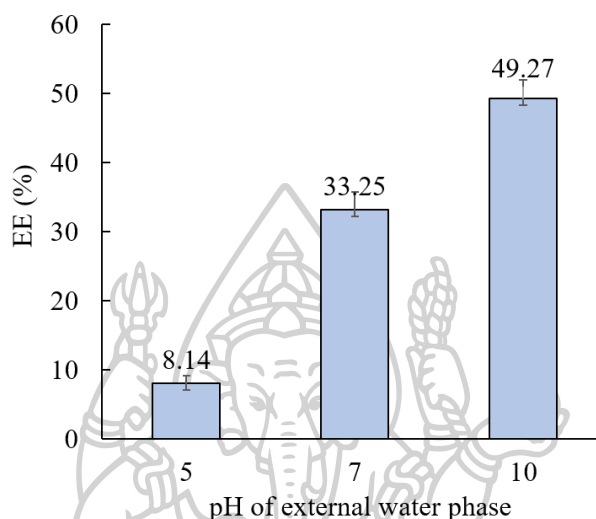


Figure 12 Effect of pH of external water phase on EE of microparticles

The solubility ratio of DPH (pK'_a value of 8.90) at pH 10 to pH 5 calculated with Equation 12 was approximately 1×10^{-4} . Due to an increase of pH of external water phase from 5 to 10 led to a decrease of drug solubility in this phase, the partition of DPH from internal phase to external water phase was decreased. For the reason, the EE of microparticles was improved. Therefore, 1% PVA solution prepared with pH 10 carbonate-bicarbonate buffer was used as an external water phase to prepare microparticles for further experiments.

4.1.2 Effect of ultrasonication time

To prepare primary W_1/O emulsion in the first emulsification step, the effect of ultrasonication time was investigated by varying the ultrasonication time from 30 to 180 s. The AMC amount of 7 g, volume of external water phase of 450 mL and stirring time in the second emulsification of 180 s were used in this study.

According to the exclusive property of dichloromethane, which had high vapor pressure (353 mmHg, 20°C), it would rapidly evaporate. So, the droplet size of primary

W_1/O emulsion cannot be directly measured under optical microscope. The effect of ultrasonication time was investigated by measuring droplet size of $W_1/O/W_2$ by light scattering particle size analyzer instead. It demonstrated that, when increasing ultrasonication time, the droplet size of freshly prepared emulsion after 1 h stirring and 3 h stirring double emulsion was in the range of 240 to 250 μm (Fig. 13). However, the smallest droplet size was obtained with the ultrasonication time of 120 s.

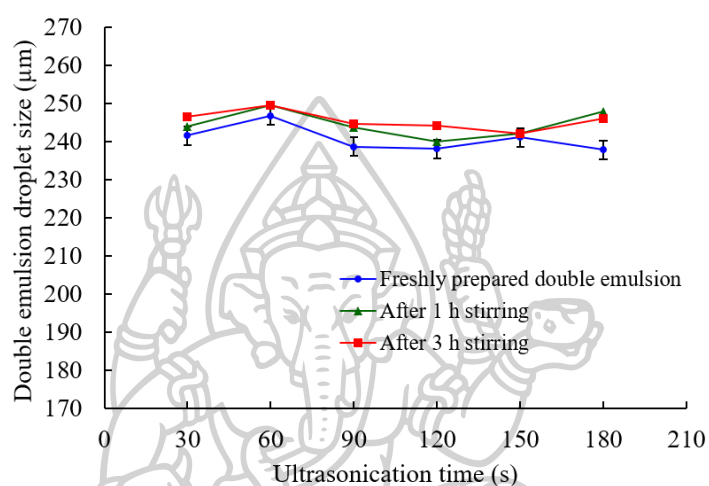


Figure 13 Effect of ultrasonication time on double emulsion droplets size

After drying, the size of microparticles was measured. The results demonstrated that the microparticle size (220-235 μm) was smaller than that of double emulsion droplets (Fig. 14).

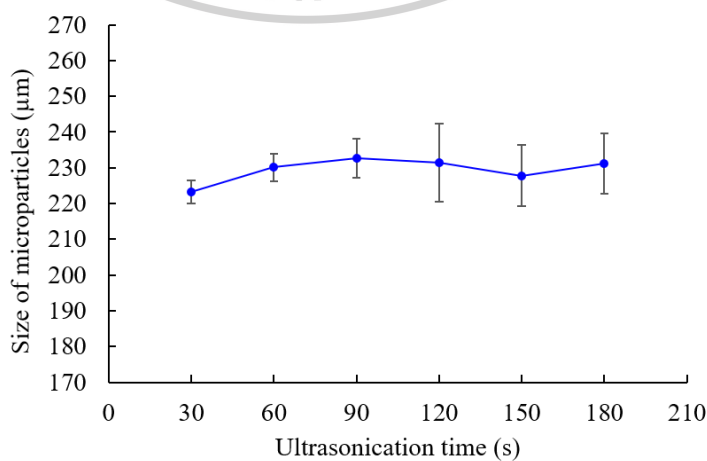


Figure 14 Effect of ultrasonication time on size of microparticles

It indicated that microparticle size was not significantly influenced by increasing of ultrasonication time. This was in a good agreement with the previous publications (16, 99), which reported that any parameters modified in the second emulsification step had a greater impact on the microparticle size than that in the first emulsification step. Therefore, the ultrasonication time was kept constant at 120 s.

4.1.3 Effect of polymer amount

Since the emulsion droplets cannot be formed with AMC amount less than 1 g while the AMC amount above 7 g was not feasible to prepare owing to an extremely high viscosity of oil phase. The effect of polymer amount on double emulsion preparation was therefore investigated by varying AMC from 1 to 7 g while other parameters were kept constant (i.e., ultrasonication time of 120 s, volume of the external water phase of 450 mL, and stirring time in the second emulsification of 180 s)

The size of double emulsion droplets was measured by light scattering particle size analyzer. The median size and span of emulsion droplets containing AMC amount of 1, 2, 3, 4, 5, 6, and 7, were 47.16 ± 1.98 , 73.17 ± 1.65 , 114.26 ± 1.73 , 132.93 ± 1.65 , 158.81 ± 1.86 , 185.13 ± 1.72 , and 217.24 ± 1.52 μm , respectively. The results demonstrated that double emulsion droplet sizes increased with increasing AMC amount.

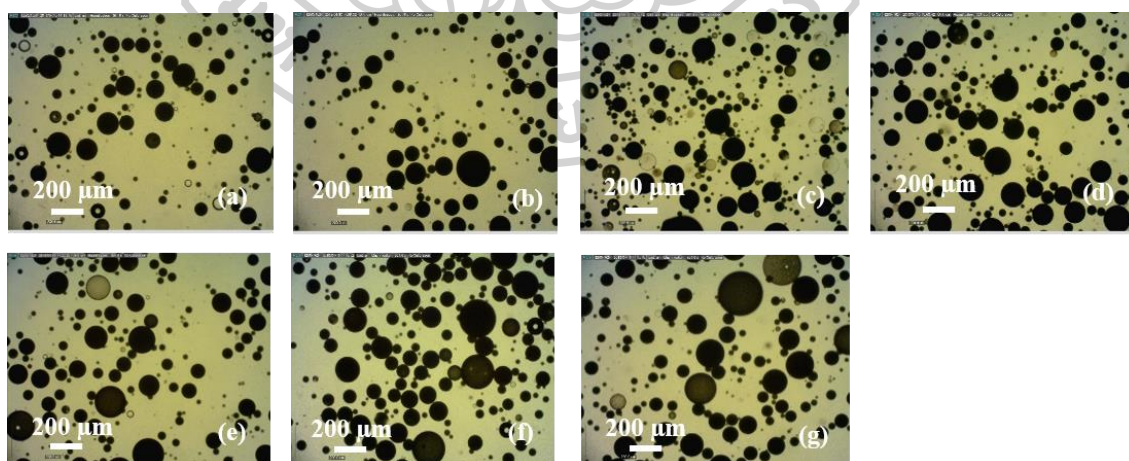


Figure 15 Optical microscopic images of emulsion droplets containing AMC amount of (a) 1, (b) 2, (c) 3, (d) 4, (e) 5, (f) 6, and (g) 7 g

The optical microscope was also used to capture the images of freshly prepared double emulsion droplets with the magnification of $\times 300$. Fig. 15 demonstrates the spherical opaque emulsion droplets with polydisperse droplet distribution. This is generally found in double emulsion prepared by two-step emulsification technique as compared to other techniques (16, 18). This phenomenon can be explained by the complexity of preparation process and its thermodynamic unstable of the system. However, the size can be controlled by cautiously adjusting the relevant parameters (16, 59)

After drying, the shape and surface morphology of microparticles were observed by SEM as shown in Fig. 16. The microparticles were in spherical shape. The surface morphology of microparticles (Fig. 17) containing AMC amount of 1, 2, 3, 4, and 5 g was rough with numerous pores, whereas that of 6 and 7 g was smooth without any pore. These pores may be developed during the solidification of microparticles due to evaporation of in oil phase. The effect of AMC amount on microparticle size is demonstrated in Fig. 18. The microparticle size significantly increased with increasing AMC amount.

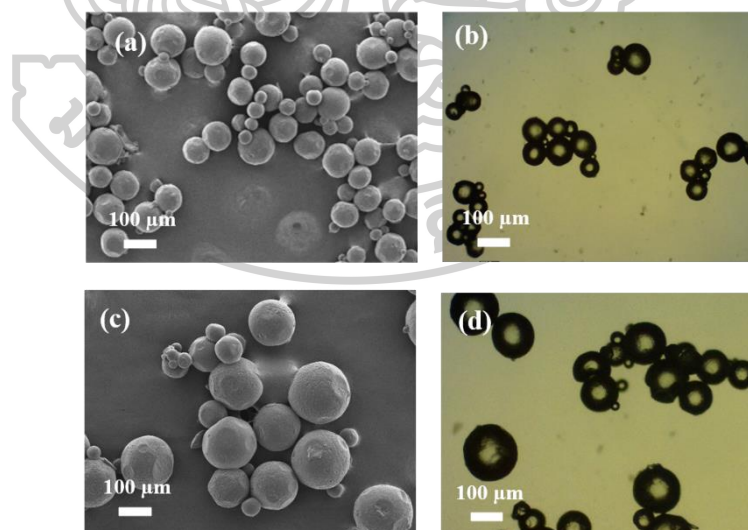


Figure 16 SEM images (left) and microscopic images (right) of microparticles containing AMC amount of (a, b) 1, and (c, d) 7 g

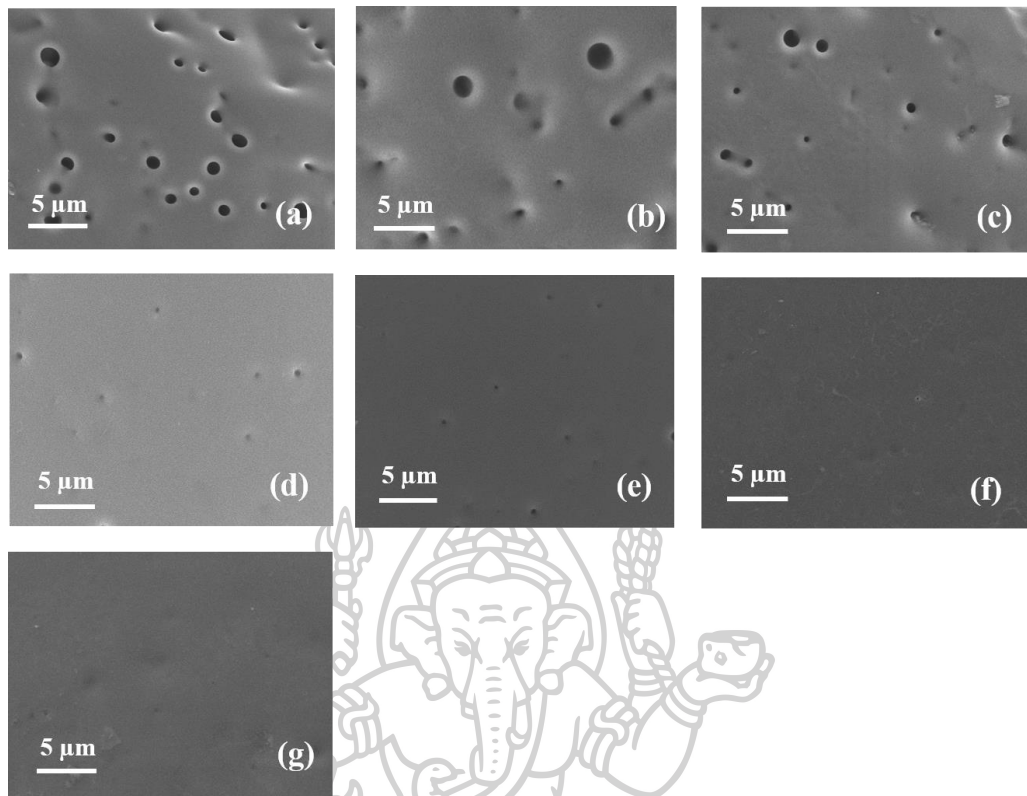


Figure 17 SEM images showing surface morphology of microparticles containing AMC amount of (a) 1, (b) 2, (c) 3, (d) 4, (e) 5, (f) 6, and (g) 7 g

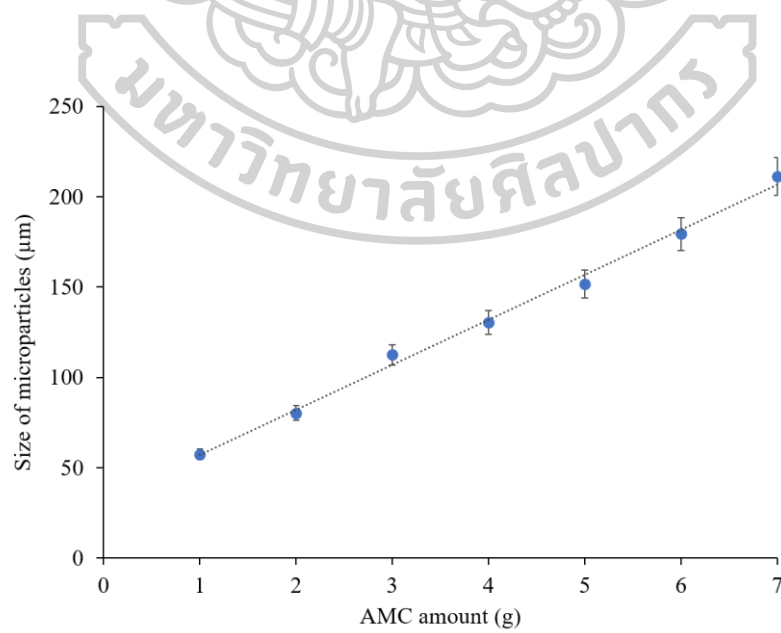


Figure 18 Size of microparticles prepared with different amounts of AMC

Fig. 19 demonstrates the *in vitro* drug dissolution of DPH-loaded microparticles. Q_5 of each formulation is shown in Fig. 20. It demonstrated a decrease in Q_5 with increased AMC amount.

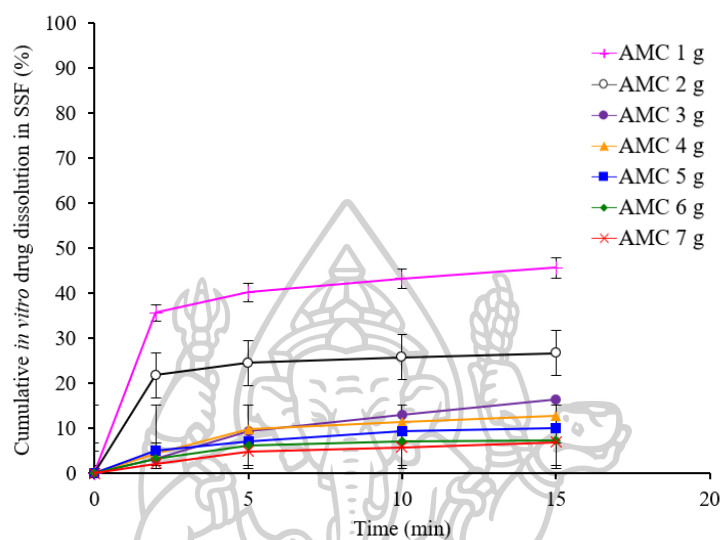


Figure 19 *In vitro* drug release profiles in SSF of DPH-loaded microparticles containing different amounts of AMC

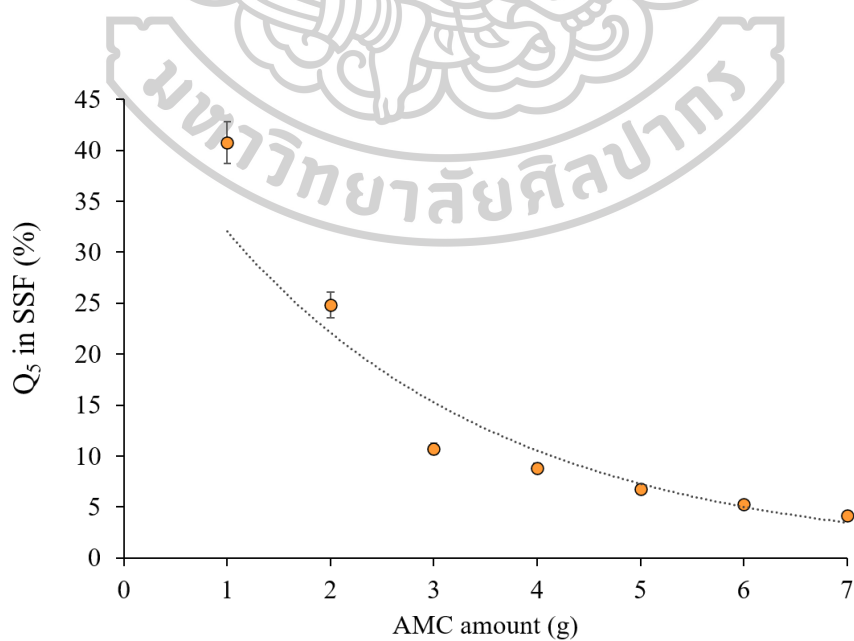


Figure 20 Q_5 in SSF of microparticles containing different amounts of AMC

The *in vitro* drug dissolution test in SGF of microparticles containing different amounts of AMC was also carried out to investigate the effect of AMC amount. The cumulative drug dissolution profiles of microparticles in SGF are demonstrated in Fig. 21. The MDT of these profiles were then calculated. The results shows that MDT increased with increasing AMC amount (Fig. 22).

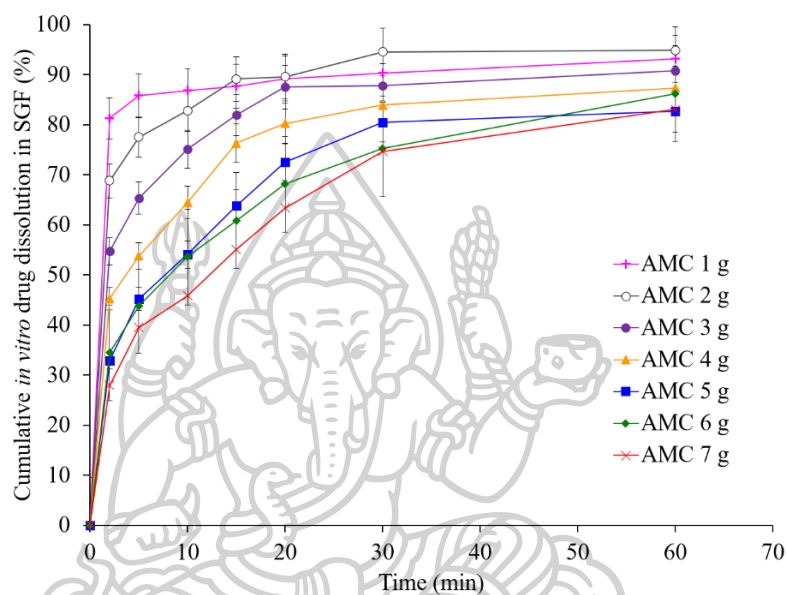


Figure 21 Cumulative *in vitro* drug dissolution in SGF of microparticles containing different amounts of AMC

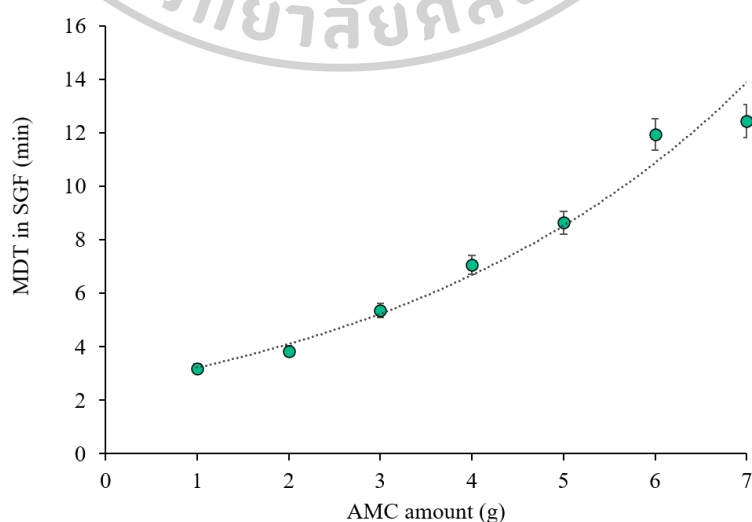


Figure 22 MDT in SGF of microparticles containing different amounts of AMC

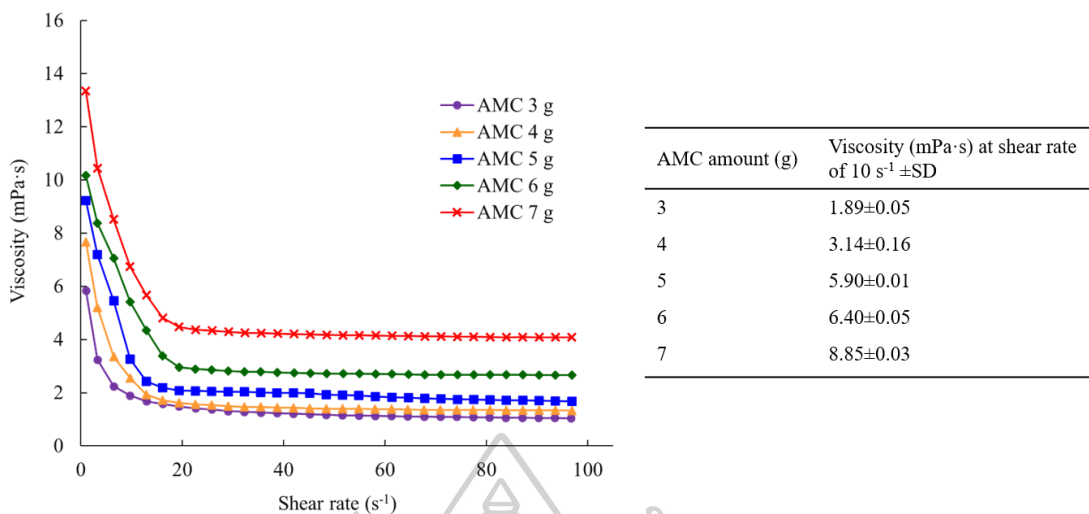


Figure 23 Viscosity profiles of oil phase containing different amounts of AMC

The effect of AMC amount on microparticle size can be explained by the viscosity of oil phase solution shown in Fig. 23. At a shear rate of 10 s⁻¹, the viscosity was increased when higher AMC amount was introduced to the oil phase. The higher agitation force may be required for breaking the primary W₁/O emulsion into double emulsion droplets in the external water phase. However, in this study, the stirring parameters were kept constant, the microparticle size was therefore increased with increasing AMC amount, which in accordance with previous studies (65, 73).

The effect of AMC amount on *in vitro* drug dissolution in SSF and SGF can be explained by the property of AMC, which is a pH-dependent polymer. It is soluble at pH up to 5 but insoluble and swellable at pH above 5. In SSF with pH of 6.75, the swollen AMC layer of the microparticles was formed. By increasing AMC amount, these layers become thicker and prevent DPH dissolution. Q₅ was therefore decreased with increasing AMC amount. Similar with that of *in vitro* drug dissolution testing in SGF (pH 1.2), an increasing of AMC amount resulted in a thicker layer of polymer, which slow drug dissolution rate in SGF. MDT in SGF was therefore increased with increasing AMC amount.

4.1.4 Effect of stirring time

In the second emulsification step, the turbine stirrer was used to prepare double emulsion. The effect of stirring time was studied by preparing microparticles with AMC amount of 3 and 7 g and varying from 30 to 180 s, whereas other parameters were kept constant.

The results show that the microparticles prepared with AMC amount of 3 g demonstrated a significant decrease in size of microparticles upon increasing the stirring time of 30 to 120 s (Fig. 24). However, the size of microparticle prepared with stirring time of 120 to 150 s was not significantly different. It was significantly decreased when the stirring time of 180 s was introduced to the emulsion. In the same way with those prepared with AMC amount of 7 g, the microparticle size decreased with increasing stirring time up to 90 s. The size of microparticle prepared with stirring time of 90 to 150 s was not significantly different. However, the microparticle size was significantly decreased with increased stirring time from 150 to 180 s.

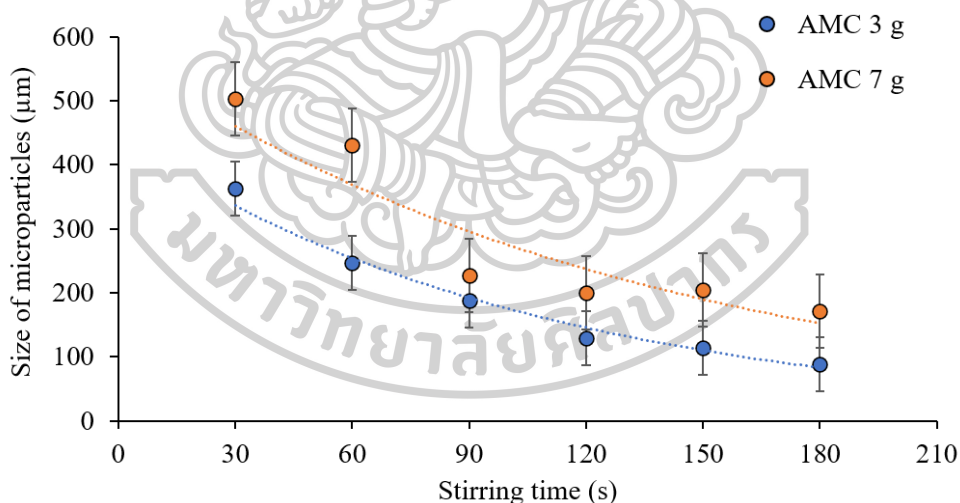


Figure 24 Size of microparticles prepared by different stirring times

The *in vitro* dissolution in SSF was carried out in to study the effect of stirring time on Q_5 . Fig. 25 demonstrates that Q_5 of microparticles prepared with AMC amount of 3 g was significantly decreased when stirring time increased from 30 to 180 s. In the same way, Q_5 of microparticles prepared with AMC amount of 7 g was significantly decreased when stirring time increased from 30 to 60, 90 to 120, and 150

to 180 s. However, Q_5 of microparticles prepared with stirring time of 60 to 90 and 120 to 150 s was not significantly different. Based on AMC amount, Q_5 of microparticles prepared with AMC amount of 3 g was greater than that of 7 g.

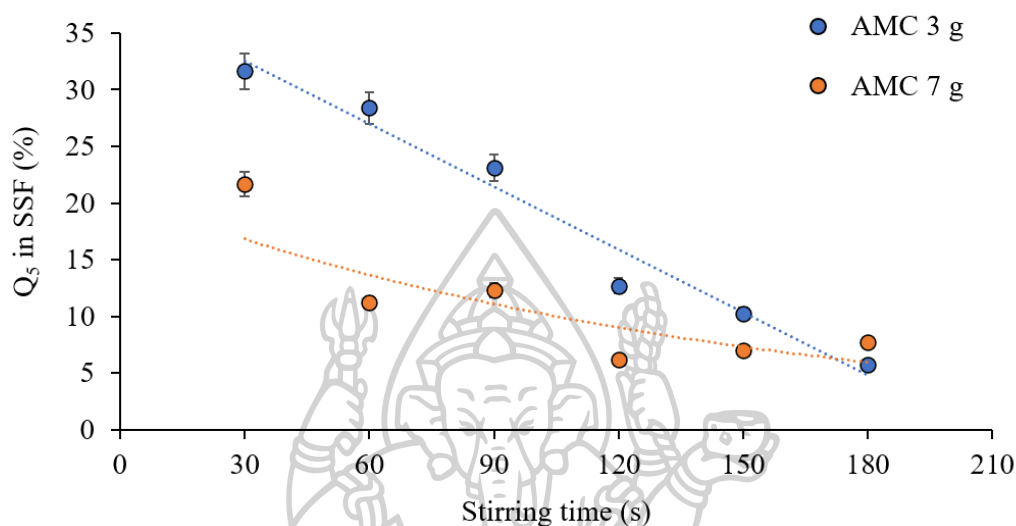


Figure 25 Q_5 in SSF of microparticles prepared by different stirring times

Then, the *in vitro* drug dissolution in SGF was carried out. Fig. 26 shows that MDT in SGF of microparticles was increased by increasing stirring time. Regarding AMC amount, MDT of microparticles prepared with AMC amount of 7 g was greater than that of 3 g. MDT of microparticles prepared with AMC amount of 3 g was significantly increased when stirring time was increased from 90 to 120 s and 150 to 180 s. However, MDT was not significantly increased with increasing stirring time of 30 to 90 s and 120 to 150 s. Similar trends were observed with that of 7 g. MDT was significantly increased when stirring time was increased from 60 to 90 s and 150 to 180 s, whereas the increasing stirring time of 30 to 60 s and 90 to 150 s did not result in a significant increase in MDT.

According to the results, increasing the stirring time in the second emulsification step increased the time interval for breaking primary W_1/O emulsion into small double emulsion droplets. Therefore, an increase of stirring time decreased microparticle size.

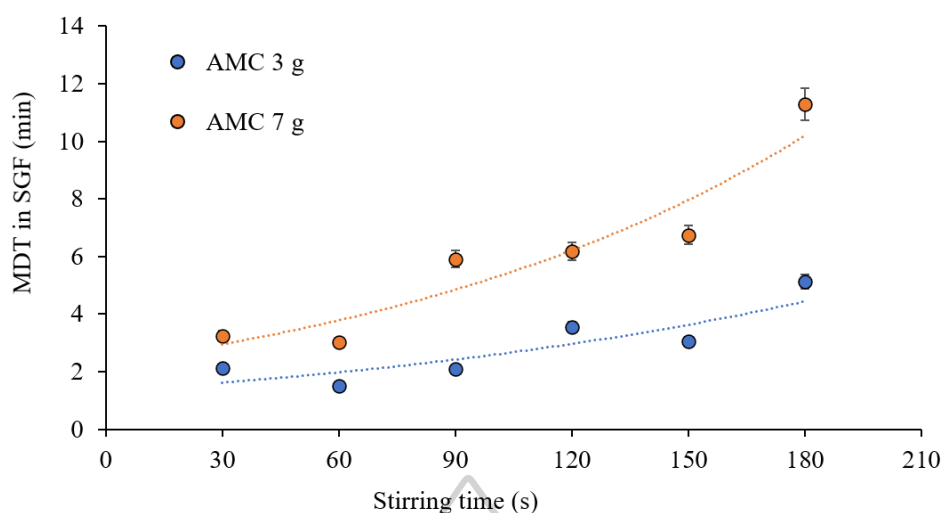


Figure 26 MDT in SGF of microparticles prepared with different stirring times

The effect of stirring time on *in vitro* drug dissolution in SSF can be explained by EE of microparticles prepared with different stirring times, as shown in Table 8. An increase in stirring time increased the chance of DPH to be lost from the microparticles to the external water phase. The EE, therefore, decreased led to low Q_5 in SSF, in accordance with previous study (65). In addition, an increase in stirring time, which resulted in a small microparticles, also facilitated a hardening of polymer layer. It may result in a dense microparticle structure and, therefore, slow drug dissolution rate in SGF or an increasing of MDT.

Table 8 EE of microparticles prepared by different stirring times and AMC amounts

| Stirring time (s) | EE (%) \pm SD | |
|-------------------|------------------|------------------|
| | AMC 3 g | AMC 7 g |
| 30 | 44.23 \pm 2.13 | 47.13 \pm 1.71 |
| 60 | 45.93 \pm 3.82 | 39.19 \pm 2.16 |
| 90 | 36.42 \pm 1.28 | 37.20 \pm 3.74 |
| 120 | 30.15 \pm 2.75 | 35.01 \pm 3.12 |
| 150 | 28.02 \pm 1.63 | 34.73 \pm 2.34 |
| 180 | 27.09 \pm 2.47 | 24.54 \pm 1.86 |

4.1.5 Effect of volume of external phase

In this study, 1% PVA in carbonate-bicarbonate buffer (pH 10) was used as an external water phase to stabilize double emulsion droplets in the second emulsification. The volume of external water phase was varied from 150 to 450 mL with two different AMC amounts (3 and 7 g), whereas other parameters were kept constant.

The effect of volume of external water phase on size of microparticles was investigated, as shown in Fig. 27. Regarding to the AMC amount, with the same volume of external phase, the size of microparticles prepared with AMC amount of 7 g was bigger than that of 3 g. The size of microparticles prepared with large volume of external water phase was smaller than that of small volume of external water phase.

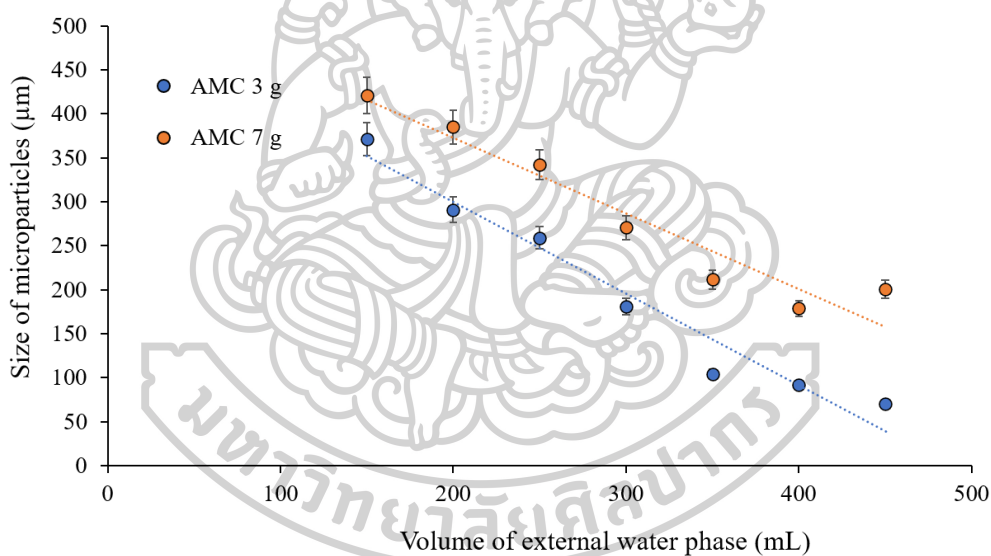


Figure 27 Size of microparticles prepared with different volumes of external water phase

Similar findings were reported by Kataras and coworkers (69). However, Zafar and coworkers (99) reported an increased size of microparticles containing ammonio methacrylate copolymer Type B (Eudragit® RS100) with increasing volume of external water phase. The results attributed to the decrease of stirring efficiency with large volume of external water phase.

The *in vitro* drug dissolution in SSF and SGF was further performed to investigate the effect of volume of external water phase. Q_5 in SSF of microparticles prepared with different volumes of external phase was demonstrated in Fig. 28. Q_5 of microparticles prepared with AMC amount of 3 g was greater than that of 7 g. Also, Q_5 of microparticles prepared with large volume of external water phase was less than that of small volume of external water phase.

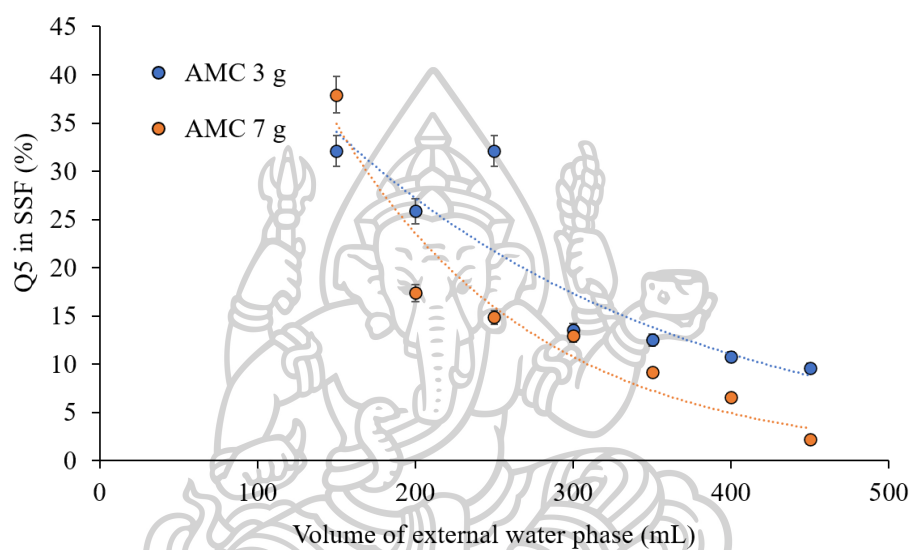


Figure 28 Q_5 in SSF of microparticles prepared by different volumes of external water phase

The *in vitro* drug dissolution in SGF was also carried out to investigate the effect of volume of external phase. MDT in SGF was calculated, as shown in Fig. 29. Based on the AMC amount, MDT of microparticles prepared with AMC amount of 7 g was greater than that of 3 g. MDT of microparticles prepared with large volume of external water phase was greater than that of small volume of external water phase.

The effect of volume of external phase on EE was also investigated. As shown in Table 8, the EE at two different AMC amounts decreased with increasing volume of external phase. This is in accordance with a previous study (65). When the volume of external phase increased, it provided large volume for the organic solvent in the oil phase to be extracted. Once the solvent was removed, it may cause DPH loss to the external water phase. The EE was therefore decreased, which led to a lower amount of

drug dissolution in SSF. The large volume of external phase may also fasten the hardening of microparticles, resulting in dense structure of microparticles. The slow rate of drug dissolution was, therefore, observed in SGF.

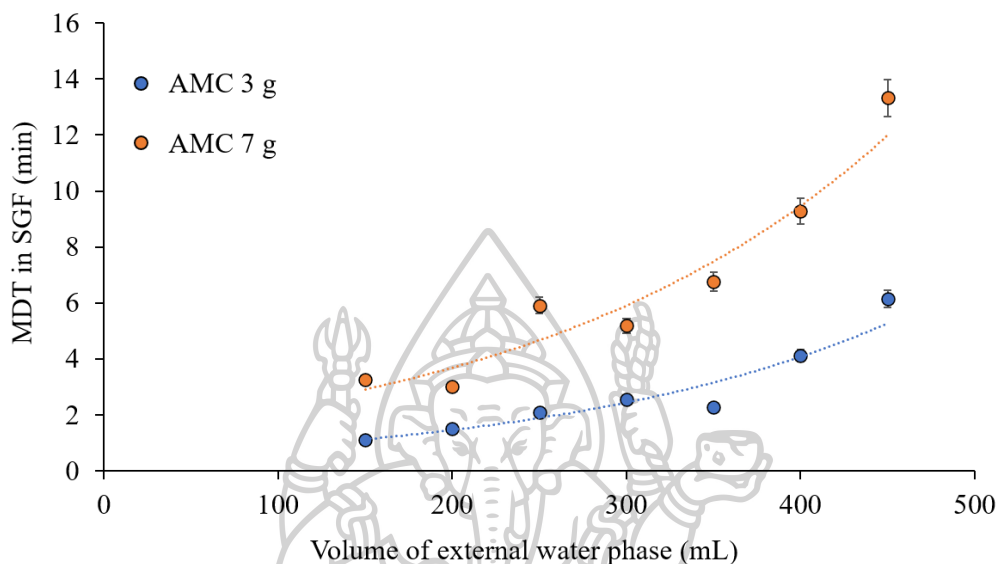


Figure 29 MDT in SGF of microparticle prepared by different volumes of external water phase

The effect of volume of external water phase on *in vitro* drug dissolution in SSF can be explained by EE of microparticles prepared with different volumes of external water phase (Table 9). An increase of volume of external water phase increased the diffusion of dichloromethane from the microparticles to the external water phase, and therefore, increased the chance of DPH loss to the external water phase. This resulted in a decrease of EE and led to a low Q_5 in SSF. Moreover, an increase in volume of external water phase provided large volume for dichloromethane to diffuse, facilitating a hardening of microparticles. This may result in a dense microparticle structure and, therefore, slow drug release rate in SGF or an increase in MDT.

Table 9 EE of microparticles prepared by different volumes of external phase and AMC amounts

| Volume of external phase (mL) | EE (%) \pm SD | |
|-------------------------------|------------------|------------------|
| | AMC 3 g | AMC 7 g |
| 150 | 38.29 \pm 1.37 | 43.47 \pm 2.12 |
| 200 | 37.13 \pm 2.87 | 45.13 \pm 2.03 |
| 250 | 32.14 \pm 1.53 | 42.13 \pm 1.31 |
| 300 | 29.31 \pm 1.92 | 37.24 \pm 1.65 |
| 350 | 33.87 \pm 2.01 | 34.13 \pm 2.19 |
| 400 | 26.23 \pm 3.23 | 30.10 \pm 2.93 |
| 450 | 24.20 \pm 1.73 | 29.03 \pm 2.28 |

4.2 Determination of factors and factor levels for optimization based on risk assessment approach

As mentioned in Chapter 2 that the CQAs of taste-masked microparticles were size of microparticles, Q₅ in SSF, and MDT in SGF.

According to FIP/AAPS guidelines to dissolution/*in vitro* release testing of novel/special dosage forms, the taste-masking is achieved when *in vitro* drug dissolution in neutral medium is less than 10% (100). Therefore, Q₅ in SSF of less than 10% was set as criteria. The ideal taste-masking technique property should only mask the unpleasant taste but should not affect drug release behavior. The *in vitro* drug dissolution testing in SGF was therefore performed to investigate this point. According to the *in vitro* drug dissolution of DPH in SGF, MDT was 4.35 min and 80% of cumulative drug dissolution was obtained within 5 min. Therefore, these criteria were set for drug dissolution testing in SGF. In this study, the microparticles were planned to incorporate in the ODTs. As microparticle size is responsible for the mouthfeel of the tablet after disintegrating in the mouth. The large microparticles can cause a strong grittiness feeling (101, 102). Therefore, the size of microparticles in the range of 100 to 200 μ m was set as criteria.

These criteria were applied for selecting the levels of AMC amount, stirring time, and volume of external phase (Table 10). By preparing microparticles with AMC amount ranged from 3 to 7 g, the average particle size of around 100 to 200 was

obtained with Q_5 in SSF of less than 10% and MDT in SGF of 5 to 12 min. In case of operating condition, the stirring rate of overhead stirrer used in the second emulsification step was kept constant at 500 rpm due to equipment limitation. The stirring time was varied in the range of 90 to 180 s, which resulted in microparticle size of around 200 μm with low Q_5 and MDT in SGF of 6 to 11 min. Using volume of external water phase of 350 to 450 mL, the size of microparticles of less than 200 μm with low Q_5 and MDT in SGF of 7 to 14 min was obtained. The effects of these processing parameters were further investigated by BBD (Table 11).

Table 10 Independent factors, level of each factor and responses in BBD of DPH-loaded microparticles preparation

| Independent factors | Level | | |
|--|----------|------------|-----------|
| | Low (-1) | Medium (0) | High (+1) |
| X ₁ : AMC amount (g) | 3 | 5 | 7 |
| X ₂ : Stirring time (s) | 90 | 135 | 180 |
| X ₃ : Volume of external water phase (mL) | 350 | 400 | 450 |
| Responses | | | |
| Y ₁ : Particle size (μm) | | | |
| Y ₂ : Q_5 in SSF (%) | | | |
| Y ₃ : MDT in SGF (min) | | | |

4.3 DoE in microparticle preparation

According to the literature and preliminary study, the properties of microparticles were influenced by independent factors, including AMC amount (X_1), stirring time (X_2), and volume of W_2 (X_3). During the experiment, the environmental factors, including temperature and relative humidity were monitored. The evaluated responses were particle size (Y_1), Q_5 in SSF (Y_2), and MDT in SGF (Y_3).

Table 11 Summary of independent factors, level of factor, and responses in Box-Behnken design of DPH-loaded microparticles preparation

| Standard run order | Independent factors | | | Experimental values of responses | | |
|-----------------------|---------------------|----------------|----------------|----------------------------------|----------------|----------------|
| | X ₁ | X ₂ | X ₃ | Y ₁ | Y ₂ | Y ₃ |
| 1 | 3 | 90 | 400 | 116.24 | 14.23 | 5.15 |
| 2 | 7 | 90 | 400 | 247.73 | 5.41 | 9.86 |
| 3 | 3 | 180 | 400 | 82.50 | 11.71 | 5.27 |
| 4 | 7 | 180 | 400 | 213.02 | 3.64 | 10.52 |
| 5 | 3 | 135 | 350 | 113.82 | 13.90 | 4.34 |
| 6 | 7 | 135 | 350 | 226.01 | 5.32 | 7.56 |
| 7 | 3 | 135 | 450 | 99.31 | 8.21 | 6.32 |
| 8 | 7 | 135 | 450 | 228.61 | 4.79 | 12.67 |
| 9 | 5 | 90 | 350 | 194.25 | 6.50 | 5.78 |
| 10 | 5 | 180 | 350 | 157.52 | 7.57 | 6.03 |
| 11 | 5 | 90 | 450 | 186.28 | 5.45 | 7.54 |
| 12 | 5 | 180 | 450 | 174.72 | 4.93 | 7.11 |
| 13 | 5 | 135 | 400 | 184.82 | 5.46 | 5.17 |
| 14 | 5 | 135 | 400 | 187.53 | 6.20 | 5.67 |
| 15 | 5 | 135 | 400 | 193.62 | 5.54 | 6.14 |
| 16 | 5 | 135 | 400 | 185.23 | 4.35 | 7.78 |
| 17 | 5 | 135 | 400 | 183.72 | 5.47 | 6.03 |

4.3.1 Particle size of DPH-loaded microparticles

The effect of independent factors on particle size of DPH-loaded microparticles was investigated. As summarized in Table 11, the particle size ranged from 82.50 to 247.73 μm . A reduced mathematical model in Equation 13 represented the relationship of independent factors on particle size in terms of coded factors. The ANOVA results (as provided in Table 12) demonstrated the reliability of the model with p -value of less than 0.05. Moreover, the p -value for lack-of-fit was 0.0954, indicating the suitability of the model. The goodness of fit was represented by R^2 value of 0.9820.

$$\text{Particle size} = 183.08 + 62.94X_1 - 14.59X_2 - 17.17X_1^2 \quad (13)$$

The ANOVA results (Table 12) showed the significant terms were X_1 , X_2 , and X_1^2 . AMC amount and stirring time significantly influenced the particle size. The effect of these factors is illustrated by three-dimensional plot (Fig. 30), showing that the particle size increased with increasing AMC amount and decreasing stirring time. This is in good agreement with the preliminary study.

Table 12 ANOVA results of the fitted model for predicting Y_1

| Source | Sum of squares | Degree of freedom | Mean square | F-value | p -value, prob > F |
|---|----------------|-------------------|-------------|---------|----------------------|
| Y_1 | | | | | |
| Model | 34641.40 | 3 | 11547.13 | 236.38 | <0.0001 |
| X_1 | 31689.03 | 1 | 31689.03 | 648.72 | <0.0001 |
| X_2 | 1703.53 | 1 | 1703.53 | 34.87 | <0.0001 |
| X_1^2 | 1248.84 | 1 | 1248.84 | 25.57 | 0.0002 |
| Residual | 635.04 | 13 | 48.85 | | |
| Lack of fit | 572.29 | 9 | 63.59 | 4.05 | 0.0954 |
| Pure error | 62.75 | 4 | 15.69 | | |
| Cor total | 35276.44 | 16 | | | |
| Regression coefficient: $R^2 = 0.9820$, adjusted $R^2 = 0.9778$, predicted $R^2 = 0.9693$ | | | | | |

Note: Cor total means corrected total sum of squares

The explanation of this phenomenon may be associated with the viscosity of oil phase. Since an increase of AMC amount increased the viscosity of oil phase, the higher stirring force and time were required to disperse the primary emulsion in external water phase (73, 77). Thus, the size of microparticles was increased.

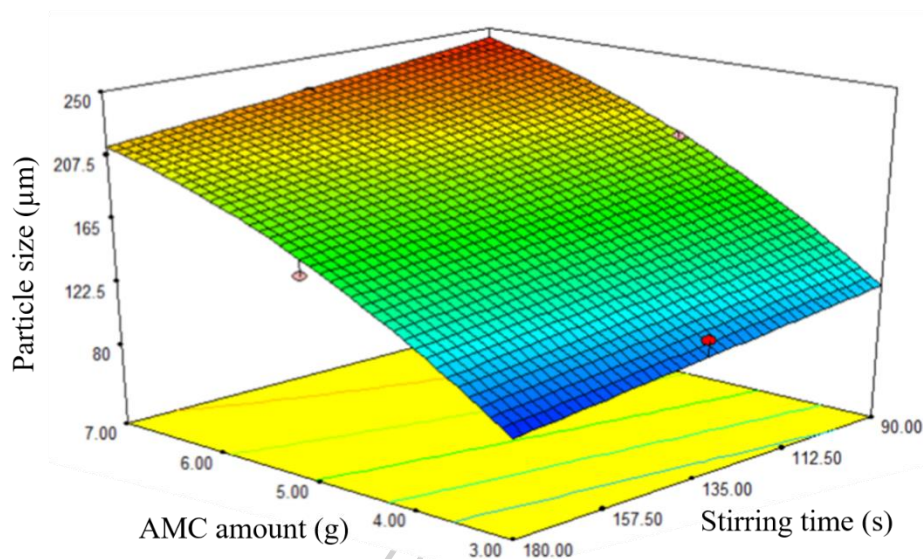


Figure 30 Three-dimensional plot showing the effect of independent factors on size of microparticles

According to the study of Pal and coworkers (103), a low shear force is recommended to disperse primary W₁/O emulsion in external water phase in the second emulsification step in order to avoid internal droplet break up. The stirring rate in this study was, therefore, kept constant at 500 rpm, whereas stirring time was varied. In case of the effect of stirring time on the size of microparticles, it showed negative association in the model. This may be due to the longer emulsification time by increasing stirring time. The particle size was, therefore, decreased, as proposed in previous publication (65).

4.3.2 Q₅ in SSF

From the results, Q₅ ranged from the lowest of 3.64% to highest of 14.23%. The ANOVA results (Table 13) showed that the model predicting Q₅ of DPH-loaded microparticles was significant with *p*-value of less than 0.05. The *p*-value for lack-of-fit of 0.1384 indicated model suitability and R² value of 0.9216 indicated the goodness of fit. A reduced mathematical model was represented in coded terms in Equation 14, indicating that AMC amount was the most significant factor and both AMC amount and volume of external water phase demonstrated negative association in the model.

$$Q_5 \text{ in SSF} = 5.72 - 3.61X_1 - 1.24X_3 + 1.29X_1X_3 + 2.68X_1^2 \quad (14)$$

Table 13 ANOVA results of the fitted model for predicting Y_2

| Source | Sum of squares | Degree of freedom | Mean square | F-value | p-value, prob > F |
|---|----------------|-------------------|-------------|---------|-------------------|
| Y_2 | | | | | |
| Model | 153.73 | 4 | 38.43 | 35.25 | <0.0001 |
| X_1 | 104.33 | 1 | 104.33 | 95.69 | <0.0001 |
| X_3 | 12.28 | 1 | 12.28 | 11.26 | 0.0057 |
| X_1X_3 | 6.66 | 1 | 6.66 | 6.11 | 0.0294 |
| X_1^2 | 30.47 | 1 | 30.47 | 27.95 | 0.0002 |
| Residual | 13.08 | 12 | 1.09 | | |
| Lack of fit | 11.31 | 8 | 1.41 | 3.19 | 0.1384 |
| Pure error | 1.77 | 4 | 0.44 | | |
| Cor total | 166.82 | 16 | | | |
| Regression coefficient: $R^2 = 0.9216$, adjusted $R^2 = 0.8954$, predicted $R^2 = 0.7923$ | | | | | |

Note: Cor total means corrected total sum of squares

The effect of AMC amount, and volume of external water phase on Q_5 in SSF is illustrated by the three-dimensional plot (Fig. 31). *In vitro* drug dissolution profiles in SSF of standard run 5, 7, 8 are illustrated in Fig. 32 (a), showing retarded drug dissolution behavior with Q_5 of 13.90, 8.21, and 4.79, respectively. It can be explained by the properties of AMC, a pH-dependent solubility polymer, which is soluble at pH of less than 5, but swellable and permeable above pH 5. An increase in AMC amount from 3 g (run 7) to 7 g (run 8) may result in the formation of thicker swellable layer of polymer in SSF, which prevented DPH dissolution from microparticles, resulting in a decreased Q_5 .

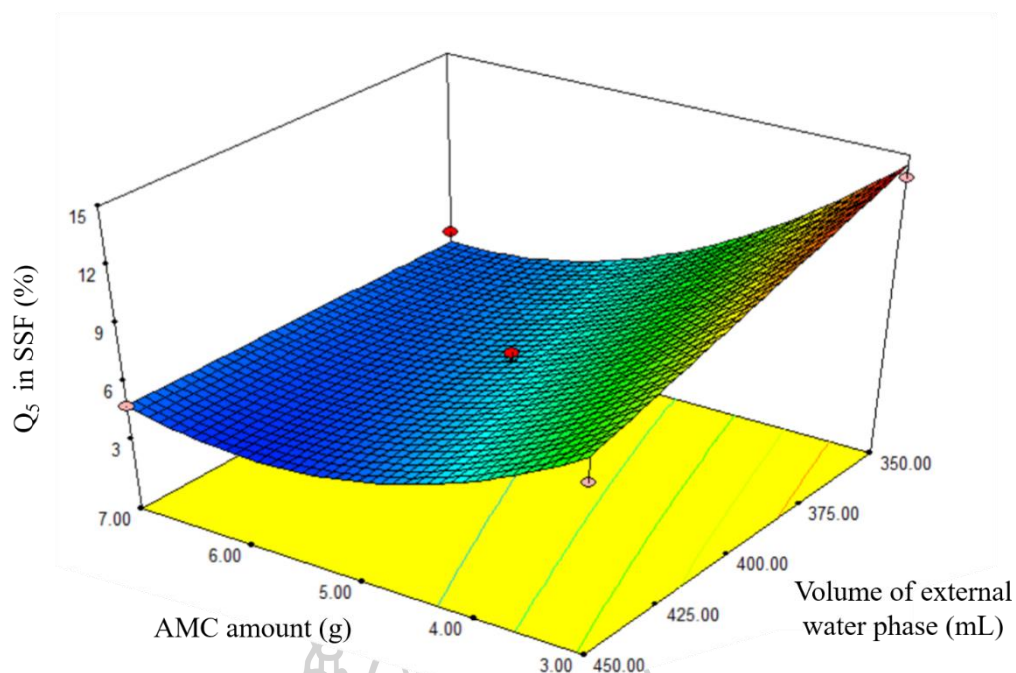


Figure 31 Three-dimensional plot showing the effect of independent factors on Q_5 in SSF

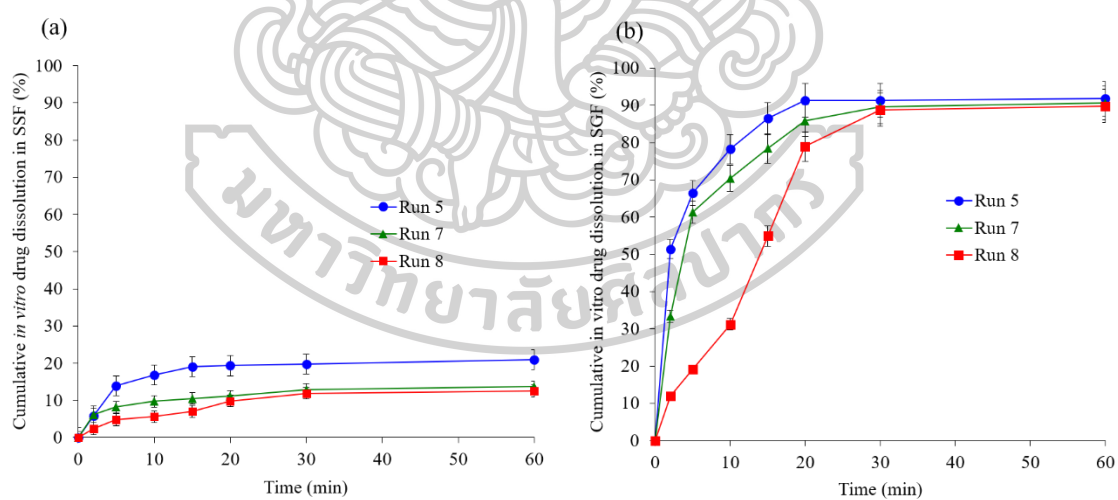


Figure 32 In vitro drug dissolution profiles of standard run 5, 7, and 8 in (a) SSF, and (b) SGF

The volume of external water phase showed negative association in the model. In vitro drug dissolution profiles of run 5 and 7 in SSF demonstrated that an increased volume of external water phase from 350 mL (run 5) to 450 mL (run 7) resulted in

lower Q_5 . The results are in good agreement with the preliminary study results, which a changed parameter was only volume of external water phase. This can be explained by the role of external water phase responsible for the last stage of solvent evaporation. The steps of microparticle hardening were briefly described as follows: diffusion of organic solvent inside emulsion droplets, diffusion of organic solvent to the intermediate boundary between dispersed emulsion droplet and external phase and, evaporation of organic solvent to ambient environment (77). An increase in volume of external water phase resulted in an accelerated diffusion of organic solvent due to large volume available for the removal of organic solvent, thus facilitating the microparticle hardening (61, 100). Therefore, it is hypothesized that this phenomenon was associated with the formation of complex microparticle structure, which resulted in low Q_5 .

4.3.3 MDT in SGF

Ideally, the taste-masking approach should only mask the unpleasant taste of drug without changing the biopharmaceutical behavior (34, 96). Therefore, the effect of independent factors on MDT in SGF was investigated.

The results showed that MDT ranged from the lowest of 4.34 min in run 5 to the highest of 12.67 min in run 8. The results of ANOVA test (Table 14) showed that a reduced mathematical model predicting MDT of DPH-loaded microparticles was significant with p -value of less than 0.05 and p -value for lack-of-fit of 0.1104, indicating model suitability. Moreover, R^2 value of 0.9379 demonstrated the goodness of fit. The model was represented in coded terms in Equation 15. The effect of AMC amount, and volume of external water phase on MDT is illustrated by the three-dimensional plot in Fig. 33.

Table 14 ANOVA results of the fitted model for predicting Y_3

| Source | Sum of squares | Degree of freedom | Mean square | F-value | p-value, prob > F |
|---|----------------|-------------------|-------------|---------|-------------------|
| Y_3 | | | | | |
| Model | 72.92 | 4 | 18.23 | 45.27 | <0.0001 |
| X_1 | 47.68 | 1 | 47.68 | 118.39 | <0.0001 |
| X_3 | 12.33 | 1 | 12.33 | 30.61 | 0.0001 |
| X_1X_3 | 2.45 | 1 | 2.45 | 6.08 | 0.0297 |
| X_1^2 | 10.47 | 1 | 10.47 | 26.00 | 0.0003 |
| Residual | 4.83 | 12 | 0.40 | | |
| Lack of fit | 4.26 | 8 | 0.53 | 3.71 | 0.1104 |
| Pure error | 0.57 | 4 | 0.14 | | |
| Cor total | 77.76 | 16 | | | |
| Regression coefficient: $R^2 = 0.9379$, adjusted $R^2 = 0.9171$, predicted $R^2 = 0.8217$ | | | | | |

Note: Cor total means corrected total sum of squares

$$\text{MDT in SGF} = 6.14 + 2.44X_1 + 1.24X_3 + 0.78X_1X_3 + 1.57X_1^2 \quad (15)$$

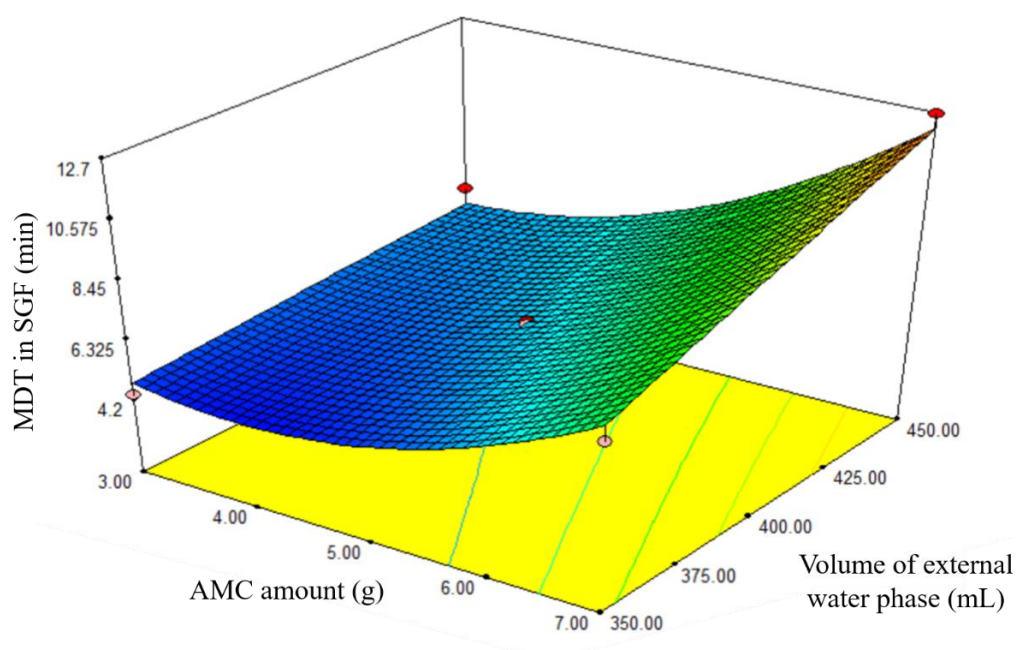


Figure 33 Three-dimensional plot showing the effect of independent factors on MDT of drug release in SGF

Fig. 32 (b) shows drug dissolution profiles of run 5, 7, 8 in SGF, showing that an increase of both AMC amount and volume of W_2 resulted in an increased of MDT. This phenomenon can be explained in a similar manner to that of Q_5 in SSF. An increase in AMC amount resulted in a thick barrier for drug release, and, therefore increased MDT. In case of the effect of volume of W_2 , the increase in this factor led to rapid emulsion harden, which strengthen microparticle structure (59, 73), resulting in an increased MDT.

4.3.4 Validation of mathematical model

The additional experiment was performed to validate the correlation between the actual value and predicted value calculated from the proposed mathematical model. Table 15 demonstrates the RMSE of particle size, Q_5 , and MDT of 11.63, 0.50, and 1.06, respectively, indicating the model effectiveness.

Table 15 Comparison of the difference between actual and predicted value of responses

| No. | Independent factors | | |
|-----|---------------------|-------------------|----------------------------|
| | AMC amount (g) | Stirring time (s) | Volume of water phase (mL) |
| F1 | 5.5 | 120 | 350 |
| F2 | 4.8 | 160 | 380 |
| F3 | 5.2 | 100 | 430 |

| No. | Responses | | |
|-----|---------------------------------|-----------------|-------|
| | Particle size (μm) | | |
| | Actual value | Predicted value | RMSE |
| F1 | 209.29 | 202.60 | 11.63 |
| F2 | 159.20 | 168.50 | |
| F3 | 217.11 | 200.55 | |

Table 15 (continued)

| No. | Responses | | |
|-----|---------------------------------|-----------------|------|
| | Particle size (μm) | | |
| | Actual value | Predicted value | RMSE |
| | Q ₅ (%) in SSF | | |
| F1 | 5.51 | 5.90 | 0.50 |
| F2 | 6.97 | 6.65 | |
| F3 | 5.43 | 4.72 | |
| | MDT (min) in SGF | | |
| F1 | 6.49 | 5.41 | 1.06 |
| F2 | 6.62 | 5.45 | |
| F3 | 8.10 | 7.19 | |

4.3.5 Optimization of DPH-loaded microparticles preparation

After validation of the model, the optimization was carried out to find the optimum conditions to prepare desired taste-masked DPH-loaded microparticles. As ODTs are designed to disintegrate in the oral cavity, the disintegrated particles may potentially cause unpleasant or grittiness feeling on the tongue, leading to poor patient compliance. Recent studies demonstrated the relationship of particle size and grittiness feeling; the smaller the particle size, the less the grittiness feeling (101, 104). They revealed that the particle size of greater than 200 μm may cause intense grittiness sensation. Therefore, criteria of particle size was set at the range of 100 - 200 μm .

Based on the guideline (100), the taste-masking is achieved while drug dissolution is less than 0.5 mg (or 10 $\mu\text{g}/\text{mL}$). However, the bitterness threshold of individual drug is also necessary to take into consideration for developing decision-making criteria. According to the result of *in vivo* taste evaluation study in human volunteers, the bitterness threshold of DPH was 56.3 ± 15.73 $\mu\text{g}/\text{mL}$, indicating that taste-masking was achieved while drug dissolution amount in the medium was under this concentration. Comparing to that of guideline (100), the evaluation of taste-

masking using Q_5 of less than 10% was selected to use as a strict interpretation for taste-masking evaluation.

As mentioned in previous part that the ideal taste-masking should not affect the biopharmaceutical properties of native drug. Regarding to the test, the *in vitro* drug dissolution testing of DPH in SGF showed MDT of 4.35 min. Moreover, the cumulative drug dissolution reached 80% within 15 min. According to the experimental results, MDT ranged from 4.34 to 12.67 min. To fulfill the purposed requirements, the criteria for MDT of less than 10 min was acceptable.

In summary, the optimization criteria to determine the optimum values for preparing DPH-loaded microparticles included the particle size ranging from 100 to 200 μm , Q_5 of less than 10%, and MDT of less than 10 min.

The optimum value of AMC amount of 5.7 g, stirring time of 148 s, and volume of external phase of 350 mL were obtained. This condition predicted particle size of 200 μm , Q_5 in SSF of 5.5%, and MDT in SGF of 5.7 min. The predicted values were validated by further measuring particle size, *in vitro* drug dissolution both in SSF and SGF of the optimized microparticles. The optimized microparticles showed particle size of $174.45 \pm 18.19 \mu\text{m}$, Q_5 in SSF of 5.04%, and MDT in SGF of 5.97 min. Comparing to the predicted value, percentage of error of particle size, Q_5 , and MDT were 14.65%, 9.13%, 4.52%, confirming the validity of the model.

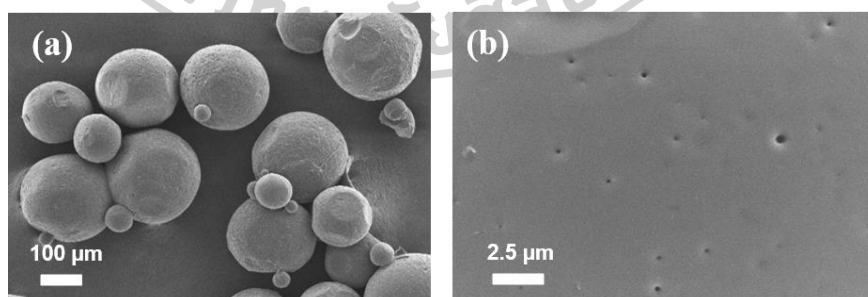


Figure 34 SEM images of (a) optimized microparticles and (a) its surface morphology

4.4 Characterization of optimized DPH-loaded microparticles

4.4.1 Residual solvent determination

Regarding to USP36-NF31 (105), dichloromethane is classified as class II residual solvent, which should be limited in drug substances, excipients, and drug products because of its inherent toxicities. Since dichloromethane was used as a solvent in oil phase in this study, residual solvent test is necessary to confirm that the residual amount of dichloromethane is in limitation criteria. The permitted daily exposure of dichloromethane is set at 6.0 mg/day while the concentration limit is 600 ppm. The amount of dichloromethane analyzed by head-space GC showed that its amount was below detection limit (less than 5 ppb) of the method. Therefore, it can be concluded that the amount of residual dichloromethane of microparticles prepared by DESE was in acceptable criteria.

4.4.2 FTIR spectroscopy

To investigate the chemical compatibility of optimized microparticles, FTIR was used to characterize the molecular behavior of DPH, AMC, PVA, physical mixture, and optimized microparticles. As shown in Fig. 35, DPH demonstrated a band at 3007.6 cm^{-1} , which was assigned to an aromatic C-H stretching. It is demonstrated that a band at 1697.2 cm^{-1} due to the stretching of C=O group on indanone moiety, and a band at 1589.0 cm^{-1} due to the vibration of aromatic C=C were observed. DPH also showed a band at 1312.9 cm^{-1} due to the C-N stretching on piperidine ring. AMC spectrum demonstrated the band at 2822.6 and 2772.0 cm^{-1} attributed to the C-H stretching of dimethyl amino group.

Additionally, a strong C-O stretching band at 1149.0 , and 1242.1 cm^{-1} and C=O band at 1731.6 cm^{-1} , indicating the present of ester group were observed. For physical mixture, the superimposed spectrum between DPH and AMC was obviously seen. Similar result was also observed in the spectrum of optimized microparticles. There was no significant deviation in characteristic band of microparticles after preparation, confirming compatibility of components.

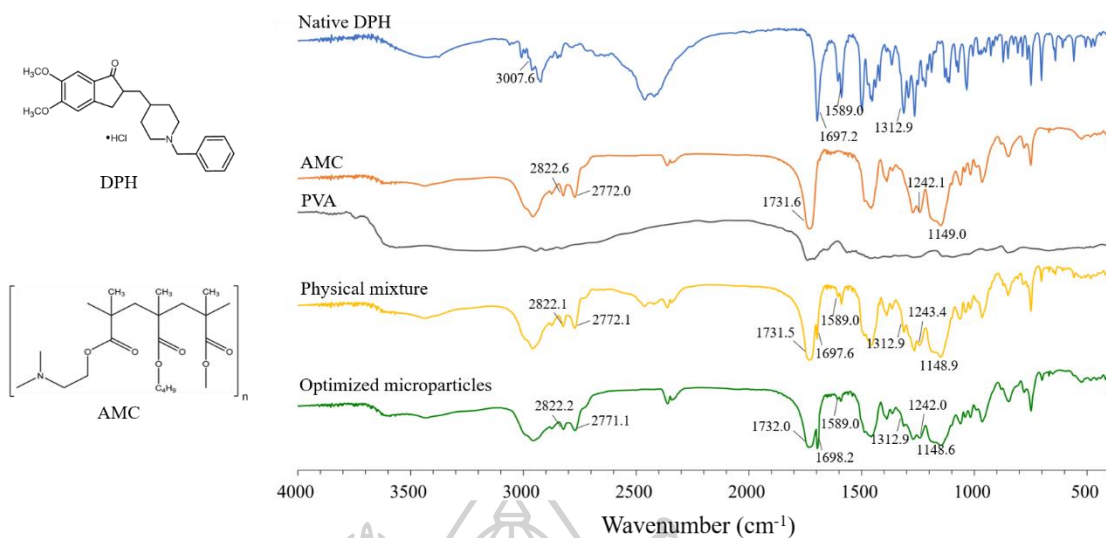


Figure 35 FTIR spectra of DPH, AMC, PVA, physical mixture, and optimized microparticles

4.4.3 PXRD

According to the PXRD pattern of native DPH illustrated in Fig. 36, sharp diffraction peaks were observed at 2-theta value of 6.5, 12.9, 16.5, 18.1, 19.5, 20.1, 21.6, 25.9, and 28.1 degree, indicating its crystalline structure. The sharp peaks were also observed in the PXRD pattern of physical mixture at 2-theta value of 18.1 and 21.6, which attributed to the crystalline peak of DPH. In case of the PXRD pattern of AMC, PVA, and optimized microparticles, a broad halo pattern was observed, which indicated the amorphous structure of these samples. Additionally, the absence of crystalline peak in PXRD pattern of optimized microparticles also confirmed the complete encapsulation of optimized microparticles.

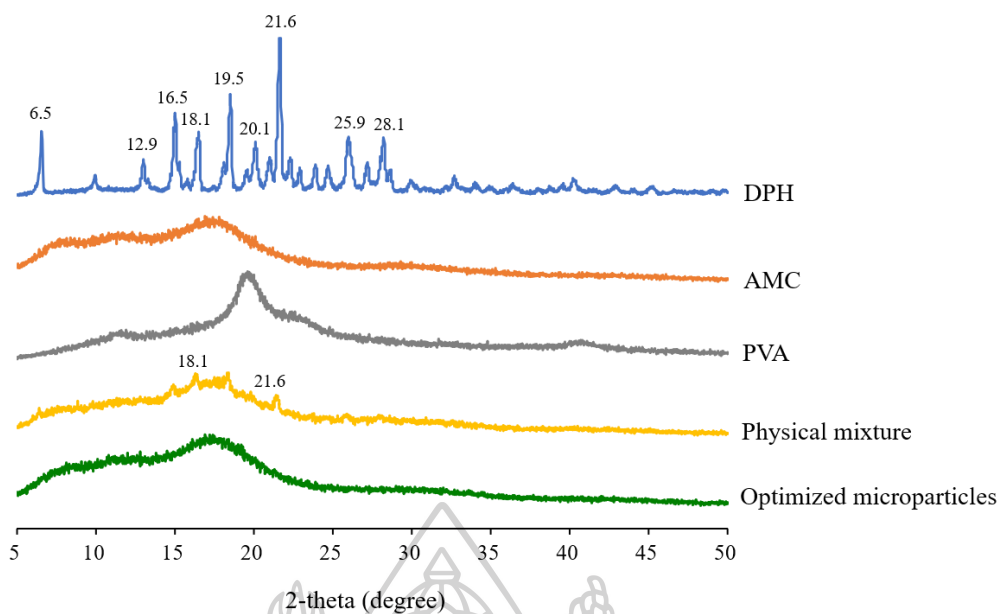


Figure 36 Powder X-ray diffraction patterns of DPH, AMC, PVA, physical mixture, and optimized microparticles

4.4.4 DSC

DSC thermograms of native DPH, AMC, PVA, physical mixture, and optimized microparticles were used to investigate the interaction between the component of resultant microparticles (Fig. 37). Regarding DSC thermogram of native DPH showed a sharp endothermic peak at 231.31°C was observed, attributing to the melting peak.

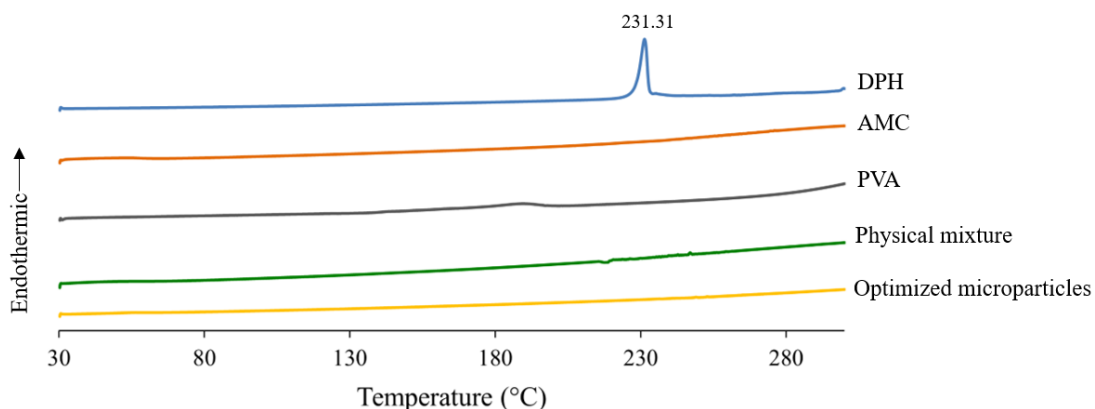


Figure 37 DSC thermograms of (a) DPH, (b) AMC, (c) PVA, (d) physical mixture, and (e) optimized microparticles

The thermogram of physical mixture showed a small endothermic peak. On the other hand, the absence of endothermic peak in the thermogram of optimized microparticles supported the PXRD result. It is suggested that the crystalline state of DPH was changed to amorphous state and it was completely incorporated in the microparticles.

4.5 Preparation and evaluation of ODTs

4.5.1 Physical properties of ODTs

The 200 mg-blank ODT (F1-ODT to F9-ODT) was first prepared by direct compression method without addition of optimized microparticles. The effect of super-disintegrant including sodium starch glycolate (F1-ODT, F2-ODT and F3-ODT), croscarmellose sodium (F4-ODT, F5-ODT and F6-ODT), and crospovidone (F7-ODT, F8-ODT and F9-ODT) at 2, 4, 6% on wetting time and *in vitro* disintegration time was studied. Table 16 demonstrates the physical properties of blank ODTs.

Table 16 Physical properties of blank ODTs

| Formulation | ODTs properties | | | | |
|-------------|-----------------------|------------------------|----------------------|--------------------------|---|
| | Diameter (mm) ± SD | Thickness (mm) ± SD | Hardness (N) ± SD | Wetting time (s) ± SD | <i>In vitro</i> disintegration time (s) ± SD |
| F1-ODT | 9.72 ± 0.02 | 2.10 ± 0.02 | 41 ± 2.49 | 17 ± 1.63 | 16 ± 0.82 |
| F2-ODT | 9.67 ± 0.03 | 2.11 ± 0.01 | 40 ± 2.87 | 20 ± 0.47 | 14 ± 0.82 |
| F3-ODT | 9.69 ± 0.02 | 2.09 ± 0.02 | 42 ± 0.47 | 20 ± 1.41 | 15 ± 2.15 |
| F4-ODT | 9.69 ± 0.01 | 2.09 ± 0.00 | 37 ± 1.25 | 21 ± 0.47 | 14 ± 1.25 |
| F5-ODT | 9.68 ± 0.00 | 2.10 ± 0.01 | 38 ± 2.49 | 20 ± 0.00 | 15 ± 0.82 |
| F6-ODT | 9.68 ± 0.00 | 2.11 ± 0.01 | 34 ± 3.56 | 21 ± 0.94 | 17 ± 0.47 |
| F7-ODT | 9.71 ± 0.04 | 2.14 ± 0.01 | 46 ± 2.05 | 12 ± 1.25 | 18 ± 0.47 |
| F8-ODT | 9.68 ± 0.02 | 2.15 ± 0.01 | 46 ± 0.94 | 10 ± 0.47 | 14 ± 1.70 |
| F9-ODT | 9.69 ± 0.00 | 2.16 ± 0.01 | 48 ± 0.82 | 9 ± 0.47 | 16 ± 0.47 |

The off-white color, round, smooth flat-face blank ODT was obtained. Although the diameter and thickness of all formulations were similar (around 9.70 mm, and 2.10 mm, respectively), the hardness was quite different. The ODTs prepared with crospovidone provided the highest hardness (46-48 N), followed with those of sodium starch glycolate (40 – 42 N) and croscarmellose sodium (34 – 38 N).

4.5.2 Wetting test and *in vitro* disintegration test

According to the USA guidance for industry: orally disintegrating tablets (8), the disintegration time is the critical factor for characterizing tablets as ODTs. It should rapidly disintegrate with an *in vitro* disintegration time of 30 s or less using USP disintegration test or alternative. Therefore, the effect of disintegrant on disintegration time of ODTs should be investigated in this study. However, there is no compendial disintegration test in pharmacopeia that particularly designed for ODTs. The test specified in general chapter <701> Disintegration assigned the tablet to be tested in 900 mL of water under vigorously agitated apparatus, which does not simulate the condition of oral cavity. Therefore, various alternative disintegration tests have been proposed. Among these tests, wetting test has received much attention to characterize the ODTs. The time required for dye solution to diffuse through the ODT and completely cover its surface was recorded as wetting time. So, this test was carried out as a quick and easy screening tool for investigating wettability of ODTs containing different super-disintegrants.

The wetting time of F1-ODT to F9-ODT is demonstrated in Table 16. The wetting time of 17-21 s was observed in F1-ODT-F6-ODT in which sodium starch glycolate and croscarmellose sodium were used as a disintegrant. However, faster wetting time of 9-12 s was achieved for F7-ODT-F9-ODT containing crospovidone. This phenomenon can be explained by high capillary effect and strong hydration capacity of crospovidone over other super-disintegrants (106). After placing on wetted filter paper, it rapidly absorbed dye solution via capillary action and, therefore, wetting time was shortened.

However, in physiological condition, there are two steps related to the disintegration of ODT in oral cavity. After placing the tablet on the tongue, the saliva absorption begins, followed by tablet disintegration into small particles due to the pressure between the tongue and upper hard palate. Only determination of wetting time may not be sufficient to characterize the ODT, since that pressure was neglected. To simulate both steps, *in vitro* disintegration time of all ODTs was also determined. The result showed a different trend compared to those of wetting test (Table 16). The disintegration time was determined, ranging from 14 to 18 s. To choose the ODT for further analysis, the information from wetting test and *in vitro*

disintegration test were taken into consideration. Therefore, sodium starch glycolate of 4% (F2-ODT), croscarmellose sodium of 2% (F4-ODT), and crospovidone of 4% (F8-ODT) were selected to prepare ODT containing optimized microparticles.

The optimized microparticles of 28.5 mg (equivalent to 5 mg of DPH) were incorporated in order to prepare F10-ODT (with 4% sodium starch glycolate), F11-ODT (with 2% croscarmellose sodium), and F12-ODT (with 4% crospovidone). After blending and tableting, the ODTs properties were determined against DPH-ODT. Similar to the appearance of blank ODT, the off-white color, round, flat face ODT with the diameter of 9.7 mm was obtained. However, the surface of ODT was rough due to homogeneously distributed microparticles and the thickness was increased to 2.34 mm. F12-ODT prepared with 4% crospovidone showed the highest hardness of 42 N, followed by F10-ODT, and F11-ODT.

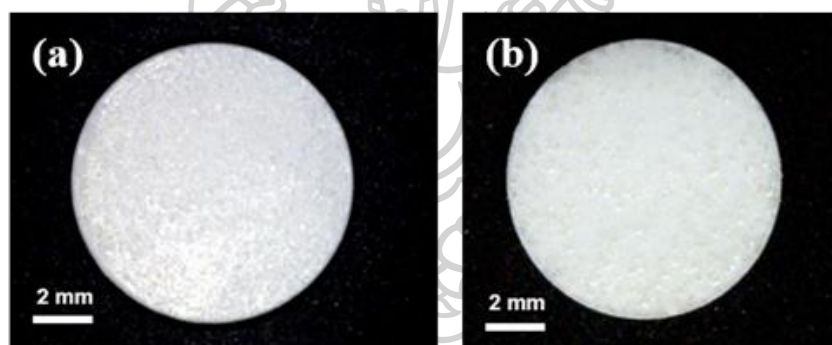


Figure 38 Microscopic images of (a) DPH-ODT and (b) F12-ODT

The wetting time and *in vitro* disintegration time results showed similar trend to that of blank ODT. Fig. 39 shows different stages of wetting time testing. The wetting time of F12-ODT was fastest (11 s) while that of F10-ODT and F11-ODT was 23 and 24 s, respectively. In contrast to the *in vitro* disintegration time of all formulations (Table 17), it was in the same range of 13 to 14 s.

In addition, the percentage of friability was also determined. The results showed that the lowest friability was obtained from F12-ODT (Table 17), which correlated well with its high hardness. This phenomenon was also reported by Mehta and coworkers (84), who reported that the hardness of multiparticulate tablets

containing crospovidone was higher than that of sodium starch glycolate and croscarmellose sodium. The binding properties of crospovidone acted as an adhesive within the tablets. The ODT was, therefore, harder and less friable (107).

Table 17 Physical properties of ODTs containing taste-masked microparticles

| Formulation | ODTs properties | | | | | | |
|-------------|---------------------------|----------------------------|--------------------------|------------------------------|--|-------------------|---|
| | Diameter (mm) \pm SD | Thickness (mm) \pm SD | Hardness (N) \pm SD | Wetting time (s) \pm SD | <i>In vitro</i> disintegration time (s) \pm SD | Friability (%) | <i>In vivo</i> disintegration time (s) \pm SD |
| F10-ODT | 9.68 \pm 0.00 | 2.26 \pm 0.02 | 37 \pm 2.05 | 23 \pm 0.94 | 14 \pm 0.94 | 1.72 | - |
| F11-ODT | 9.68 \pm 0.01 | 2.28 \pm 0.01 | 34 \pm 1.70 | 24 \pm 1.63 | 13 \pm 1.25 | 1.90 | - |
| F12-ODT | 9.70 \pm 0.00 | 2.34 \pm 0.05 | 42 \pm 0.82 | 11 \pm 0.82 | 14 \pm 1.25 | 0.76 | 18.78 \pm 1.73 |
| DPH-ODT | 9.71 \pm 0.01 | 2.18 \pm 0.02 | 38 \pm 2.83 | 10 \pm 1.70 | 13 \pm 0.82 | 0.90 | 22.57 \pm 3.41 |

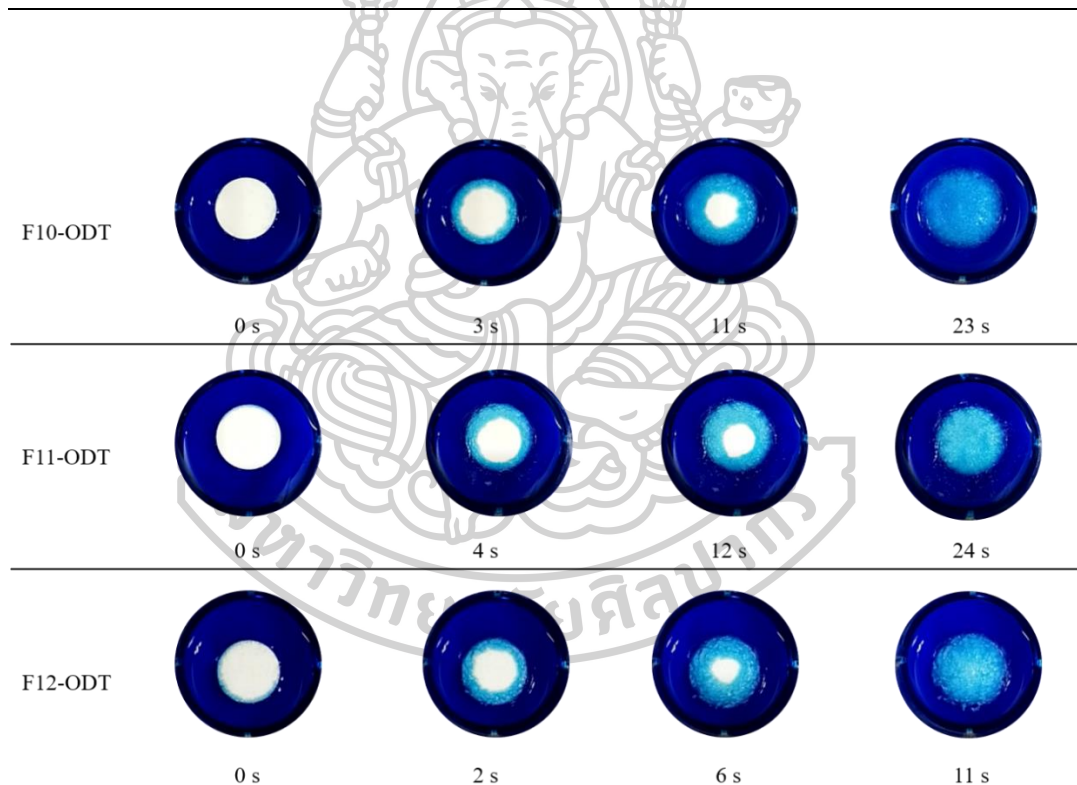


Figure 39 Stages of wetting test of F10-ODT (with 4% sodium starch glycolate), F11-ODT (with 2% croscarmellose sodium), and F12-ODT (with 4% crospovidone)

4.5.3 *In vitro* dissolution test

The *in vitro* drug dissolution of native DPH, DPH-ODT, optimized microparticles, and F12-ODT was determined in both SSF, and SGF. The dissolution

profiles of DPH, and DPH-ODT in SSF in Fig. 40 (a) showed a rapid drug dissolution of more than 80% in 5 min with Q_5 of 81.38 and 83.11%, respectively. In contrast to the optimized microparticles, and F12-ODT demonstrated a low drug dissolution behavior with Q_5 of 5.04, and 4.48%. These two formulations met the taste-masking acceptance criteria of Q_5 less than 10%.

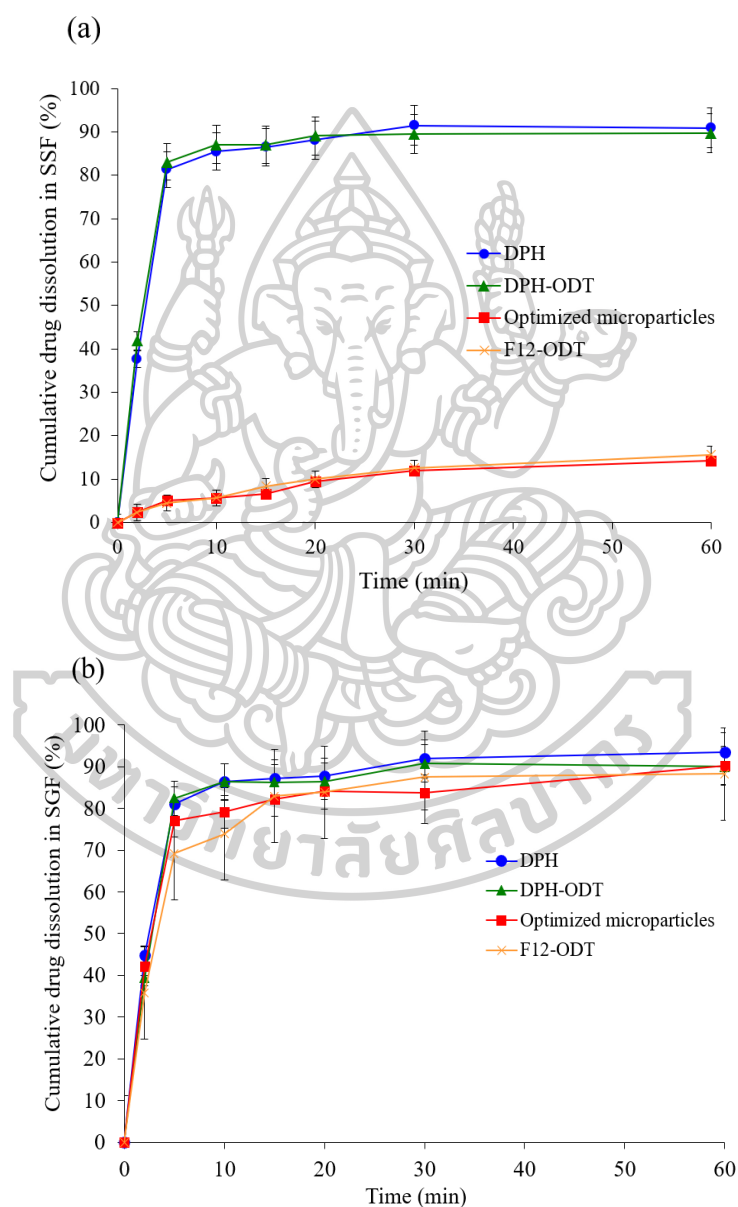


Figure 40 In vitro drug dissolution profiles of native DPH, DPH-ODT, optimized microparticles, and F12-ODT in (a) SSF, and (b) SGF

Drug dissolution testing in SGF was also carried out to determine drug dissolved in pH 1.2 medium to simulate gastric conditions. A rapid drug dissolution of more than 80% within 5 min was observed in DPH, and DPH-ODT. However, the drug dissolution from optimized microparticles, and F12-ODT was slower and reached 80% within 15 min with MDT of 5.97 and 5.01 min, which were acceptable with regards to the criteria.

4.5.4 *In vivo* evaluation

The *in vivo* evaluation began with the determination of perception and bitterness threshold of DPH. The results from six volunteers showed the perception threshold of 41.7 $\mu\text{g/mL}$ (ranged from 25.0 to 62.5 $\mu\text{g/mL}$, SD of 13.81). The bitterness threshold of DPH was found to be 56.3 $\mu\text{g/mL}$ (ranged from 37.5 to 75.0 $\mu\text{g/mL}$, SD of 15.72), which is in a good agreement with previous studies (12, 26).

The volunteers were also asked to evaluate the disintegration time of the samples. The results showed that the average disintegration time of DPH-ODT, and F12-ODT was 20.74 ± 1.90 and 18.78 ± 1.73 s, respectively. After the tablet completely disintegrated, the volunteers were asked to hold it in their mouth for 30 s. Then, they were asked to evaluate the score for bitterness, tablet handling, grittiness, and overall palatability by drawing line on 100-mm length VAS line. The VAS score of ODT was presented as median with range in box-whisker plot in Fig. 41. A statistically significant difference among two samples was noted by asterisk at *p*-value of less than 0.05.

The median VAS bitterness score of F12-ODT (92.5) was significantly lower than that of DPH-ODT (6), indicating that the bitterness of DPH was successfully suppressed. On the other hand, the median of VAS tablet handling of DPH-ODT, and F12-ODT was almost similar (91.5 and 91, respectively), meaning that the tablet handling of these tablets was not significantly different. The VAS results in Fig. 41 (c) presented that the median grittiness score of F12-ODT was significantly greater than that of DPH-ODT, indicating that the grittiness feeling of F12-ODT was pronounced over that of DPH-ODT. This result may be related with the large particle size of optimized microparticles of 174.45 ± 18.19 μm . However, the median of VAS score for

overall palatability of F12-ODT was significantly greater than that of DPH-ODT, indicating that F12-ODT was acceptable.

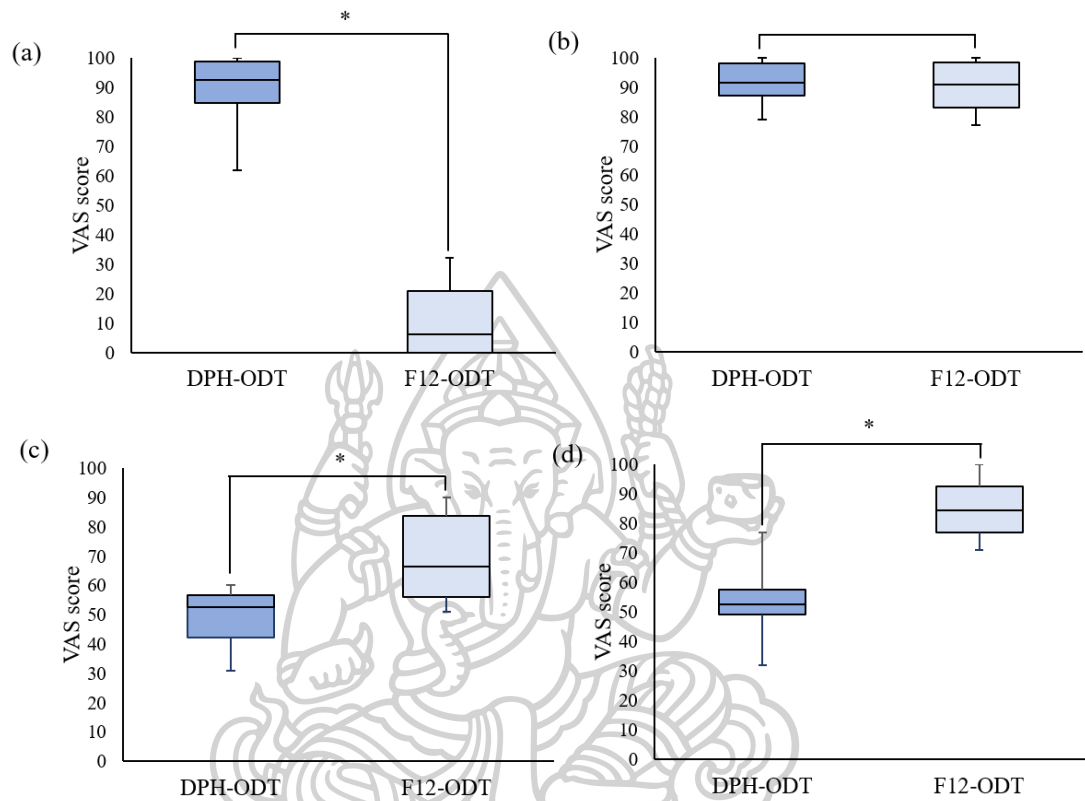


Figure 41 VAS scores of (a) bitterness, (b) tablet handling, (c) grittiness, and (d) overall palatability

CHAPTER 5

Conclusion and future prospect

Drug microencapsulation by DESE may potentially be used for taste-masking of DPH. However, the preparation of W/O/W double emulsion is a complex process and associated with several factors including formulation factors, operating conditions, and environmental factors, the implement of DoE may be beneficial in helping determine the effect of each factor and optimization.

Firstly, the preliminary study was performed to determine a suitable range of AMC amount (1-7 g) and ultrasonication time (120 s) used for double emulsion preparation. The fishbone diagram was constructed to demonstrate relevant factors throughout microparticle preparation process. The risk assessment approach was then employed to prioritize risk value of each factor based on the information from literature. The high-risk factors were amount and volume of materials, pH of external water phase, and ultrasonication and stirring rate and time. The effect of independent factors including AMC amount (3-7 g), stirring time (90-180 s), and volume of external water phase (350-450 mL) on particle size, Q_5 in SSF, and MDT in SGF were investigated using BBD. The results demonstrated that particle size increased with increasing AMC amount and decreasing stirring time. Both AMC amount and volume of external water phase had a significant impact on Q_5 in SSF. On the other hand, these two factors had a significant impact on MDT in SGF. Furthermore, the optimization was then carried out to find the optimum conditions for taste-masked microparticle preparation based on the acceptance criteria. The optimum conditions were AMC amount of 5.7 g, stirring time of 148 s, and volume of external phase of 350 mL.

The optimized microparticles were then incorporated in ODTs, which prepared by direct compression method. The effect of super-disintegrant including sodium starch glycolate, croscarmellose sodium, and crospovidone at 2, 4, 6% on wetting time and *in vitro* disintegration time was investigated. Since F12-ODT containing 4% of crospovidone showed a sufficient hardness, low friability, short wetting time and *in vitro* disintegration time, this formulation was then selected for further studied.

The *in vivo* ODT evaluation was then conducted in 6 healthy volunteers. The perception threshold and bitterness threshold were first determined before tablet evaluation. The results showed that the bitterness score of F12-ODT was significantly lower than that of DPH-ODT while tablet handling score was not significant different. It is suggested that successful taste-masking of DPH with acceptable tablet handling was achieved. Although the grittiness score of F12-ODT was significantly higher than that of DPH-ODT, the overall palatability was acceptable.

According to the results obtained from all experiments, it can be concluded that the microencapsulation by DESE can effectively use for taste-masking the bitter taste of DPH. DoE approach using BBD can help explain the effect of independent factor and optimization. Eventually, the ODT containing taste-masked microparticles with acceptable properties was successfully prepared.

Although the characterization part of this study demonstrated that the encapsulation process had no effect on chemical characteristics, only crystal structure changed observed, the *in vivo* bioavailability of microparticles should be conducted. In addition to bitterness taste of DPH, gastrointestinal adverse event is frequently reported due to the fluctuation of plasma drug level of conventional product. Future research should emphasize on controlled release product to maintain steady DPH level. The nanotechnology-based formulation for transdermal or intranasal administration may be an excellent alternative route to overcome this problem.

REFERENCES

1. Alzheimer's association. 2020 Alzheimer's disease facts and figures. *Alzheimers Dement.* 2020;16(3):391-460.
2. Patterson C. World Alzheimer's report 2018: the state of the art of dementia research: new frontiers 2018 [Available from: <https://www.alzint.org/u/WorldAlzheimerReport2018.pdf>].
3. Zvěřová M. Alzheimer's disease and blood-based biomarkers - potential contexts of use. *Neuropsychiatr Dis Treat.* 2018;14:1877-82.
4. Anil S, Vellappally S, Hashem M, Preethanath RS, Patil S, Samaranayake LP. Xerostomia in geriatric patients: a burgeoning global concern. *J Investig Clin Dent.* 2016;7(1):5-12.
5. Mobley AS, Rodriguez-Gil DJ, Imamura F, Greer CA. Aging in the olfactory system. *Trends Neurosci.* 2014;37(2):77-84.
6. Morishima-Kawashima M, Ihara Y. Alzheimer's disease: β -amyloid protein and tau. *J Neurosci Res.* 2002;70(3):392-401.
7. Manabe T, Teramoto S, Tamiya N, Okochi J, Hizawa N. Risk factors for aspiration pneumonia in older adults. *PloS one.* 2015;10(10):e0140060.
8. Center for drug evaluation and research. Guidance for industry: orally disintegrating tablets 2008 [Available from: <https://www.fda.gov/media/70877/download>].
9. Slavkova M, Breitkreutz J. Orodispersible drug formulations for children and elderly. *Eur J Pharm Sci.* 2015;75:2-9.
10. Liew KB, Tan YT, Peh KK. Characterization of oral disintegrating film containing donepezil for Alzheimer disease. *AAPS PharmSciTech.* 2012;13(1):134-42.
11. Liew KB, Tan YT, Peh KK. Taste-masked and affordable donepezil hydrochloride orally disintegrating tablet as promising solution for non-compliance in Alzheimer disease patients. *Drug Dev Ind Pharm.* 2015;41(4):583-93.

12. Yan YD, Woo JS, Kang JH, Yong CS, Choi HG. Preparation and evaluation of taste-masked donepezil hydrochloride orally disintegrating tablets. *Biol Pharm Bull.* 2010;33(8):1364-70.
13. Han X, Yan J, Ren L, Xue M, Yuan Z, Wang T, et al. Preparation and evaluation of orally disintegrating film containing donepezil for Alzheimer's disease. *J Drug Deliv Sci Technol.* 2019;54:101321.
14. Kim JI, Cho SM, Cui JH, Cao QR, Oh E, Lee BJ. In vitro and in vivo correlation of disintegration and bitter taste masking using orally disintegrating tablet containing ion exchange resin-drug complex. *Int J Pharm.* 2013;455(1-2):31-9.
15. Liu T, Wan X, Luo Z, Liu C, Quan P, Cun D, et al. A donepezil/cyclodextrin complexation orodispersible film: effect of cyclodextrin on taste-masking based on dynamic process and in vivo drug absorption. *Asian J Pharm Sci.* 2019;14(2):183-92.
16. Iqbal M, Zafar N, Fessi H, Elaissari A. Double emulsion solvent evaporation techniques used for drug encapsulation. *Int J Pharm.* 2015;496(2):173-90.
17. Ding S, Serra CA, Vandamme TF, Yu W, Anton N. Double emulsions prepared by two-step emulsification: history, state-of-the-art and perspective. *J Control Release.* 2019;295:31-49.
18. Garti N, Bisperink C. Double emulsions: progress and applications. *Curr Opin Colloid Interface Sci.* 1998;3(6):657-67.
19. Montgomery DC. *Design and analysis of experiments.* 8th ed. Hoboken, NJ: John Wiley & Sons; 2013.
20. Bartus RT, Dean RL, Beer B, Lippa AS. The cholinergic hypothesis of geriatric memory dysfunction. *Science.* 1982;217(4558):408-14.
21. Whitehouse PJ, Price DL, Struble RG, Clark AW, Coyle JT, Delon MR. Alzheimer's disease and senile dementia: loss of neurons in the basal forebrain. *Science.* 1982;215(4537):1237-9.
22. Sugimoto H, Ogura H, Arai Y, Iimura Y, Yamanishi Y. Research and development of donepezil hydrochloride, a new type of acetylcholinesterase inhibitor. *Jpn J Pharmacol.* 2002;89(1):7-20.

23. Asiri YA, Mostafa GAE. Donepezil. Profiles of Drug Substances, Excipients and Related Methodology. Amsterdam: Academic Press; 2010. p. 117-50.
24. Moffat AC, Olselton MD, Widdop B, Watts J. Clarke's analysis of drugs and poisons. 4th ed. London: Pharmaceutical Press; 2011.
25. Ruela AL, Carvalho FC, Pereira GR. Exploring the phase behavior of monoolein/oleic acid/water systems for enhanced donepezil administration for Alzheimer disease treatment. *J Pharm Sci.* 2016;105(1):71-7.
26. Zainuddin R, Kulkani A, Chavan H, Patil G, Zaheer Z. Taste masking of donepezil hydrochloride using different ion exchange resin - a comparative study. *Indones J Pharm.* 2013;24(2):107-15.
27. Alzheimer's Association. FDA-approved treatments for Alzheimer's 2019 [Available from: <https://www.alz.org/media/documents/fda-approved-treatments-alzheimers-ts.pdf>].
28. Eisai Co. Ltd. Aricept (donepezil hydrochloride) label 2012 [1-14]. Available from: https://www.accessdata.fda.gov/drugsatfda_docs/label/2012/020690s035,021720s008,022568s0051bl.pdf.
29. Román GC, Rogers SJ. Donepezil: a clinical review of current and emerging indications. *Expert Opin Pharmacother.* 2004;5(1):161-80.
30. Boada-Rovira M, Brodaty H, Cras P, Baloyannis S, Emre M, Zhang R, et al. Efficacy and safety of donepezil in patients with Alzheimer's disease: results of a global, multinational, clinical experience study. *Drugs Aging.* 2004;21(1):43-53.
31. Rogers SL, Doody RS, Mohs RC, Friedhoff LT. Donepezil improves cognition and global function in Alzheimer disease: a 15-week, double-blind, placebo-controlled study. *Clin Chem.* 1998;158(9):1021-31.
32. Harada T, Uchida T, Yoshida M, Kobayashi Y, Narazaki R, Ohwaki T. A new method for evaluating the bitterness of medicines in development using a taste sensor and a disintegration testing apparatus. *Chem Pharm Bull.* 2010;58(8):1009-14.
33. Douroumis D. Practical approaches of taste masking technologies in oral solid forms. *Expert Opin Drug Deliv.* 2007;4(4):417-26.

34. Sohi H, Sultana Y, Khar RK. Taste masking technologies in oral pharmaceuticals: recent developments and approaches. *Drug Dev Ind Pharm.* 2004;30(5):429-48.
35. Guo X, Chang R-K, Hussain MA. Ion-exchange resins as drug delivery carriers. *J Pharm Sci.* 2009;98(11):3886-902.
36. Imbimbo BP. Pharmacodynamic-tolerability relationships of cholinesterase inhibitors for Alzheimer's disease. *CNS Drugs.* 2001;15(5):375-90.
37. Jann MW, Shirley KL, Small GW. Clinical pharmacokinetics and pharmacodynamics of cholinesterase inhibitors. *Clin Pharmacokinet.* 2002;41(10):719-39.
38. Park JK, Choy YB, Oh JM, Kim JY, Hwang SJ, Choy JH. Controlled release of donepezil intercalated in smectite clays. *Int J Pharm.* 2008;359(1-2):198-204.
39. Eisai Co. Ltd. Eisai amends license agreement with Teikoku Pharma USA for Aricept transdermal patch system 2012 [Available from: <http://www.eisai.com/news/news201217.html>].
40. Icure Pharmaceutical Inc. A multinational, multi-center, randomized , double-blind, active comparator, phase III clinical trial to evaluate the efficacy and safety of donepezil transdermal patch in patients with Alzheimer's disease 2017 [Available from: <https://clinicaltrials.gov/ct2/show/NCT03197740>].
41. Choi J, Choi MK, Chong S, Chung SJ, Shim CK, Kim DD. Effect of fatty acids on the transdermal delivery of donepezil: in vitro and in vivo evaluation. *Int J Pharm.* 2012;422(1-2):83-90.
42. Galipoğlu M, Erdal MS, Güngör S. Biopolymer-based transdermal films of donepezil as an alternative delivery approach in Alzheimer's disease treatment. *AAPS PharmSciTech.* 2015;16(2):284-92.
43. Mendes IT, Ruela ALM, Carvalho FC, Freitas JTJ, Bonfilio R, Pereira GR. Development and characterization of nanostructured lipid carrier-based gels for the transdermal delivery of donepezil. *Colloids Surf B Biointerfaces.* 2019;177:274-81.

44. Wu H, Fang F, Zheng L, Ji W, Qi M, Hong M, et al. Ionic liquid form of donepezil: preparation, characterization and formulation development. *J Mol Liq.* 2020;300:112308.
45. Saluja S, Kasha PC, Paturi J, Anderson C, Morris R, Banga AK. A novel electronic skin patch for delivery and pharmacokinetic evaluation of donepezil following transdermal iontophoresis. *Int J Pharm.* 2013;453(2):395-9.
46. Kim JY, Han MR, Kim YH, Shin SW, Nam SY, Park JH. Tip-loaded dissolving microneedles for transdermal delivery of donepezil hydrochloride for treatment of Alzheimer's disease. *Eur J Pharm Biopharm.* 2016;105:148-55.
47. Kearney MC, Caffarel-Salvador E, Fallows SJ, McCarthy HO, Donnelly RF. Microneedle-mediated delivery of donepezil: potential for improved treatment options in Alzheimer's disease. *Eur J Pharm Biopharm.* 2016;103:43-50.
48. Guo W, Quan P, Fang L, Cun D, Yang M. Sustained release donepezil loaded PLGA microspheres for injection: preparation, in vitro and in vivo study. *Asian J Pharm Sci.* 2015;10(5):405-14.
49. Agrawal M, Saraf S, Saraf S, Antimisiaris SG, Chougule MB, Shoyele SA, et al. Nose-to-brain drug delivery: an update on clinical challenges and progress towards approval of anti-Alzheimer drugs. *J Control Release.* 2018;281:139-77.
50. Crowe TP, Greenlee MHW, Kanthasamy AG, Hsu WH. Mechanism of intranasal drug delivery directly to the brain. *Life Sci.* 2018;195:44-52.
51. Rohrer J, Lupo N, Bernkop-Schnürch A. Advanced formulations for intranasal delivery of biologics. *Int J Pharm.* 2018;553(1-2):8-20.
52. Bhavna, Md S, Ali M, Ali R, Bhatnagar A, Baboota S, et al. Donepezil nanosuspension intended for nose to brain targeting: in vitro and in vivo safety evaluation. *Int J Biol Macromol.* 2014;67:418-25.
53. Al Asmari AK, Ullah Z, Tariq M, Fatani A. Preparation, characterization, and in vivo evaluation of intranasally administered liposomal formulation of donepezil. *Drug Des Devel Ther.* 2016;10:205-15.
54. Yasir M, Sara UVS, Chauhan I, Gaur PK, Singh AP, Puri D, et al. Solid lipid nanoparticles for nose to brain delivery of donepezil: formulation, optimization

- by Box–Behnken design, in vitro and in vivo evaluation. *Artif Cells Nanomed B.* 2018;46(8):1838-51.
55. Khunt D, Shrivastava M, Polaka S, Gondaliya P, Misra M. Role of omega-3 fatty acids and butter oil in targeting delivery of donepezil hydrochloride microemulsion to brain via the intranasal route: a comparative study. *AAPS PharmSciTech.* 2020;21(2):45.
56. Topal GR, Mészáros M, Porkoláb G, Szecskó A, Polgár TF, Siklós L, et al. ApoE-targeting increases the transfer of solid lipid nanoparticles with donepezil cargo across a culture model of the blood–brain barrier. *Pharmaceutics.* 2021;13(1).
57. Andrade J, Wright AJ, Corredig M. In vitro digestion behavior of water-in-oil-in-water emulsions with gelled oil-water inner phases. *Food Res Int.* 2018;105:41-51.
58. Muschiolik G. Multiple emulsions for food use. *Curr Opin Colloid Interface Sci.* 2007;12(4):213-20.
59. Aserin A. *Multiple emulsion: technology and applications*: John Wiley & Sons; 2008. 352 p.
60. Vladisavljević GT, Williams RA. Recent developments in manufacturing emulsions and particulate products using membranes. *Adv Colloid Interface Sci.* 2005;113(1):1-20.
61. Nakashima T, Shimizu M, Kukizaki M. Particle control of emulsion by membrane emulsification and its applications. *Adv Drug Deliv Rev.* 2000;45(1):47-56.
62. Piacentini E, Drioli E, Giorno L. Membrane emulsification technology: twenty-five years of inventions and research through patent survey. *J Memb Sci.* 2014;468:410-22.
63. Lee TY, Choi TM, Shim TS, Frijns RAM, Kim SH. Microfluidic production of multiple emulsions and functional microcapsules. *Lap Chip.* 2016;16(18):3415-40.
64. Vladisavljević GT, Al Nuamani R, Nabavi SA. Microfluidic production of multiple emulsions. *Micromachines.* 2017;8(3):75.

65. Alex R, Bodmeier R. Encapsulation of water-soluble drugs by a modified solvent evaporation method. I. effect of process and formulation variables on drug entrapment. *J Microencapsul.* 1990;7(3):347-55.
66. Pisani E, Fattal E, Paris J, Ringard C, Rosilio V, Tsapis N. Surfactant dependent morphology of polymeric capsules of perfluorooctyl bromide: influence of polymer adsorption at the dichloromethane-water interface. *J Colloid Interface Sci.* 2008;326(1):66-71.
67. Uchida T, Yoshida K, Goto S. Preparation and characterization of polylactic acid microspheres containing water-soluble dyes using a novel w/o/w emulsion solvent evaporation method. *J Microencapsul.* 1996;13(2):219-28.
68. Hombreiro-Pérez M, Siepmann J, Zinutti C, Lamprecht A, Ubrich N, Hoffman M, et al. Non-degradable microparticles containing a hydrophilic and/or a lipophilic drug: preparation, characterization and drug release modeling. *J Control Release.* 2003;88(3):413-28.
69. Karataş A, Sonakin O, Kiliçarslan M, Baykara T. Poly (epsilon-caprolactone) microparticles containing levobunolol HCl prepared by a multiple emulsion (w/o/w) solvent evaporation technique: effects of some formulation parameters on microparticle characteristics. *J Microencapsul.* 2009;26(1):63-74.
70. Cohen-Sela E, Chorny M, Koroukhov N, Danenberg HD, Golomb G. A new double emulsion solvent diffusion technique for encapsulating hydrophilic molecules in PLGA nanoparticles. *J Control Release.* 2009;133(2):90-5.
71. Hashimoto Y, Tanaka M, Kishimoto H, Shiozawa H, Hasegawa K, Matsuyama K, et al. Preparation, characterization and taste-masking properties of polyvinylacetal diethylaminoacetate microspheres containing trimebutine. *J Pharm Pharmacol.* 2002;54(10):1323-8.
72. Jiang HH, Kim TH, Lee S, Chen X, Youn YS, Lee KC. PEGylated TNF-related apoptosis-inducing ligand (TRAIL) for effective tumor combination therapy. *Biomaterials.* 2011;32(33):8529-37.
73. Gaignaux A, Réeff J, Siepmann F, Siepmann J, De Vriese C, Goole J, et al. Development and evaluation of sustained-release clonidine-loaded PLGA microparticles. *Int J Pharm.* 2012;437(1-2):20-8.

74. Ghasemian E, Vatanara A, Rouholamini Najafabadi A, Rouini MR, Gilani K, Darabi M. Preparation, characterization and optimization of sildenafil citrate loaded PLGA nanoparticles by statistical factorial design. *DARU J Pharm Sci.* 2013;21(1):68.
75. Bouriche S, Cózar-Bernal MJ, Rezgui F, Rabasco Álvarez AM, González-Rodríguez ML. Optimization of preparation method by w/o/w emulsion for entrapping metformin hydrochloride into poly (lactic acid) microparticles using Box-Behnken design. *J Drug Deliv Sci Technol.* 2019;51:419-29.
76. Rowe RC, Sheskey PJ, Quinn ME. *Handbook of Pharmaceutical Excipient.* 6th ed. London: Pharmaceutical Press; 2009. 23-7 p.
77. Li M, Rouaud O, Poncelet D. Microencapsulation by solvent evaporation: state of the art for process engineering approaches. *Int J Pharm.* 2008;363(1-2):26-39.
78. Joshi S, Petereit HU. Film coatings for taste masking and moisture protection. *Int J Pharm.* 2013;457(2):395-406.
79. Bitar A, Zafar N, Valour JP, Agusti G, Fessi H, Humbert P, et al. Elaboration of sponge-like particles for textile functionalization and skin penetration. *Colloid Polym Sci.* 2015;293(10):2967-77.
80. Walsh J, Ranmal SR, Ernest TB, Liu F. Patient acceptability, safety and access: a balancing act for selecting age-appropriate oral dosage forms for paediatric and geriatric populations. *Int J Pharm.* 2018;536(2):547-62.
81. Douroumis D. Orally disintegrating dosage forms and taste-masking technologies; 2010. *Expert Opin Drug Deliv.* 2011;8(5):665-75.
82. Badgajar BP, Mundada AS. The technologies used for developing orally disintegrating tablets: a review. *Acta Pharm.* 2011;61(2):117-39.
83. Gittings S, Turnbull N, Roberts CJ, Gershkovich P. Dissolution methodology for taste masked oral dosage forms. *J Control Release.* 2014;173:32-42.
84. Lacombe V, Lacout C, Lozac'h P, Ghali A, Gury A, Lavigne C, et al. Unstimulated whole saliva flow for diagnosis of primary Sjögren's syndrome: time to revisit the threshold? *Arthritis Res Therapy.* 2020;22(1):38.

85. Rudney JD, Ji Z, Larson CJ. The prediction of saliva swallowing frequency in humans from estimates of salivary flow rate and the volume of saliva swallowed. *Arch Oral Biol.* 1995;40(6):507-12.
86. Dey P, Maiti S. Orodispersible tablets: a new trend in drug delivery. *J Nat Sci Biol Med.* 2010;1(1):2-5.
87. Park JH, Holman KM, Bish GA, Krieger DG, Ramlose DS, Herman CJ. An alternative to the USP disintegration test for orally disintegrating tablets. *Pharm Technol.* 2008;32:54-8.
88. Bi Y, Sunada H, Yonezawa Y, Danjo K, Otsuka A, Iida K. Preparation and evaluation of a compressed tablet rapidly disintegrating in the oral cavity. *Chem Pharm Bull.* 1996;44(11):2121-7.
89. Morita Y, Tsushima Y, Yasui M, Termoz R, Ajioka J, Takayama K. Evaluation of the disintegration time of rapidly disintegrating tablets via a novel method utilizing a CCD camera. *Chem Pharm Bull.* 2002;50(9):1181-6.
90. Fu Y, Jeong SH, Callihan J, Kim J, Park K. Preparation of fast dissolving tablets based on mannose. *ACS Symposium Series.* ACS Symposium Series. 924: American Chemical Society; 2006. p. 340-51.
91. Narazaki R, Harada T, Takami N, Kato Y, Ohwaki T. A new method for disintegration studies of rapid disintegrating tablet. *Chem Pharm Bull.* 2004;52(6):704-7.
92. Scheuerle RL, Gerrard SE, Kendall RA, Tuleu C, Slater NK, Mahbubani KT. Characterising the disintegration properties of tablets in opaque media using texture analysis. *Int J Pharm.* 2015;486(1-2):136-43.
93. Collins LM, Dziak JJ, Li R. Design of experiments with multiple independent variables: a resource management perspective on complete and reduced factorial designs. *Psychol Methods.* 2009;14(3):202-24.
94. World Health Organization. WHO Expert Committee on Specifications for Pharmaceutical Preparations. 2011.
95. Samaha D, Shehayeb R, Kyriacos S. Modeling and comparison of dissolution profiles of diltiazem modified-release formulations. *Dissolution Technol.* 2009;16(2):41-6.

96. Hoashi Y, Tozuka Y, Takeuchi H. Development of a novel and simple method to evaluate disintegration of rapidly disintegrating tablets. *Chem Pharm Bull.* 2013;61(9):962-6.
97. British Pharmacopoeia Commission. *British Pharmacopoeia 2013.* London: The Stationary Office; 2013.
98. Shoghi E, Fuguet E, Bosch E, Ràfols C. Solubility-pH profiles of some acidic, basic and amphoteric drugs. *Eur J Pharm Sci.* 2013;48(1-2):291-300.
99. Zafar N, Bitar A, Valour JP, Fessi H, Elaissari A. Elaboration of ammonio methacrylate copolymer based spongy cationic particles via double emulsion solvent evaporation process. *Mater Sci Eng C.* 2016;61:85-96.
100. Siewert M, Dressman J, Brown CK, Shah VP. FIP/AAPS guidelines to dissolution/in vitro release testing of novel/special dosage forms. *AAPS PharmSciTech.* 2003;4(1):E7.
101. Kimura S, Uchida S, Kanada K, Namiki N. Effect of granule properties on rough mouth feel and palatability of orally disintegrating tablets. *Int J Pharm.* 2015;484(1-2):156-62.
102. Tung NT, Tran CS, Nguyen TL, Hoang T, Trinh TD, Nguyen TN. Formulation and biopharmaceutical evaluation of bitter taste masking microparticles containing azithromycin loaded in dispersible tablets. *Eur J Pharm Biopharm.* 2018;126:187-200.
103. Pal R. Rheology of simple and multiple emulsions. *Curr Opin Colloid Interface Sci.* 2011;16(1):41-60.
104. Nakano Y, Maeda A, Uchida S, Namiki N. Preparation and evaluation of unpleasant taste-masked pioglitazone orally disintegrating tablets. *Int J Pharm.* 2013;446(1-2):160-5.
105. United States Pharmacopeial Convention. *United States Pharmacopeia and National Formulary (USP 36-NF 31).* Rockville: United States Pharmacopeial Convention; 2013.
106. Desai PM, Liew CV, Heng PWS. Review of disintegrants and the disintegration phenomena. *J Pharm Sci.* 2016;105(9):2545-55.

107. Mehta S, De Beer T, Remon JP, Vervaet C. Effect of disintegrants on the properties of multiparticulate tablets comprising starch pellets and excipient granules. *Int J Pharm.* 2012;422(1-2):310-7.





VITA

NAME Lalinthip Sutthapitaksakul

DATE OF BIRTH 25 September 1990

INSTITUTIONS ATTENDED Faculty of Pharmacy, Silpakorn University, Thailand

HOME ADDRESS 41/9 M.7 Lambua sub-district, Nakhon Chaisri district, Nakhon Pathom, Thailand

PUBLICATION

- Sutthapitaksakul, L., & Sriamornsak, P. (2019). Influence of process parameters on the characteristics of hydrophilic drug-loaded microparticles through double emulsion solvent evaporation technique. *Key Eng Mater*, 819, 252-257.
- Sutthapitaksakul, L., & Sriamornsak, P. (2020). Effect of processing parameters on release profiles of donepezil hydrochloride-loaded microparticles. *Key Eng Mater*, 859, 283-288.
- Sutthapitaksakul, L., Dass, C. R., & Sriamornsak, P. (2021). Donepezil—an updated review of challenges in dosage form design. *J Drug Deliv Sci Technol*, 63, 102549. doi:<https://doi.org/10.1016/j.jddst.2021.102549>

